Cardiff
Catalysis Institute

Sefydliad Catalysis
Caerdydd

Selective Oxidation of *n*-Butanol Using Heterogeneous Platinum Metal Nanoparticulate-Based Catalysts

Thesis submitted in accordance with the requirement of Cardiff University for the degree of Doctor of Philosophy

Shaimaa Alghareeb

School of Chemistry

Cardiff University

2019

Declarations

STATEMENT 1

This thesis is being submitted in partial fulfilment of the requirements for the degree of PhD

Signed ……

Date ……..……..……

STATEMENT 2

This work has not been submitted in substance for any other degree or award at this or any other university or place of learning, nor is being submitted concurrently in candidature for any degree or other award (outside of any formal collaboration agreement between the University and a partner organisation)

Signed ……

Date ……..……..……

STATEMENT 3

I hereby give consent for my thesis, if accepted, to be available online in the University's Open Access repository (or, where approved, to be available in the University's library and for inter-library loan), and for the title and summary to be made available to outside organisations, subject to expiry of a University-approved bar on access if applicable.

Signed ……

Date ……..……..……

DECLARATION

This thesis is the result of my own independent work, except where otherwise stated, and the views expressed are my own. Other sources are acknowledged by explicit references. The thesis has not been edited by a third party beyond what is permitted by Cardiff University's Policy on the Use of Third Party Editors by Research Degree Students Procedure.

Signed ……

Date ……..……..……

WORD COUNT Approximately 31749 words

(Excluding summary, acknowledgment, declarations, contents pages, appendices, tables, diagrams and figures, references, bibliography, footnotes and endnotes)

Acknowledgements

I would like to express that completing a PhD is not something that one goes through alone, and here I offer my heartfelt gratitude to the people who have helped, guided, and supported me both academically and non-academically throughout my studies.

Foremost I would like to thank my supervisor, Prof. Stuart Taylor, for his technical support, advice and encouragement throughout this process.

I would like to thank Drs. Robert Armstrong, James Hayward and Mark Douthwaite for taking the time to read and correct this thesis.

I would also like to thank Drs David Morgan and Thomas Davies for their contribution to the XPS and SEM work presented in this thesis. To multi-skilled Drs Greg Shaw, and Michal Perdjon, Steven Morris, Simon Waller and Chris Morgan for their continual technical assistance and advice.

A special thank you goes to Moira Northam and George Summers for their continued guidance and support.

To my CCI colleagues, thank you for all the experiences and memorable moments in Cardiff.

Thank you to all my family and friends. To my parents and son (Barack) for their unending love, support and understanding throughout the process.

Throughout my life my mother has motivated me to work hard and achieve, and I take great pleasure in making her proud.

Thank you.
Shaimaa Alghareeb

Abstract

The selective oxidation of alcohols plays a significant role for the manufacturing of valuable organic compounds. Currently, the chemical industry uses organic and inorganic stoichiometric oxidants to produce carbonyl compounds, it is therefore highly desirable to use a heterogeneous catalyst with oxygen as oxidant as an alternative to this. The research presented herein, utilizes *n*-butanol as a model substrate. The activity and selectivity of various heterogeneous catalysts towards the corresponding aldehyde is examined, to draw conclusions on how the physicochemical properties of the catalyst influences viability in this oxidative transformation. In addition, there have been recent developments for producing *n*-butanol via sustainable methods, providing an additional motive for its selection as a model compound. This research focusses on the base free selective oxidation of *n*-butanol with O_2 in the aqueous phase over supported Pt nanoparticles. A sol-immobilization technique was used to synthesize different catalysts. The 1 wt.Pt/TiO_2 catalyst displayed activity (30 %) and selectivity towards butyraldehyde (91 %), however Pt was observed to leach (5.2 %), even in the presence of small concentrations of butyric acid, during the reaction (100 °C, 3 bar O_2). However, this catalyst was observed to deactivate after 2 h of reaction. This was evidenced by a stop in the butanol conversion after 2 h. It has been suggested that the inhibition of the reaction by the presence of a product affects the conversion of *n*- butanol. It was observed that exposing the catalyst to a reductive pre-treatment under 5 vol.%H_2/Ar at 200 °C for 2 hours, could enhance the catalysts activity (43 %). In order to improve catalyst performance and limit the deactivation, additional experiments were conducted in aerobic and anaerobic conditions, to better understand the conditions which influence catalytic performance. Based on this observation the effect of the concentration of oxygen was studied. It was found that the best pressure, which gives the highest conversion, is 2 bar (conversion 38 %).To improve the performance of platinum catalyst, the preparation of a Pt-base bimetallic can be an effective route, the elements Al, Zn, Sn, Bi and Pb were selected and added to the Pt for the selective oxidation of *n*-butanol at 100 °C, 2 bar O_2 for 2 h. The addition of Pb and Sn show higher activity for *n*-butanol. Accordingly, it was decided to carry on the work focussing on the 1 wt.%Pt-0.5 wt.%Pb/TiO_2 and 1 wt.%Pt-1 wt.%Sn/TiO_2 catalysts. It seems that the addition of Pb and Sn improve the catalyst performance, and suppress the poisoning, due to product formation, observed with Pt alone. The interaction between the metal and supports plays an important role in the properties of the catalyst. Generally, this electronic interaction has a positive effect towards the enhancement of catalytic

properties and stability. Based on this observation it has been decided to prepare Pt using a carbon support. Changing the support is likely to have an effect, such that with Pt/C the oxygen may assist with the removal or oxidation of inhibiting species. It was also found that the Pt leaching reduced from 3.1 % to 1.5 % under operating conditions (100 °C, 2 bar O_2 for 2 h) when changing supports. In order to determine the effect of the support and promoter on the structural and electronic properties of the Pt catalysts characterisation including ICP, XRD, BET, TGA, XPS, SEM and TEM were performed.

GLOSSARY

Å	Angstrom (10^{-10} meters)
BET	Brauner, Emmet and Teller
Cm	Centimetre
cm^{-1}	Reciprocal Centimetre
°C	Degrees Celsius
eV	Electron Volts
FID	Flame ionisation detector
FTIR	Fourier transform infrared spectroscopy
g	Gram
GC	Gas Chromatography
h	Hours
ICP-MS	Inductively Coupled Plasma Mass Spectroscopy
M	Molar
mg	Milligram (10^{-3} g)
mol	Moles
min	Minutes
nm	Nanometre (10^{-9} m)
SMSI	Strong metal support interaction
SEM	Scanning electron microscopy
TGA	Thermogravimetric analysis
wt. %	Weight percent
XPS	X-ray photoelectron spectroscopy
XRD	X-ray diffraction
μL^{-1}	Micromoles (10^{-6} L)
Conv.	Conversion
Sel.	Selectivity
n-BuOH	*n*-Butanol
BuALD	Butyraldehyde
BuAC	Butyric Acid

Table of Contents

Chapter 1: Introduction

1.1. Green chemistry

Green chemistry, also known as sustainable chemistry, is the design, manufacture and application of chemical products that reduce or eliminate the generation of substances that are hazardous to human health and the environment. It is a science-based, non-regulatory, economically driven approach toward sustainable development that has grown substantially since the concept fully emerged in the 1990's.[1] Today the following 12 Principles of Green Chemistry are used; they were developed by Paul Anastas and John Warner [2] and are used as guidelines and criteria by chemical scientists:

1. Waste prevention not remediation.
2. Maximize incorporation of all materials into the final product (atom economy).
3. Less hazardous chemical synthesis.
4. Benign solvents and auxiliaries.
5. Improve energy efficiency.
6. Use of renewable raw material.
7. Reduce derivatives.
8. Use catalytic reagents.
9. Design degradable products
10. Design methods for the prevention of pollution
11. Design safe chemical process.
12. Designing safer chemicals.

By using a selective heterogeneous catalyst, many of these criteria can be met by minimizing the uses of toxic solvents in the chemical processes and analyses, as well as avoiding generation of residues resulting from these processes.[3]

1.2. Biofuels and biobutanol

Liquid biofuels such as biobutanol have the potential to reduce the need for petroleum fuels, and also can reduce greenhouse gas emissions when compared with petroleum-based fuels (**Scheme 1.1**).[4-6] The start of the biofuel movement came with the first generation of alternative fuel sources, directly from edible agricultural food sources. First generation liquid biofuel can come from a number of edible resources including: starches, sugars, animal fats, and vegetable oils.

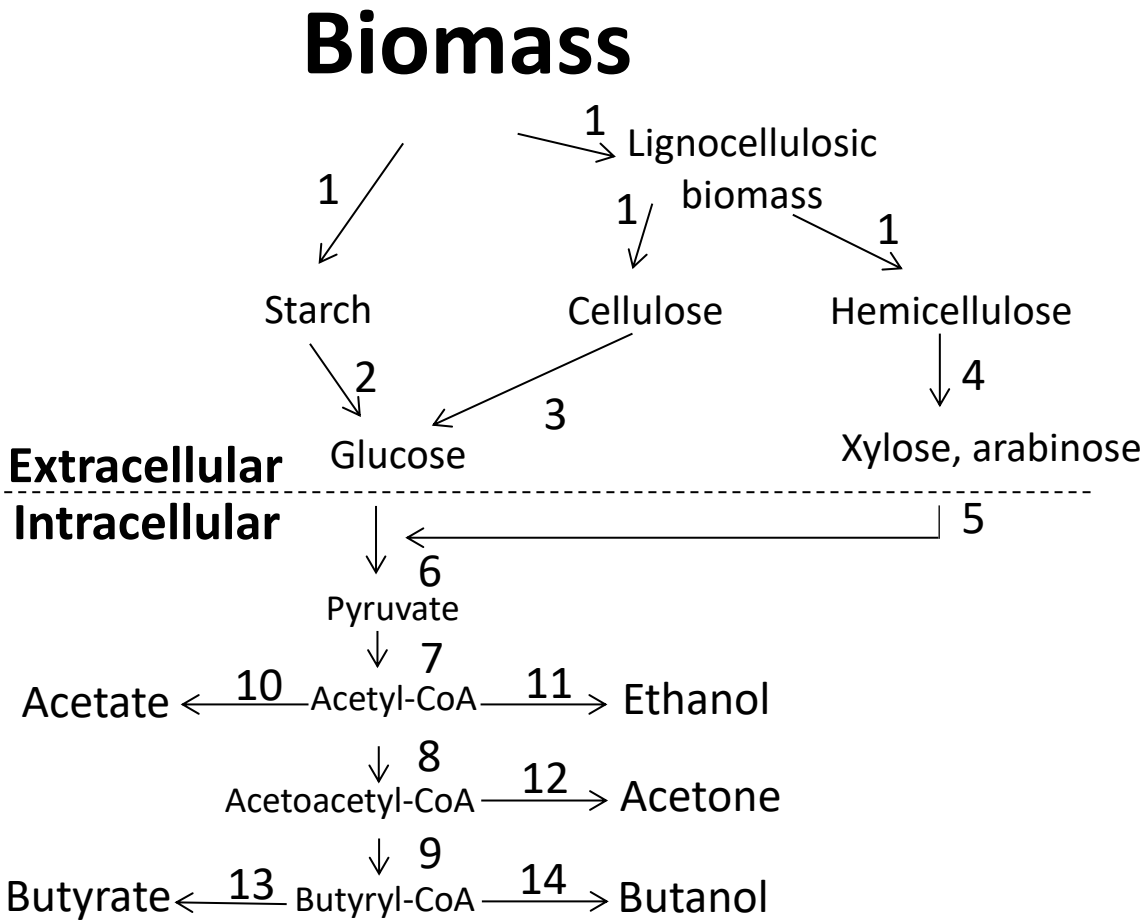

Scheme 1.1. Bioproduction of butanol from biomass.[6]

The most commonly used feed stock sources for first generation biofuel are sugar cane, wheat, and corn stock. Sugar beets, rapeseed and peanuts were also once considered a plausible source for first-generation biofuels. Ethanol is derived from these feedstocks and has the ability to supply sufficient power, but because of the negative impact it holds on the food supply available and the agricultural economy it is a less appealing option as a long term solution to fossil fuels. What separates the second generation biofuels from the first generation biofuels is the fact that second-generation biofuels are not made from food crops or edible biomass crops.[7] For example, *n*-butanol (*n*-BtOH) can be considered a 2nd generation bio-fuel if produced from inedible plants or plant parts.[8] This biobutanol could become a key building block in future biorefineries. Biobutanol has several advantages over other biofuels, such as better infrastructure compatibility, higher energy, lower water adsorption, better blending ability and could also be a potential substitute for gasoline in automobile fuel.[9-11] Also, bio-butanol is non-poisonous, non-corrosive, and biodegradable and does not lead to soil and water pollution.[9, 12]

1.3. Bio-butanol for chemicals production

The selective oxidation of butanol into butyraldehydes is of great importance at both laboratory and industrial levels. Butyraldehyde is an intermediate for the chemical industry; for example, it is used for the manufacture of extractant in the production of drugs and natural substances such as antibiotics, hormones, vitamins, alkaloids and camphor, solvent for dyes, e.g. in printing inks, additive in polishes and cleaners, e.g. floor cleaners and stain removers, solubilizer in the textile industry, e.g. additive in spinning baths or carrier for coloring plastics, acetals to be used as fuel additive (i.e 1,1-diethoxbutane). The selective synthesis of aldehyde from aqueous alcohol is challenging because the aldehyde can go through oxidation into acid in the presence of water.[13] Several studies have previously shown that supported metal (Au/Pd/Pt) nanoparticles can be effective catalysts for the oxidation of alcohols to aldehydes.[14-16] The reported route to synthesise butyraldehyde is greener compared with hydroformylation of propylene, through the selective oxidation of biobutanol,[17] which can be obtained by the acetone-butanol-ethanol (ABE) fermentation of biomass (**Scheme 1.2**).[18, 19]

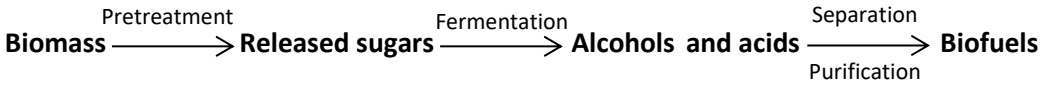

Scheme 1.2. Flow diagram of biofuel production from biomass.[19]

There is also significant interest in the conversion of *n*-butanol to butyric acid, as this process gives access to valuable products such as butyrate esters (which are used as non-toxic solvents for a variety of industrial applications) [20] and butyrate cellulose esters. Cellulose acetate butyrate polymer is used widely in coatings, sheeting and film products and is tougher, has a lower moisture absorption and better compatibility with plasticisers than cellulose acetate.[21]

1.4. Heterogeneous catalysis for green chemistry

Heterogeneous catalysis has played a leading role in boosting the worldwide economy. Heterogeneous catalysts can help to achieve reduction of the formation of unwanted side products and a decrease in energy consumption during reactions. Catalysts do this by offering lower energy pathways to the desired products. It is not only the economy that has been supported; without effective catalysis the manufacture of many materials, pharmaceuticals and foodstuffs would not be possible. Therefore, it is not surprising that this field has gained a lot of interest across the scientific world.

1.5. Catalytic oxidation

The selective oxidation in the liquid phase of alcohols provides access to fine chemical and pharmaceutical intermediates. Unfortunately, stoichiometric quantities of inorganic oxidants (hypochlorites, high-valent metal oxidation agents such as chromates and active manganese dioxide, mineral acids) are often used in halogenated organic solvents. This produces relatively large amounts of hazardous or toxic wastes, and therefore the oxidation process suffers from low atom efficiency and high waste production.[22-24] It is well known that primary alcohols can be oxidised to either aldehydes or carboxylic acids depending on reaction conditions.[25] In the case of the formation of carboxylic acids, the alcohol is first oxidised to an aldehyde, which is then oxidised further to the acid. In traditional methods a homogeneous oxidising agent such as potassium dichromate is used to dehydrogenate the sample as shown in **Scheme 1.3**.

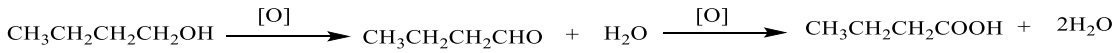

Scheme 1.3. Oxidation of *n*-butanol, in this case the oxidant is dichromate.

When simplified this scheme is effective, but there are two limitations which this possess. It was shown in 1962 that this is acid catalysed, which leads to the formation of an array of side products.[26] These products are formed due to carbon-carbon bond fission, and it was shown that this takes place via the enol form of the aldehyde in the first stage of the oxidation. This is also homogeneously catalysed so the catalyst is not easily recovered. This breaks many of the 12 principles of green chemistry.

Chromium oxidants can cause problems during work-up of the products and disposal of the toxic residues. Catalytic alternatives to these well-tried methods are therefore attractive, but must demonstrate clear advantages over these systems, be reliable and easy to use, and be applicable to a wide range of substrates. One of the more successful attempts was made using tetra-*n*-butylammonium per-ruthenate (TBAP reagent) and tetra-n-propylammonium per-ruthenate (TPAP reagent).[27] Griffith *et al*, showed a percentage yield of 94 % in the oxidation of *n*-butanol to butyraldehyde over 0.8 h at room temperature, but again this presents problems, mainly in the area of green chemistry. The reaction requires a CH_2Cl_2 medium, which is not consistent with the aqueous medium in which biobutanol is received.[27] A reaction with an aqueous medium is therefore required.

Alcohol oxidation by enzymes is an environmentally friendlier alternative; however, product separation and waste production remain a problem. Homogeneous catalysis is

another efficient alternative; however, catalyst recovery, reactant recycling, and reactor corrosion limit its utilisation on an industrial scale.[28]

Heterogeneous catalysis represents a greener alternative. Therefore, heterogeneous catalysts for the oxidation of alcohols to carbonyl compounds are attracting interest from industry and academics alike.[25, 29, 30] A recent review by Mallat *et* al.[31] gives an extensive survey of "green" methods for heterogeneously catalysed alcohol oxidation. Noble metal-catalysed alcohol oxidation with cheap oxidants, such as air or molecular oxygen, is inexpensive and non-toxic.[31-33] It is a clean and elegant alternative with variable reaction conditions, with which high selectivities can be obtained.[34, 35]

As stated before, heterogeneous supported metal nanoparticles can selectively oxidise primary alcohols.[36] F. Wang *et al*, showed that a high conversion and high yield from oxidation of *n*-butanol to butraldehyde can be achieved with a 'Au/M390' catalyst. The number after the M indicates the reduction temperature, in this case 390 °C.[37] The M stands for MoO_x. This catalyst shows similar behaviour across a wide range of alcohol reactants, as shown in **Table 1.1**.[37]

Table 1.1. Aerobic oxidation of various alcohols[a].

Entry	Catalyst[b]	Substrate	t (h)	Conv. (%)[c]	Yield(%)[d]
1	Au/M390	benzyl alcohol	14	>99	94
2	Au/M390	p-chlorobenzylalcohol	16	>99	90
3	Au/M390	cyclohexanol	10	>99	93
4	Au/M390	2-phenylethanol	8	>99	94
5	Au/M390	*n*-butanol	20	>99	88
6	Au/M390	2-butanol	12	>99	92
7	Au/M390	1-hexanol	18	>99	87
8	Au/M390	2-hexanol	18	>99	85
9	Au/M390	1-octanol	15	>99	89
10	Au/M390	2-octanol	15	>99	90
11	Au/M390[e]	Benzyl alcohol	14	11	-

[a] Typical reaction conditions: 5 mmol alcohol, 15 mmol K_2CO_3, 100 mg catalyst, 5 mL acetonitrile, 50 °C. Experiments were conducted in a quartz reactor. Pure oxygen gas (1 atm) was supplied by a balloon. Samples were withdrawn at intervals to track the reaction by TLC. [b] M390 indicates the catalyst support was reduced in 5 % H_2 balanced with Ar at 390 °C. The loading amount of Au was 1.1 wt % in all catalysts as analysed by ICP-mass spectometry. [c] The conversion was determined by gas chromatography. [d] Products were isolated on silica gel using hexane/ethyl acetate (2.5:1) as effluent solution.

As shown in **Table 1.1** this catalyst is very active and selective for the oxidation of alcohols. For the Au/M390 catalyst to be active, the reaction must be completed under basic conditions. The reaction did not occur in the absence of base (Table 1, entry 11). However, basic conditions can lead to a reactor corrosion passing additional costs on to the end user, in addition the presence of butyric acid can reduce reactor lifetime.[38]

1.6. Oxidation of *n*-butanol

1.6.1. Mechanism of oxidation of alcohols

The partial oxidation of alcohols involves the loss of hydrogen to form the corresponding carbonyl compound. Secondary alcohols form ketones, while primary alcohols form aldehydes before becoming carboxylic acids with further oxidation. A loss of a carbon dioxide molecule will occur under more forcing oxidation conditions. In order to determine the mechanism of alcohol oxidation and the Rate Determining Step (RDS), researchers have tried to oxidise isotopically labelled alcohols.[39]

Scheme 1.4. Proposed mechanism for the oxidation of an alcohol.[40]

The dissociation mechanism happens when the alcohol adsorbs on the metal by forming an alkoxide (the conjugate base of an alcohol), and hydrogen, occupies two adjacent active sites (**Scheme 1.4**). It is also proposed that the alcohol can be adsorbed associatively as a whole molecule on the catalyst surface and then will undergo dehydrogenation.[41] The adsorbed alcohol or alkoxide then may react with a free active site * in an acidic medium, an adsorbed oxygen O*, if there is a high oxygen surface coverage, and/or an adsorbed hydroxyl OH* in an alkaline medium to abstract the H – α from the reactant. [34]It was originally suggested that the alcohol would undergo the following route within a basic medium (Equation 1.1 – 1.3):[42]

I) $R-CH_2OH_{ads} + OH^- \leftrightarrow R-CH_2O^-_{ads} + H_2O$ Equation 1.1

II) $R-CH_2O^-_{ads} + * \rightarrow R-CHO_{ads} + H^-_{ads}$ Equation 1.2

III) $H^-_{ads} + O_{ads} \rightarrow OH^-_{ads} + *$ Equation 1.3

This was later rejected since deprotonation of a weak acid in alkaline medium is unlikely. [34, 43] The pathway shown in Equation 1.4 – 1.7 was suggested:

I) $R-CH_2OH_{ads} + * \leftrightarrow R-CH_2O_{ads} + H_{ads}$ Equation 1.4

II) $R-CH_2O_{ads} + * \rightarrow R-CHO_{ads} + H_{ads}$ Equation 1.5

III) $\frac{1}{2}O_2 + * \rightarrow O_{ads}$ Equation 1.6

IV) $2H_{ads} + O_{ads} \rightarrow H_2O + 3*$ Equation 1.7

In this pathway the first reaction is fast and the second one is the Rate Determining Step (RDS). An adsorbed oxygen (O_{ads}) or adsorbed hydroxyl (OH_{ads}) can replace the active site * depending on the oxygen coverage and pH. In electrochemical studies, Kluytmans *et al*.[29] proposed that the catalyst acts as a short-circuited cell where the alcohol dehydrogenates on the surface which causes the desorption of H^+ and OH^- from (H_{ads}) and (OH_{ads}) (Equation 1.8 – 1.12).

(I) $\frac{1}{2}O_2 + * \rightarrow O_{ads}$ Equation 1.8

(II) $R-CH_2OH_{ads} + O* \leftrightarrow R-CH_2O_{ads} + OH_{ads}$ Equation 1.9

(III) $R \text{——} CH_2O_{ads} \rightarrow R \text{——} CHO_{ads} + H^+ + e^-$ Equation 1.10

(IV) $e^- + OH_{ads} \rightarrow OH^- + *$ Equation 1.11

(V) $H^+ + OH^- \rightarrow H_2O$ Equation 1.12

Therefore, the ketone formation (III) and the hydroxyl reduction (IV) may happen at different sites on the catalyst, while electrons are transported by conduction and the proton by diffusion (V) guided by Fick's first law. It becomes apparent that there is no agreement on the mechanism of the alcohol oxidation.[44] Gallezot notes that the oxidation could be affected by the solution pH, the state of metal oxidation, the nature of adsorbed species, and the oxygen coverage.[45]

Since C-C bonds are difficult to break under mild reaction conditions, the oxidation of secondary alcohols yield ketones, and the carbon chain is preserved.[34] However, primary alcohols are oxidised to aldehydes, and can further undergo catalysis to yield carboxylic acids. A high pH or an aqueous media increases the carboxylic acid yield considerably, unless the hydroxyl function is adjacent to a C=C bond or an aromatic ring that stabilize the carbonyl group.[25] It's worth noting that the comparison of catalyst activity with respect to product selectivity should be made at equal levels of conversion of the substrate. The transition metal catalysts are desirable materials for rapid alcohol oxidation due to their tunability towards product selectivity.[17] It becomes apparent that the selectivity of oxidation is greatly affected by the nature and promotion of the catalyst, the reaction conditions, and by the solvent. The different aspects from these approaches are disclosed in the following section.

1.6.2. Heterogeneous catalysts for *n*-butanol oxidation

The heterogeneous oxidation of alcohols with noble metals has been exponentially improved since it was first studied 150 years ago.[34, 46] However, before the industry can apply heterogeneous catalysts on a large scale for the production of carbonyl compounds and invest in new processes, it is crucial to investigate and optimise the catalytic oxidation of alcohols.

Unlike stoichiometric oxidants that produce chemical wastes, heterogeneous catalysis can effectively use stoichiometric oxidants such as H_2O_2 or TBHP (Tert-butyl hydroperoxide) to produce only water as side-products, and can be operated under range of temperature and pressure conditions. From a cost-efficiency point of view, supported catalysts have an advantage over homogeneous catalysts by being easily recoverable and they can be used in continuous flow regimes.[28]

It has been previously shown that Au–Pd/TiO_2 nanoparticles prepared by sol-immobilisation method displayed the narrowest particle size distribution (average size 2.2 nm) and the best performance in *n*-butanol oxidation (92 % butyric acid selectivity at 90 % *n*-butanol conversion).[47] Under operating conditions it was reported that the catalyst showed no metal leaching and maintained its activity during reaction cycles. Many studies reported that Au-Pd/TiO_2 prepared by sol-immoblisation method showed a high activity in the oxidation of other alcohols.[48-50] Selective oxidation of alcohols into butyraldehyde is important for the synthesis of fine chemicals and their intermediates. The production of butyraldehyde from *n*-butanol is challenging, as butyraldehyde oxidises to butyric acid at 100 °C in the absence of a catalyst.[47] To overcome the rapid conversion of aldehyde to acid,[51] a catalyst that is active for the oxidation of *n*-butanol to butyraldehyde, but does not catalyse its transformation into butyric acid has to be developed. Additionally, the catalyst has to be stable under the operating conditions.

Gandarias *et al*. have more recently shown that this can be achieved by using TiO_2 as a support.[47] Molecular oxygen was used as the oxidant. They used bimetallic Au-Pd nanoparticles supported on titania (P25) as the catalyst, which was synthesized using the sol-immobilization technique. Polyvinyl alcohol (PVA) was the most effective stabilizing agent as it gave the catalyst with the smallest average particle size. The catalyst was not only active and selective towards butyric acid, but was also stable under operating conditions. This work is used as the basis for this project. Table 1.2 contains oxidation data from the literature for a comparison.

Table 1.*2*. A list of catalyst (with reaction conditions) shown to be active for the oxidation of *n*-butanol.

Entry	Catalyst	Conv. (%)	Sel. (%)		Reaction conditions	Ref.
			BuALD	BuA		
1	Au/M390[a]	>99	88	-	5 mmol *n*-butanol, 15 mmol K_2CO_3, 100 mg catalyst, 5 mL acetonitrile, 50 °C, 1 bar O_2, 20 h	[37]
2	Au-Pd/TiO_2	89.7	0.3	92.5	5 mmol *n*-butanol, 8 mL H_2O, 0.15 g catalyst, 3 bar O_2, 100 °C, 6 h	[47]
3	Mo-V-O	33	>99	<1	0.7 mmol *n*-butanol, toluene 1.6 mL, catalyst 0.03 g, 80 °C, 24 h, 1 L oxygen cylinder (1 atm)	[37]

Conversion (Conv.), Selectivity (Sel.), Butyraldehyde (BuALD), Butyric Acid (BuAC), Reference (Ref.)

Cai *et* al,[52] have reported the doping effect of Ru, Rh, Ir and Pd on Co/ZnO catalysts for the conversion of bio-butanol into various derivatives and observed an increase in activity and a decreased deactivation.

1.6.3. Pt catalysed *n*-butanol oxidation

The discovery that platinum can be used as a catalyst to oxidise alcohols with molecular oxygen was discovered one and a half centuries ago.[34] Platinum has a high affinity to

adsorb hydrogen which allows it to dehydrogenate alcohols to yield the corresponding carbonyl compound. Gallezot noted that the activity and selectivity of platinum catalysts are strongly affected by the nature of the support, the particle size, the reaction medium and the substrate, which underlines the importance of investigating the effects of these conditions.[45] The main challenge is to maintain the selectivity towards the carbonyl intermediate without producing by-products or deactivating the catalyst. A novel way of achieving this goal is with the help of promoters.[52] Many investigations have been done on the use of Pt or Pd/C catalysts for the oxidation of water-soluble carbohydrates with molecular oxygen.[45, 53]

In 2012 T. Lu *et al*, reported that base- free selective oxidation of *n*-butanol to butyric acid is possible in the liquid phase.[54] The Pt supported catalysts were prepared using the deposition-precipitation method. It was found that the reduction temperature of the catalysts had a great effect on the catalytic activity of Pt/Bi_2O_3. For example, when the reduction temperature was between 150 and 250 °C a higher conversion of *n*-butanol was observed ~60 to 68 %, respectively. At a higher reduction temperature (300 °C) the catalyst deactivated under the same reaction conditions (2.5 mmol substrate, 0.20 g catalyst, 2mL H_2O, 90 °C, 0.1 MPa O_2, 5 h).[54] Low activity of the uncalcined catalyst could be ascribed to the presence of platinum oxides.

Table 1.3. A list of catalyst (with reaction conditions) shown to be active for the oxidation of *n*-butanol.

Entry	Catalyst	Conv. (%)	Sel. (%)		Reaction conditions	Ref.
			BuALD	BuA		
1	Pt/BiO_3	99	1	99	2.5 mmol *n*- butanol, 0.20 g catalyst, 2 mL H_2O, 90 °C, 0.1 MPa O_2, 5 h	[54]
2	Pt/TiO_2	31.4	78.8	21.2	540 mmol *n*- butanol in H_2O, 0.072 g catalyst, 100 °C, 0.3 MPa O_2, 6 h.	[55]
3	Pt/C	77.6	37.9	61.7	540 mmol *n*- butanol in H_2O, 0.072 g catalyst, 100 °C, 0.3 MPa O_2, 6 h.	[55]

Conversion (Conv.), Selectivity (Sel.), Butyraldehyde (BuALD), Butyric Acid (BuAC), Reference (Ref.)

Recent studies show that supported Pt was active and selective towards butyraldehyde in the oxidation of *n*-butanol by O_2 in an aqueous phase.[55] By changing the catalyst support and preparation method, they were able to synthesize stable Pt metal nanoparticles. Gandarias *et al*. find that 1 wt. % Pt/TiO_2 gives the highest selectivity toward butyraldehyde (78.8 %) with a total *n*-butanol conversion of 31.4 %, however, Pt was observed to leach (31.4 %), even in the presence of small concentration of butyric acid.[55] XPS and TEM suggests that the observed Pt leaching is related to both

the metal-support interaction and the size of the metal nano-particles. Using carbon (Cabot Vulcan XC-72R) as the support and CVI (Chemical vapour impregnation) as the preparation method an active and selective catalyst (Pt/C $^{CVI\text{-}RED400}$) was synthesised. By changing the catalyst support and preparation method, the Pt leaching reduced to < 1 % under operating conditions used (100 °C, 3 bar of O_2). The study of product evolution with reaction time revealed that butyraldehyde selectivity decreased with increasing *n*-butanol conversion. This was ascribed to *n*-butanol acting as a radical inhibitor in the uncatalysed oxidation of butyraldehyde to butyric acid.

1.6.3.1. Deactivation of platinum catalysts during primary alcohol oxidation

It is worth noting that platinum metal based catalysts could undergo irreversible deactivation; this is a major reason that delays the application of PGM catalyst in the fine chemical industry.[56] It becomes important to identify the causes of such deactivation and investigate any possible solutions. Mallat and Baiker [34], Gallezot [45](1997) and Vleeming *et al*.,[57] have shown that the following major factors can cause catalyst deactivation:

1. Deposition of species such as carbon (fouling/coking).
2. Metal leaching
3. Strongly adsorbed oxygen (oxidation) on the catalyst surface.
4. Substrate adsorption poisoning on the active sites (chemisorption).

Metal leaching is defined as the loss of active metal during the catalysis in the solution. After leaching occurs, a metal ion may be re-deposited on another metal particle causing, an increase in particle size through agglomeration which decreases the efficiency. Catalyst can be also deactivated by thermal sintering.

1.6.3.2. Proposed mechanism of Pt-catalyst deactivation

1.6.3.2.1. Deactivation through oxidation of Pt (0)

The solubility of oxygen increases with increasing pressure according to Henry's law. While the presence of oxygen is essential to remove adsorbed hydrogen and other by-products for the regeneration of free sites, a high oxygen coverage will decrease the reaction rate.[58] Working at low oxygen partial pressure prevents the catalyst from being oxidised, although the adsorbed hydrogen formed from alcohol dehydrogenation may react then with another substrate to generate unwanted by-products instead of being oxidised to form water.[59] Keresszegi *et al*.[44] found that the oxidation of primary alcohols such as 1-octanol and benzyl alcohol can yield CO by decarbonylation, which deactivates the catalyst. The reaction rate can then be dramatically enhanced by the

introduction of oxygen which removes adsorbed carbon monoxide. Working at high oxygen partial pressure tends to deactivate the catalyst by oxidizing the metal and occupying the active sites.[60] A catalyst is oxidised or covered with oxygen when the catalyst potential is higher than 0.8V vs the Reversible Hydrogen Electrode (RHE). The catalyst is reduced or covered with hydrogen/CO when the potential is lower than 0.4V vs. RHE.[56] (The optimum catalyst potential then lies between 0.4 and 0.8V vs. RHE as illustrated in **Figure 1.4**). Extensive modelling work on oxidation can be found in the following references.[61-63]

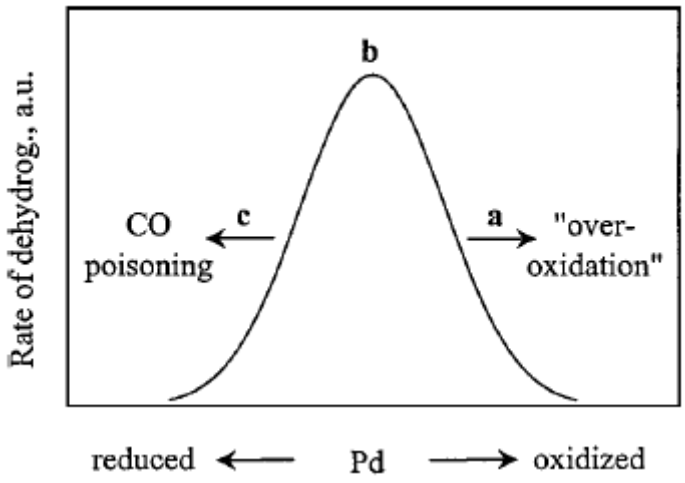

Figure 1.4. Illustration on the catalyst state. [58]

Kluytmans *et al*.[29] and Markusse *et al.*[56] note that stopping the oxygen flow during the oxidation reaction allows the alcohol to reduce the oxidised Pt catalyst, therefore reactivating it. The addition of promoters can be another way of overcoming poisoning by surface oxidation. The addition of non-noble metals such as bismuth controls the oxygen supply to the noble metal and prevents the formation of adsorbed hydrogen and carbon monoxide.[64] Hence, an optimum oxygen concentration exists that is high enough to oxidise adsorbed hydrogen and by-products without oxidising the catalyst. Many researchers have recommended working in the oxygen mass transfer limited regime to prevent any oxidation, since working in a kinetic regime results in rapid catalyst deactivation.[59, 61, 65, 66] The selectivity towards the partially oxidised intermediate of the reaction is also dependant on the oxygen concentration. While ketones and carboxylic acids are resistant to further oxidation under mild conditions, aldehydes can easily be further oxidised to carboxylic acids in oxygen rich systems, when reacting in an aqueous or alkaline medium.[34]

1.6.3.2.2. Product-mediated catalyst poisoning

Poisoning is the strong adsorption of substrate or impurities on catalytic active site (chemisorption). A good example is the presence of H_2S in feeds for the steam reforming of CO on nickel based catalysts. The formation of Ni_3S_2 is irreversible and thus eventually renders the catalyst inert.[67] In the case of alcohol oxidation, a strongly adsorbed substrate is referred to as chemical poisoning and can occur due to alcohol, carbonyl species or other by-products bonding to the active metal. The adsorbed molecule may dissociate and bond chemically to the metal surface. Hence, poisoning is highly dependent on the identity of the substrate. Carboxylic acids,[29] ketones,[57, 68] and even alcohols[34] may deactivate the catalyst by strong adsorption. Similarly to the rate of adsorption, the rate of desorption is expected to follow an Arrhenius-like form, $k_d = Ae^{-Ea/RT}$, where typical energies for desorption are 100 kJ/mol.[69] It is crucial to have the rate of product desorption faster than the rate of reactant adsorption in order to regenerate active sites. While substrate can physisorb and/or chemisorb, it is only the latter that inhibits the active sites due to the strong bonding with the metal.

Poisonous substrates can be classified into two types: non-oxygenated hydrocarbons and molecules containing the CO group. Carbon monoxide or carbonyl compounds can be re-oxidised to form carbon dioxide at a high catalyst electro-potential while hydrocarbons can be hydrogenated to break the RC-M (carbon-metal bond) and form RC-H in order to prevent deactivation. Primary alcohols exhibit more CO poisoning than secondary alcohols, and as the carbon chain length increases, the carbonyl poisoning decreases.[70, 71] For example, the oxidation of methanol or propanol deactivates the catalyst with a decrease in the potential of the latter up to 0.5 V vs. RHE [72] which means the catalyst has a high coverage of CO. The oxidation of benzyl alcohol decreases the potential down to 0.3V vs. RHE [71] since non-oxygenated rings such as benzene adsorb strongly on the catalyst, lowering the potential. Oxidation of glucose with platinum shows the best example for chemical poisoning.[73, 74] The intermediates gluconic acid, gluconate and smaller fragments bind strongly on the Pt surface which deactivates the catalyst as can be illustrated in **Figure 1.5**.[75]

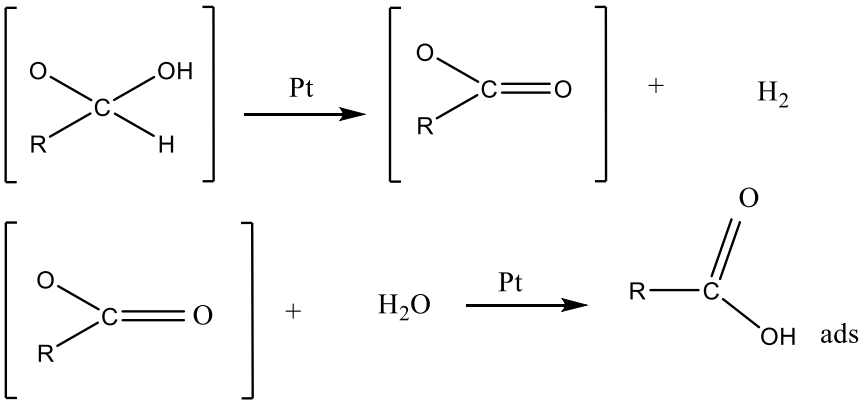

Figure 1.5. Gluconic acid poisoning on platinum.[74]

Poisonous substrates can also be created by possible side reactions which lead to decreases in selectivity towards the intermediate carbonyl. Oxidation of an aldehyde molecule creates carboxylic acids, which strongly adsorb on the surface.[68] Other reported side reactions are polymerization and aldol condensation in strongly basic or acidic solutions can occur.[76] Selectivity is also affected if the adsorbed hydrogen is not removed from the metal surface since hydrogenation may occur, thus forming different by-products.[59] In an anaerobic basic medium, fructose was oxidised into gluconate with platinum, and the adsorbed hydrogen hydrogenated the fructose into mannitol and sorbitol.[45]

1.6.3.2.3. Deactivation through product-mediated Pt-leaching

The presence of certain species, specifically anions and carbohydrates, can enhance the loss of the active metal into the solution.[57] Schuurman *et al*.[41] notes that the loss of activity for the oxidation of alpha-D-glucopyranoside is due to re-deposition of platinum ions, which is known as the Ostwald effect. The Ostwald ripening involves small crystallites which tend to increase in size to bring the surface to volume condition to a favourable low free energy state.[77] Whilst poisoning and oxidation are reversible processes, leaching and agglomeration are irreversible and may render the catalyst completely inactive.[34]

To better understand Pt-catalyst performance Gandarias *et al*., prepared catalysts using sol-immoblisation and a CVI method with different supports. There XPS results suggest that using C-based catalysts show lower Pt leaching as compared to TiO_2 based catalysts. This can be ascribed to well-known high resistance of carbon supports to acidic and chelating media.[30, 55] In the summary of their TEM data, the degree to which Pt is leached from the catalysts is related to both the metal support interaction

and metal particle size. The metal support interaction is affected by the type of support and by catalyst preparation method.

1.6.3.2.4. Deactivation through thermal sintering

It has been found that there are different causes for the loss of metal particle surface area in solution, the sintering of active metal or the sintering of the support. The common deactivation cause is thermal sintering where a high temperature causes the support to collapse.[78] Therefore, thermal deactivation is not a common phenomenon in liquid phase oxidation due to the lower temperature used.

Recent study shows TEM characterisation of the Pt/C $^{CVI\text{-}RED400}$ (the catalyst prepared by chemical vapour impregnation and reduced at 400 °C for 3 h) identified the particle size of fresh and used catalyst as shown in **Figure 1.6**.[55]

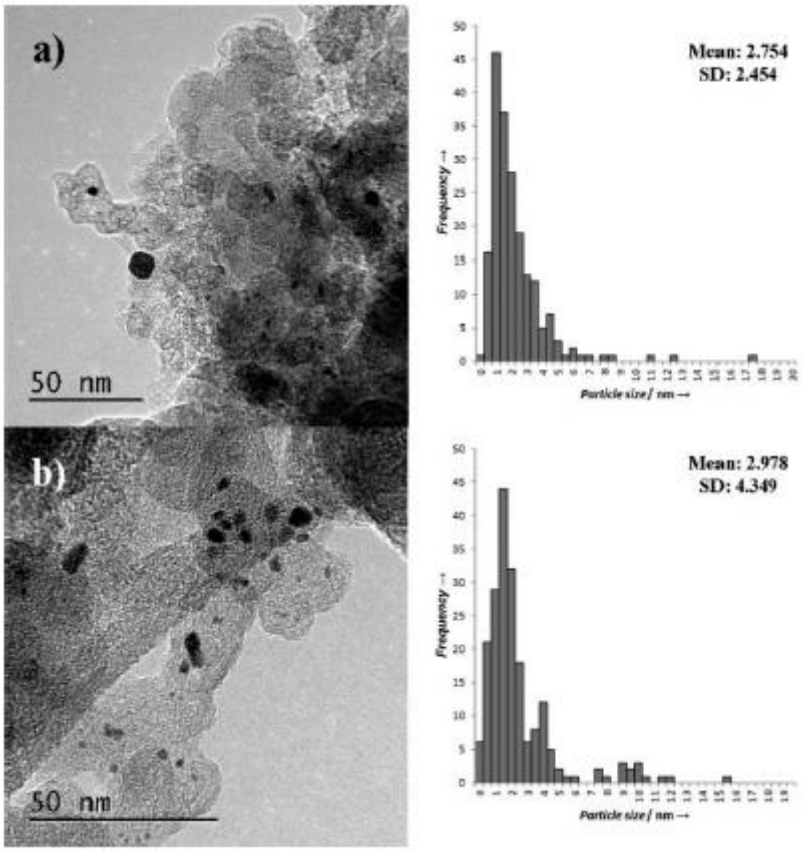

Figure 1.6. TEM images and associated PSDs of Pt/C$^{CVI\text{-}RED400}$ a) fresh and b) used.

The used Pt/C$^{CVI\text{-}RED400}$ catalyst showed a slight increase in average particle size compared to the fresh catalyst (Fig. 1.6 b), although this may be skewed by the larger

particles that were present in the analysed region. The bi-modal nature of the particle size distribution makes it difficult to objectively analyse the average particle size. It is interesting to note that this is the catalyst which displayed the lowest degree of Pt leaching and that the PSD (particle size distribution) in the range of 1–7 nm, which is comparable for both the fresh and used catalysts.

1.6.3.3. Approaches towards preventing catalyst deactivation

1.6.3.3.1. Addition of promoters

It has been reported in the literature that adding promoters was a major step forward for the heterogeneous oxidation of alcohols, since it dramatically affected the performance of the catalyst and its life-time.[64] Although adding "non-noble" metals such as bismuth, lead and tin to Platinum Group Metals (PGM) affects the activity and increases the selectivity of the reaction, the role of the promoter was not entirely understood. Mallat *et al*.,[79] found that there are three major possible effects of the bismuth promoter:

1. A geometric effect; bismuth adatoms act as site blockers which change the orientation of the adsorbing alcohol. This phenomenon was witnessed for the oxidation of glycerol.[80] Furthermore, adatoms prevent the presence of a large active metal surface, responsible for the "ensemble effect", which causes C-C bond cleavage that decreases selectivity.[81, 82]

2. As a non-noble metal, bismuth is much more likely to adsorb oxygen than the PGM.[79, 83] Accordingly it creates a new active centre on the catalyst that contributes to the oxidation of alcohol by supplying the required oxidising species for the reaction. Gallezot,[45] suggested the following mechanism for the oxidation of glucose (**Figure 1.7**):

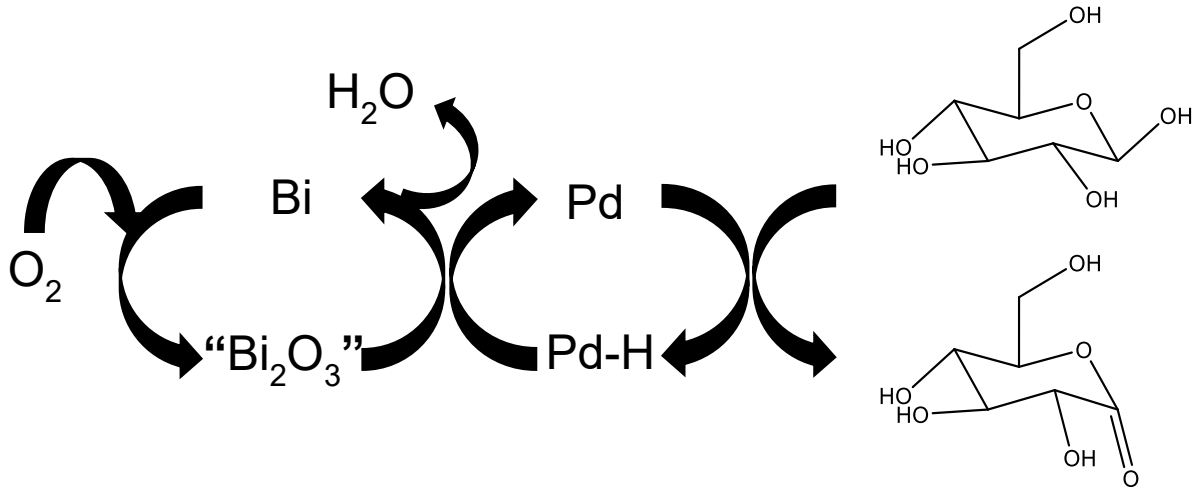

Figure 1.7. Scheme for the mechanism of glucose oxidation on Pd-Bi catalysts proposed by Gallezot.

3. Bismuth metal increases the selectivity and activity by preventing the adsorption of hydrogen by-product (and other substrates) via occupying active sites on PGM, which will prevent the hydrogen from reacting to yield unwanted by products. [70, 82, 83]

Keresszegi *et al*. studied the effect of adding bismuth to platinum for the oxidation of phenylethanol[65]. The presence of bismuth increases the conversion from 30 % to 80 %. The selectivity towards acetophenone was also increased from 70 % to 95 %. Also, Keresszegi *et al.* [65] used a simple technique to evaluate the role of bismuth on activity by comparing the alcohol dehydrogenation with argon and air for promoted and unpromoted catalysts. It was found that the bismuth led to an increased selectivity in the presence of air, but had no effect in argon. Accordingly, it was deduced that bismuth increases the oxygen transfer to remove the by-products and hence creates available active sites. Bismuth is therefore also used to protect the PGM catalyst from "oxidation" which happens when the alcohol is unable to reduce the oxygen coverage on the metal surface resulting in the deactivation of the catalyst.[45] However, Wenkin *et al.*[82] have proposed that the bismuth may have a homogenous role by leaching and forming complexes with the substrate that facilitates the dehydrogenation step. This was shown by adding a solution of bismuth during the oxidation of glucose. On the other hand, Keresszegi *et al.*[66] showed that bismuth is in the metallic form by in situ XAS studies that proved the presence of bismuth during the oxidation of phenylethanol.

1.6.3.3.2. N_2 purge cycles

The process of deactivation of metal catalysts by impurities has been studied widely by Mallat *et al.*,[34, 83-87] The deactivation of the reaction, due to by-products or reaction products, was named “chemical deactivation” or “self-poisoning”. Side products consisting of polymeric carbonyl species were detected by chromatographic and spectroscopic methods, in the oxidation of 1-methoxy-2-propanol with air and these species were identified as the primary cause of deactivation. Since chemical deactivation favours further deactivation by oxidation, deactivation could be efficiently suppressed by increasing the reaction rate (e.g. by working at higher temperatures) or by changing temporarily the air flow to nitrogen.[35] In most cases the distinction between the two types of surface poisoning was unclear. Irreversible poisoning of adsorbed by-products was also invoked in the case of cinnamyl alcohol oxidation [86] and in 1-phenyl-ethanol oxidation.[88] In the latter case, the poisoning was attributed to the dissociative adsorption of the alcohol leading to irreversibly adsorbed species. The origin of catalyst deactivation of liquid phase oxidation reactions by oxidation of the metal surface has been a subject of great importance. The dynamic balance of competitive adsorption of organic substrate and oxygen controls the initial reaction rate, and the equilibrium tends to shift towards predominant oxygen coverage as the substrate concentration decreases. By flowing nitrogen instead of air the activity was usually regenerated, but less activity was regenerated in successive cycles of reaction with alternating flow of air and nitrogen. Because of the progressive loss of reactivation efficiency, it was proposed that oxygen atoms penetrate more and more deeply into the subsurface, or even into the platinum bulk.[89] Depending upon the starting procedure (with the platinum surface reduced or oxidised to different extents) and reaction conditions (ethanol concentration, partial oxygen pressure), different steady states for the oxidation of ethanol on platinum have been measured.[90] The structure of the oxygen-covered surface was the subject of a number of studies. Recent *in situ* EXAFS experiments on platinum particles during cyclohexanol oxidation showed that the platinum surface in the deactivated state was not entirely oxidised since the Pt–O distances lie between those observed for adsorption of cyclohexanol on metal (2.1Å) and those of platinum oxide (2.06Å).[91] The lowest degree of oxidation was found after a reductive start-up, whereas the oxidative start-up with the lowest reactant concentration resulted in an almost completely oxidised platinum surface.

1.6.3.3.3. pH control

The heterogeneously catalysed oxidation of alcohols over catalysts has been studied in a weakly acidic or alkaline medium (pH 6–11). The pH effect on alcohol oxidation is complex and difficult to study, as the pH can affect the reaction in several direct and

indirect ways .[34] Several studies on the influence of pH have been reported. First, the rate of oxidation increases in an alkaline medium with an increase in pH.[41, 92-94] Second, as pH increases the selectivity towards the aldehyde intermediate decreases.[95, 96] Third, in acidic medium (pH < 6), there is product inhibition, where products adsorb to the catalyst strongly and inhibit the reaction.[97] Finally, in a highly basic medium (pH > 11), the formation of by-products or leaching of the catalyst inhibits the reaction.[84, 98] However, there is no effect of the pH on oxidation rate in the case of alcohols with low acidity (high p*K*a value) and strong reducing ability.[39, 40, 84] Vleeming *et al*. showed that with Pt on graphite catalysts, the rate of initial oxidation decreases with an increase in pH from 8 to 10.[96] In an earlier study with Pt on carbon catalyst, a linear increase of the rate at pH > 8.5 was reported.[41] These differences may be due to the multiple influences of pH, on the interaction of the catalyst support with adsorbed reactant alcohol and/or oxygen species, the concentration of intermediate aldehyde and (side) products, and catalyst deactivation due to oxidation. In the literature some efforts have been made to model the possible effects of pH on alcohol oxidation. Schuurman *et al*. performed initial rate kinetic modelling by considering two reaction paths; involved adsorbed alcohol dominating at low pH and at high pH (involved alcohol anion dominating).[41] In previous work, another approach was shown in electrochemical kinetic modelling through oxygen and oxide reduction, which are proton concentration-dependent steps.[56, 61] However, these models are inadequate for describing the effects of pH associated with catalyst deactivation due to oxidation.

1.6.3.3.4. Solvent selection

The choice of solvent influences certain processes depending on many of its characteristics.[99] Firstly, the gaseous reactant should be soluble enough in the medium in order not to slow the reaction. Secondly, both liquid and gaseous reactants should have a high diffusivity coefficient in the given solvent to be transported to the catalyst particle. Thirdly, solvents have characteristic macroscopic and structural effects.

The dielectric constants and dipole moments strongly influence the charged transition state. Solvents having a high dielectric constant enhance the dissociation of a bond to form charges, while solvents with a low dielectric constant tend to neutralise charged species by forming bonds.[100] However, a solvent interaction with solute and catalyst cannot be predicted based solely on macroscopic properties, since the solvent molecule structure also plays a considerable intermolecular role that has been difficult to investigate. Solvents may be classified into two categories: non-polar and polar. Non-polar solvents have a low dipole moment and dielectric constants, with the opposite being true of polar solvents. Polar solvents can be further divided between protic, which form hydrogen bonds, and aprotic, which do not form hydrogen bonds.

Non-polar solvents such as heptane, toluene, and p-xylene are often used due to their inertness and higher oxygen solubility than alcohols.[34, 65] Another advantage of apolar solvents is their lack of interaction toward catalysts. Different solvents including polar and non-polar have been tested for alcohol oxidation.[101] It was deduced that reactions performed in non-polar solvents, such as toluene, tend to have a higher reaction rate since polar solvents such as acetonitrile would compete with reactants to adsorb on active metallic sites, hence lowering the reaction rate. If the solvent has a low dipole moment and dielectric constant it becomes hydrophobic and could have detrimental effects on conversion. One of the by-products of oxidation with molecular oxygen is water which is produced in equimolar amounts with the carbonyl product. However, water can strongly adsorb on noble metals and on metal oxide supports such as alumina, titania and silica *via* H-bonding thus blocking active sites from reactants. Keresszegi *et al*. [65] used a water surfactant to remove adsorbed water on Pt/Alumina, since the hydrophobic toluene and cyclohexane were unable to remove adsorbed water. Gallezot *et al*,[45] substituted the silica and titania supported platinum with carbon supported platinum due to the excessive H-bonding of glyoxal hydrogen-bonded to the hydroxyl groups of the oxide supports. Therefore, in order to achieve a satisfactory reaction rate, products should be miscible enough in solvents to be removed from the catalyst surface while reactants should not have to compete for metal site adsorption. The ideal solvent for green chemistry would be water since it is the least toxic. However water has many limitations, such as insolubility with organic compounds, and low oxygen solubility. Also, due to its high polarity, water may strongly adsorb on the catalyst. Mallat *et al.,*[34] suggested the use of water-detergent systems that are more environmentally friendly than organic solvents and are as efficient, such as dodecylbenzenesulfonic acid sodium salt. Solvents may also help tune or determine the production distribution of a certain reaction. When a substrate can undergo different reaction pathways resulting in different possible products, the solvent can favour one path over the other. For example, the use of a dioxane solvent leads to the production of benzaldehyde from benzyl alcohol oxidation. On the other hand, dioxane/water mixtures led to the production of benzoic acid.[102] Hence, depending on the nature and polarity of a solvent, one product may be more favoured than another. In the current work water has been used as solvent media. Although the majority of literature reports the use of mixed solvent, liquid water offers a sustainable and environmentally friendly alternative to expensive inorganic oxidant and harmful organic solvents. [103] Hence, to obtain high butyraldehyde yields, a catalyst that is active and selective in the oxidation of *n*-butanol to butyraldehyde under aqueous conditions has to be developed.[55]

1.7. Catalyst support materials

Precious metal catalysts are often supported on materials to provide greater dispersion, stability and active surface area when compared to the bulk.[104, 105] In the development of a novel catalyst, much research and many trials are performed to find the most appropriate support since it will influence the metal particle size, structure, charge and form the specific active sites at the metal–support boundary.[106]

A wide range of inorganic materials have been used as catalyst supports including zeolites,[107] hydrotalcites,[23] and washcoated ceramic foams.[108] Depending on the chemical reactivity of the support, metal oxides can be classified as acidic inert (e.g. SiO_2) and reactive (e.g. CeO_2) metal oxides.[109] Among the metal oxides alumina (Al_2O_3), iron oxide (Fe_2O_3), silica (SiO_2), titania (TiO_2) and ceria (CeO_2) are some of the most commonly employed supports. Depending on the method of preparation, the surface area and pore sizes may vary considerably. However, a high surface area (>100 m^2/g) and highly porous supports (~1-5 nm pore diameter) are usually used for commercial catalysts in order to maximise the dispersion of the often expensive active metal.[78] In some cases, the support can act as a Lewis acid, affecting the surface chemistry by accepting a pair of electrons. The potential of a support to act as a Lewis acid can subsequently affect the conversion and selectivity observed for a given reaction. Strong Lewis acids such as alumina and iron oxide may have Al^{3+} and Fe^{3+} ions in their structure which exhibit strong affinities towards oxidation of substrates, and thus usually facilitate a higher activity at an expense of selectivity. Supports using alkaline earth metals such as magnesium oxide were shown to be active as well, since platinum had a higher tendency to form small metal particles on the support.[110] The support may play a direct role in the catalysis other than dispersing the active metal. In the case of gold based catalysts, it is the lattice oxygen of the support that participates in the oxidation, while gaseous oxygen replenishes the vacancy created in the absence of basic conditions.

1.7.1. Titania

Titania is considered as an important support in heterogeneous catalysis due to its commercial availability and high stability in electrochemical environments.[111, 112] TiO_2 used as a support has an electronic affect and bifunctional mechanism, which has an influence on heterogeneous catalysts.[111, 113] TiO_2 displays an electronic effect where the hypo-d-electronic Ti^{3+} promotes electrocatalytic features of hyper-d-electronic noble catalyst surface atoms.[114] Thus it, decreases the adsorption energy of CO intermediates, whilst improving the mobility of CO groups. At the same time, the adsorption of OH species on TiO_2 tends to enhance the conversion of the catalytically

toxic CO intermediates in CO_2, consequently improving the durability of the heterogeneous catalyst.[115, 116] The factors above indirectly assist the dispersion and adsorption of the heterogeneous catalyst particles.[116]

Titania (TiO_2) is a reducible support that exhibits a strong metal-support interaction (SMSI) with Pt group metals and is broadly used in heterogeneous catalysis due to its tuneable surface area and pore distribution. SMSI is one method of altering catalytic performance changing the properties of the metal catalyst due to the interaction with the support material.[117, 118] The literature indicates that the SMSI effect also impacts on the catalytic performance of supported metals in hydrogenation and hydrogenolysis reactions.[118] Several explanations proposed for the interpretation of SMSI were based on electronic and structural effects.[118, 119] Additionally, the dispersion and loading of platinum nanoparticles onto TiO_2 support is controlled by the structure and porosity of titania.[111]

The nature of the metal-support interactions can affect the dispersion, electronic, chemisorptive, and catalytic properties of Pt in reactions in which O_2 participates as a reactant. Additional desirable physical properties include: Lewis acidity, redox properties, thermal stability and mechanical strength.[111] Titania improves the performance of catalysts, allowing the modulation of catalytic activities for many reactions, including dehydrogenation,[111, 120, 121] hydrodesulphurisation,[122] water gas shift,[123] and thermal catalytic decomposition.[124]

In the current work TiO_2 powder (Degussa, P-25) is used. TiO_2 consists of anatase and rutile phases in a ratio of about 3:1.[125] Bickley et al. were one of the first people to investigate the proposed synergistic effect between anatase and rutile, believed to be responsible for the fairly high photoreactivity of Degussa P25.[126] Ohno et al. reported the close contact between rutile and anatase in P25 to be prerequisite for the synergistic effect.[125] According to Hurum *et.al.*, the rutile phase plays a key role in separating the electrons from the holes.[127] Electrons that are photoexcited in rutile can migrate to the conduction band of anatase; the holes remain in the rutile. Thereby, the recombination is effectively suppressed.

A study on Pt catalysts supported on TiO_2 (R-rutile) and TiO_2 (A-anatase) revealed that there are differences in catalytic activity between the two catalysts and this is mainly explained by the degree of Pt dispersion in these catalysts.[128] Hajime et al. has reported XPS and CO-TPD measurements on Pt/TiO_2 (R) and Pt/TiO_2 (A), that show strong electronic effects of the support on Pt.[128]

1.7.2. Carbon

Many different carbon materials are used as catalytic supports in heterogeneous catalysis, such as carbon blacks (e.g. acetylene black, Ketjen Black, Black Pearl or Vulcan XC-72), activated carbons and graphitized materials.[129] Carbons are typically activated by either chemical or physical activation.[129] Chemical activation involves the addition of activating agents, such as H_3PO_4 or $ZnCl_2$, to raw organic materials and is subsequently heated to temperatures of up to 1073 K. The physical preparation involves the heating of pre-carbonized material in absence of air or under steam at temperatures up to 1073 K. The activation of carbon can create a considerable number of pores and hence, substantially increases the materials surface area. While graphite has an average surface area of 10-50 m^2/g, the surface area of activated carbons can be 800-1200 m^2/g.[129] Furthermore, the organic precursor used can greatly affect the final morphology of the carbon.

Carbon supports typically offer a greater stability in acidic and basic mediums compared to other conventional supports such as alumina and silica. It can also be combusted at fairly low temperatures, which can assist with the recovery of the active metal components.[130] Given the versatility and advantages of carbon supports, they have been widely used for oxidation processes as supports for precious metals.[22, 81] Unlike metal oxides, carbon supports are electronically inert but extremely conductive, which can dramatically affect the catalytic performance of the supported metal component.[131] Among the different carbon black materials, Vulcan XC-72R (industrially produced by Cobat corporation) has attracted special attention due to its good compromise between adequate surface area (~250 $m^2\ g^{-1}$) and high electric conductivity (~2.77 Scm^{-1}).[129, 132-141] The carbon support materials for Pt catalysts are widely manufactured by the pyrolysis of hydrocarbons, such as natural gas or oil fractions from petroleum processes. Vulcan XC-72R is one of the most popular commercial carbon support materials for Pt catalysts in fuel cells because of its low cost and high activity.[142] Pt and/or Pt-based alloy catalysts are formed on the carbon support material by various chemical synthesis methods, such as impregnation-reduction,[143] colloidal methods,[144] sol-immobilisation methods,[55] etc.

Carbon applications involve interfacial interactions, where different reactants and ions interact with the carbon surface. Consequently, much effort has been conducted to study the effect of carbon black on electrochemical performance for energy conversion and storage devices, such as super capacitors, polymer electrolyte membrane fuel cells (PEMFC) and electrolysers.[134, 140, 145-149] The chemical introduction of oxygen-containing species on carbon structure has been broadly investigated.[134, 140, 150-155] Various

chemical oxidation procedures have been studied using oxidising solutions (such as NaClO, HNO_3 or H_2O_2) or gases (e.g. CO_2, O_3, O_2,NO, etc.),[135, 156, 157] which result in the generation of different oxygen functionalities on carbon surfaces, such as carboxyls, carbonyls, phenols, quinones or lactones.[141]

1.8. Aim and Objective

The overall aim of the current project was to design and synthesise a selective and stable Pt supported catalyst for the oxidation of *n*-Butanol into butyraldehyde. The research herein discussed different strategies that were invoked to reduce, or prevent over oxidation of butyraldehyde into butyric acid, along with corresponding justifications for the experiments. Understanding the role of the oxidation catalysts in the reaction and the kinetics associated with each oxidation step in this reaction is crucially important, as both can feed back into the catalyst design process.

Investigating the deactivation mechanism of the catalyst is also important from a viability perspective. Previous studies have confirmed that the experimental conditions can drastically influence the catalytic activity and reaction selectivity. For this reason, it was important to establish how the reaction conditions effected the performance of the Pt supported catalysts for this reaction. As discussed, the nature of the support material can also be influential on catalytic performance and as such, the effect of support on structural and electronic properties of Pt catalyst was investigated and the results were correlated to oxidation performance.

Finally, by incorporating the learnings from the above two Chapters some additional experiments were conducted in order to assess whether the catalytic performance could be further improved through the addition of a secondary metal. These catalysts were thoroughly characterised by XRD, SEM, TEM, TGA, ICP and IR spectroscopy in order to correlate catalytic performance with physicochemical properties.

1.9. References

1. P. T. Anastas, L. G. Heine and T. C. Williamson, ACS Symp. Ser., 2000, 767, 1-6.

2. P. Anastas and J. Warner, Green Chemistry: Theory and Practice, Oxford Univ Press, 1998.

3. B. A. de Marco, B. S. Rechelo, E. G. Tótoli, A. C. Kogawa and H. R. N. Salgado, Saudi Pharmaceutical Journal, 2018, DOI: https://doi.org/10.1016/j.jsps.2018.07.011.

4. L. D. Gottumukkala, B. Parameswaran, S. K. Valappil, K. Mathiyazhakan, A. Pandey and R. K. Sukumaran, Bioresour. Technol., 2013, 145, 182-187.

5. X. Zhao, L. Wei, J. Julson, Z. Gu and Y. Cao, Korean J. Chem. Eng., 2015, 32, 1528-1541.

6. T. C. Ezeji, N. Qureshi and H. P. Blaschek, Curr. Opin. Biotechnol., 2007, 18, 220-227.

7. J. A. C. II, in McNair Scholars Research Journal, Scholarly Commons, 2014, vol. 1.

8. R. Luque, L. Herrero-Davila, J. M. Campelo, J. H. Clark, J. M. Hidalgo, D. Luna, J. M. Marinas and A. A. Romero, Energy Environ. Sci., 2008, 1, 542-564.

9. G.-j. ten Brink, I. W. C. E. Arends and R. A. Sheldon, Science 2000, 287, 1636-1639.

10. V. K. Puthiyapura, D. J. L. Brett, A. E. Russell, W. F. Lin and C. Hardacre, Chem. Commun. , 2015, 51, 13412-13415.

11. P. Duerre, Biotechnol. J., 2007, 2, 1525-1534.

12. L. Tao, X. He, E. C. D. Tan, M. Zhang and A. Aden, Biofuels, Bioprod. Biorefin., 2014, 8, 342-361.

13. I. Gandarias, E. Nowicka, B. J. May, S. Alghareed, R. D. Armstrong, P. J. Miedziak and S. H. Taylor, Catal. Sci. Technol., 2016, 6, 4201-4209.

14. D. I. Enache, J. K. Edwards, P. Landon, B. Solsona-Espriu, A. F. Carley, A. A. Herzing, M. Watanabe, C. J. Kiely, D. W. Knight and G. J. Hutchings, Science (Washington, DC, U. S.), 2006, 311, 362-365.

15. K. Mori, T. Hara, T. Mizugaki, K. Ebitani and K. Kaneda, J. Am. Chem. Soc., 2004, 126, 10657-10666.

16. A. Abad, P. Concepcion, A. Corma and H. Garcia, Angew. Chem., Int. Ed., 2005, 44, 4066-4069.

17. S. E. Davis, M. S. Ide and R. J. Davis, Green Chem., 2013, 15, 17-45.

18. C. Bellido, M. Loureiro Pinto, M. Coca, G. Gonzalez-Benito and M. T. Garcia-Cubero, Bioresour. Technol., 2014, 167, 198-205.

19. M. K. Mahapatra and A. Kumar, J. Clean Energy Technol., 2017, 5, 27-30.

20. M. Mascal, Biofuels, Bioprod. Biorefin., 2012, 6, 483-493.

21. J. Laskar, F. Vidal, O. Fichet, C. Gauthier and D. Teyssié, Polymer, 2004, 45, 5047-5055.

22. A. F. Lee, J. J. Gee and H. J. Theyers, Green Chem., 2000, 2, 279-282.

23. N. Dimitratos, A. Villa, D. Wang, F. Porta, D. Su and L. Prati, J. Catal., 2006, 244, 113-121.

24. G. Cainelli and G. Cardillo, Chromium oxidations in organic chemistry, Springer-Verl., Berlin; Heidelbarg; New York; Tokyo, 1984.

25. J. Muzart, Tetrahedron, 2003, 59, 5789-5816.

26. J. A. Barnard and N. Karayannis, Analytica Chimica Acta, 1962, 26, 253-258.

27. W. P. Griffith, S. V. Ley, G. P. Whitcombe and A. D. White, Journal of the Chemical Society, Chem. Commun., 1987, DOI: 10.1039/C39870001625, 1625-1627.

28. M. T. Kreutzer, F. Kapteijn, J. A. Moulijn and J. J. Heiszwolf, Chem. Eng. Sci., 2005, 60, 5895-5916.

29. J. H. J. Kluytmans, A. P. Markusse, B. F. M. Kuster, G. B. Marin and J. C. Schouten, Catal. Today, 2000, 57, 143-155.

30. M. Besson and P. Gallezot, Catal. Today, 2003, 81, 547-559.

31. T. Mallat and A. Baiker, Chem. Inform., 2004, 35, 3037.

32. R. A. Sheldon, I. W. C. E. Arends and A. Dijksman, Catal. Today, 2000, 57, 157-166.

33. B. Z. Zhan and A. Thompson, Tetrahedron, 2004, 60, 2917-2935.

34. T. Mallat and A. Baiker, Catal. Today, 1994, 19, 247-283.

35. M. Besson and P. Gallezot, Catal. Today, 2000, 57, 127-141.

36. S. Carrettin, P. McMorn, P. Johnston, K. Griffin and G. J. Hutchings, Chemical Communications, 2002, 696-697.

37. F. Wang, W. Ueda and J. Xu, Angew. Chem., Int. Ed., 2012, 51, 3883-3887.

38. M. Kumar, J. DePasquale, N. J. White, M. Zeller and E. T. Papish, Organometallics, 2013, 32, 2135-2144.

39. R. DiCosimo and G. M. Whitesides, J. Phys. Chem., 1989, 93, 768-775.

40. J. A. A. van den Tillaart, B. F. M. Kuster and G. B. Marin, Appl. Catal., A, 1994, 120, 127-145.

41. Y. Schuurman, B. F. M. Kuster, K. Van der Wiele and G. B. Marin, Appl. Catal., A, 1992, 89, 31-46.

42. P. J. M. Dijkgraaf, M. J. M. Rijk, J. Meuldijk and K. Van der Wiele, J. Catal., 1988, 112, 329-336.

43. V. R. Gangwal, J. van der Schaaf, B. F. M. Kuster and J. C. Schouten, J. Catal., 2005, 229, 389-403.

44. C. Keresszegi, D. Ferri, T. Mallat and A. Baiker, J. Catal., 2005, 234, 64-75.

45. P. Gallezot, Catalysis Today, 1997, 37, 405-418.

46. H. Wieland, Ber. Dtsch. Chem. Ges. B, 1921, 54B, 2353-2376.

47. I. Gandarias, P. J. Miedziak, E. Nowicka, M. Douthwaite, D. J. Morgan, G. J. Hutchings and S. H. Taylor, ChemSusChem, 2015, 8, 473-480.

48. A. Villa, D. Wang, G. M. Veith, F. Vindigni and L. Prati, Catal. Sci. Technol., 2013, 3, 3036-3041.

49. G. L. Brett, Q. He, C. Hammond, P. J. Miedziak, N. Dimitratos, M. Sankar, A. A. Herzing, M. Conte, J. A. Lopez-Sanchez, C. J. Kiely, D. W. Knight, S. H. Taylor and G. J. Hutchings, Angew. Chem., Int. Ed., 2011, 50, 10136-10139.

50. V. Peneau, Q. He, G. Shaw, S. A. Kondrat, T. E. Davies, P. Miedziak, M. Forde, N. Dimitratos, C. J. Kiely and G. J. Hutchings, Phys. Chem. Chem. Phys., 2013, 15, 10636-10644.

51. R. Anderson, K. Griffin, P. Johnston and P. L. Alsters, Adv. Syn. Catal., 2003, 345, 517-523.

52. W. Cai, P. R. de la Piscina and N. Homs, Appl. Catal., B, 2014, 145, 56-62.

53. D. d. W. P. Vinke, A. T. J. W. de Goede, H. van Bek- and M. kumar, Elsevier, Amsterdam, 1992, vol. 72, 1-19.

54. T. Lu, Z. Du, J. Liu, H. Ma and J. Xu, Green Chemistry, 2013, 15, 2215-2221.

55. I. Gandarias, E. Nowicka, B. J. May, S. Alghareed, R. D. Armstrong, P. J. Miedziak and S. H. Taylor, Catal. Sci. Technol., 2016, 6, 4201-4209.

56. A. P. Markusse, B. F. M. Kuster and J. C. Schouten, Catal. Today, 2001, 66, 191-197.

57. J. H. Vleeming, B. F. M. Kuster, G. B. Marin, F. Oudet and P. Courtine, J. Catal., 1997, 166, 148-159.

58. C. Keresszegi, T. Bürgi, T. Mallat and A. Baiker, J. Catal., 2002, 211, 244-251.

59. C. Hardacre, E. A. Mullan, D. W. Rooney and J. M. Thompson, J. Catal., 2005, 232, 355-365.

60. H. Kimura, A. Kimura, I. Kokubo, T. Wakisaka and Y. Mitsuda, Appl. Catal. A Gen., 1993, 95, 143-169.

61. V. R. Gangwal, B. G. M. van Wachem, B. F. M. Kuster and J. C. Schouten, Chem. Eng. Sci., 2002, 57, 5051-5063.

62. V. R. Gangwal, J. v. d. Schaaf, B. F. M. Kuster and J. C. Schouten, Catal. Today, 2004, 96, 223-234.

63. V. R. Gangwal, J. van der Schaaf, B. F. M. Kuster and J. C. Schouten, J. Catal., 2005, 232, 432-443.

64. C. Mondelli, D. Ferri, J.-D. Grunwaldt, F. Krumeich, S. Mangold, R. Psaro and A. Baiker, J. Catal., 2007, 252, 77-87.

65. C. Keresszegi, T. Mallat, J.-D. Grunwaldt and A. Baiker, J. Catal., 2004, 225, 138-146.

66. C. Keresszegi, J.-D. Grunwaldt, T. Mallat and A. Baiker, J. Catal., 2004, 222, 268-280.

67. T. R. Smith, A. Wood and V. I. Birss, Appl. Catal. A. Gen., 2009, 354, 1-7.

68. J. W. Nicoletti and G. M. Whitesides, J. Phys. Chem., 1989, 93, 759-767.

69. P. Atkins and J. de Paula, Atkins' Physical Chemistry, 7th Edition, Oxford University Press, 2002.

70. R. Parsons and T. VanderNoot, J. Electroanal. Chem. Interfacial. Electrochem., 1988, 257, 9-45.

71. L. W. H. Leung and M. J. Weaver, Langmuir, 1990, 6, 323-333.

72. E. Pastor, S. Wasmus, T. Iwasita, M. C. Arevalo, S. Gonzalez and A. J. Arvia, J. Electroanal. Chem., 1993, 350, 97-116.

73. K. D. Popović, N. M. Marković, A. V. Tripković and R. R. Adžić, J. Electroanal. Chem. Interfacial. Electrochem., 1991, 313, 181-199.

74. K. D. Popovic, A. V. Tripkovic and R. R. Adzic, J. Electroanal. Chem., 1992, 339, 227-245.

75. I. T. Bae, X. Xing, C. C. Liu and E. Yeager, J. Electroanal. Chem. Interfacial Electrochem., 1990, 284, 335-349.

76. T. Tsujino, S. Ohigashi, S. Sugiyama, K. Kawashiro and H. Hayashi, J. Mol. Catal., 1992, 71, 25-35.

77. G. F. Bennett, J. Hazard. Mater., 2008, 160, 688-689.

78. C. G. Vayenas, S. Bebelis, et al., Electrochemical Activation of Catalysis - Promotion, Electrochemical Promotion, and Metal-Support Interactions, Springer - Verlag, 2001.

79. T. Mallat, Z. Bodnar, P. Hug and A. Baiker, J. Catal., 1995, 153, 131-143.

80. H. Kimura, K. Tsuto, T. Wakisaka, Y. Kazumi and Y. Inaya, Appl. Catal. A Gen., 1993, 96, 217-228.

81. H. H. C. M. Pinxt, B. F. M. Kuster and G. B. Marin, Appl. Catal. A Gen., 2000, 191, 45-54.

82. M. Wenkin, P. Ruiz, B. Delmon and M. Devillers, J. Mol. Catal. A Chem., 2002, 180, 141-159.

83. T. Mallat, Z. Bodnar, A. Baiker, O. Greis, H. Strubig and A. Reller, J. Catal., 1993, 142, 237-253.

84. T. Mallat, A. Baiker and L. Botz, Appl. Catal. A Gen., 1992, 86, 147-163.

85. T. Mallat, Z. Bodnar and A. Baiker, in Studies in Surface Science and Catalysis, eds. M. Guisnet, J. Barbier, J. Barrault, C. Bouchoule, D. Duprez, G. Pérot and C. Montassier, Elsevier, 1993, vol. 78, 377-384.

86. T. Mallat, Z. Bodnar, M. Maciejewski and A. Baiker, in Studies in Surface Science and Catalysis, eds. V. C. Corberán and S. V. Bellón, Elsevier, 1994, vol. 82, 561-570.

87. C. Broennimann, Z. Bodnar, P. Hug, T. Mallat and A. Baiker, J. Catal., 1994, 150, 199-211.

88. T. Mallat, Z. Bodnar and A. Baiker, ACS Symp. Ser., 1993, 523, 308-317.

89. P. J. M. Dijkgraaf, H. A. M. Duisters, B. F. M. Kuster and K. Van der Wiele, J. Catal., 1988, 112, 337-344.

90. L. Jelemensky, B. F. M. Kuster and G. B. Marin, Catal. Lett., 1994, 30, 269-277.

91. A. P. Markusse, B. F. M. Kuster, D. C. Koningsberger and G. B. Marin, Catal. Lett., 1998, 55, 141-145.

92. K. Heyns and H. Paulsen, Adv. Carbohydr. Chem. Biochem., 1962, 17.

93. H. G. J. de Wilt and H. S. van der Baan, Industrial and Engineering Chemistry Product Research and Development, 1972, 11, 374-378.

94. Y. Önal, S. Schimpf and P. Claus, J. Catal., 2004, 223, 122-133.

95. J. M. H. Dirkx and H. S. van der Baan, J. Catal., 1981, 67, 14-20.

96. J. H. Vleeming, B. F. M. Kuster and G. B. Marin, Carbohydrate Research, 1997, 303, 175-183.

97. A. Abbadi and H. van Bekkum, J. Mol. Catal. A: Chem., 1995, 97, 111-118.

98. P. Vinke, W. van der Poel and H. van Bekkum, in Studies in Surface Science and Catalysis, 1991, vol. 59, 385-394.

99. R. A. Rajadhyaksha and S. L. Karwa, Chem. Eng. Sci., 1986, 41, 1765-1770.

100. F. A. Carey and R. J. Sundberg, 2007.

101. T. Kawabata, Y. Shinozuka, Y. Ohishi, T. Shishido, K. Takaki and K. Takehira, J. Mol. Catal. A Chem., 2005, 236, 206-215.

102. P. Korovchenko, C. Donze, P. Gallezot and M. Besson, Catal. Today, 2007, 121, 13-21.

103. B. N. Zope, D. D. Hibbitts, M. Neurock and R. J. Davis, Science (Washington, DC, U. S.), 2010, 330, 74-78.

104. C. W. Hills, M. S. Nashner, A. I. Frenkel, J. R. Shapley and R. G. Nuzzo, Langmuir, 1999, 15, 690-700.

105. A. Abad, A. Corma and H. Garcia, Chem. - Eur. J., 2008, 14, 212-222.

106. Z. Qu, W. Huang, S. Zhou, H. Zheng, X. Liu, M. Cheng and X. Bao, J. Catal., 2005, 234, 33-36.

107. N. Srinivas, V. Radha Rani, M. Radha Kishan, S. J. Kulkarni and K. V. Raghavan, J. Mol. Catal. A Chem., 2001, 172, 187-191.

108. M. V. Twigg and J. T. Richardson, Chem. Eng. Res. Design, 2002, 80, 183-189.

109. J. M. Campelo, D. Luna, R. Luque, J. M. Marinas and A. A. Romero, Chem. Sus. Chem., 2009, 2, 18-45.

110. C.-G. Jia, F.-Y. Jing, W.-D. Hu, M.-Y. Huang and Y.-Y. Jiang, J. Mol. Catal., 1994, 91, 139-147.

111. S. Bagheri, N. Muhd Julkapli and S. Bee Abd Hamid, Sci. World J., 2014, 2014, 21.

112. S. J. Tauster, S. C. Fung, R. T. K. Baker and J. A. Horsley, Science (Washington, D. C., 1883-), 1981, 211, 1121-1125.

113. L. Si, Z. a. Huang, K. Lv, D. Tang and C. Yang, J. Alloys Compd., 2014, 601, 88-93.

114. N. M. Julkapli, S. Bagheri and S. B. Abd Hamid, Sci. World J., 2014, 692326.

115. X. L. Sui, Z. B. Wang, M. Yang, L. Huo, D. M. Gu and G. P. Yin, J. Power Sources, 2014, 255, 43-51.

116. G. R. Bamwenda, S. Tsubota, T. Nakamura and M. Haruta, Catal. Lett., 1997, 44, 83-87.

117. O. S. Alexeev, S. Y. Chin, M. H. Engelhard, L. Ortiz-Soto and M. D. Amiridis, J. Phys. Chem. B, 2005, 109, 23430-23443.

118. R. T. K. Baker, S. J. Tauster, J. A. Dumesic and Editors, ACS Symposium Series, No. 298: Strong Metal Support Interactions. [Developed from a Symposium at the 189th Meeting of the American Chemical Society, Miami Beach, Fla., April 28-May 3, 1985], American Chemical Society, 1986.

119. O. S. Alekseev and Y. A. Rundin, Usp. Khim., 1992, 61, 765-791.

120. G. Liang, L. He, H. Cheng, W. Li, X. Li, C. Zhang, Y. Yu and F. Zhao, J. Catal., 2014, 309, 468-476.

121. Q. Luo, M. Beller and H. Jiao, J. Theor. Comput. Chem., 2013, 12, 1330001-1330028.

122. R. Palcheva, L. Dimitrov, G. Tyuliev, A. Spojakina and K. Jiratova, Appl. Surf. Sci., 2013, 265, 309-316.

123. S. Bagheri, K. Shameli and S. B. Abd Hamid, J. Chem., 2013, 848205.

124. H. Kominami, J.-I. Kato, Y. Takada, Y. Doushi, B. Ohtani, S.-I. Nishimoto, M. Inoue, T. Inui and Y. Kera, Catal. Lett., 1997, 46, 235-240.

125. T. Ohno, K. Sarukawa, K. Tokieda and M. Matsumura, J. Catal., 2001, 203, 82-86.

126. R. I. Bickley, T. Gonzalez-Carreno, J. S. Lees, L. Palmisano and R. J. D. Tilley, J. Solid State Chem., 1991, 92, 178-190.

127. D. C. Hurum, A. G. Agrios, K. A. Gray, T. Rajh and M. C. Thurnauer, J. Phys. Chem. B, 2003, 107, 4545-4549.

128. H. Iida and A. Igarashi, Appl. Catal., A, 2006, 298, 152-160.

129. E. Auer, A. Freund, J. Pietsch and T. Tacke, Appl. Catal. A Gen., 1998, 173, 259-271.

130. L. Prati, A. Villa, C. Campione and P. Spontoni, Top. Catal., 2007, 44, 319-324.

131. N. Dimitratos, J. A. Lopez-Sanchez, D. Morgan, A. Carley, L. Prati and G. J. Hutchings, Catal. Today, 2007, 122, 317-324.

132. C. W. B. Bezerra, L. Zhang, H. Liu, K. Lee, A. L. B. Marques, E. P. Marques, H. Wang and J. Zhang, Journal of Power Sources, 2007, 173, 891-908.

133. M. Noked, A. Soffer and D. Aurbach, J. Solid State Electrochem., 2011, 15, 1563.

134. E. Antolini, Appl. Catal. B: Environmental, 2009, 88, 1-24.

135. J. L. Figueiredo, M. F. R. Pereira, M. M. A. Freitas and J. J. M. Órfão, Carbon, 1999, 37, 1379-1389.

136. K. Jurewicz, C. Vix-Guterl, E. Frackowiak, S. Saadallah, M. Reda, J. Parmentier, J. Patarin and F. Béguin, J. Phys. Chem. Solids, 2004, 65, 287-293.

137. E. Frackowiak and F. Béguin, Carbon, 2001, 39, 937-950.

138. K. Fic, E. Frackowiak and F. Béguin, J. Mater. Chem., 2012, 22, 24213-24223.

139. S. Tang, G. Sun, J. Qi, S. Sun, J. Guo, Q. Xin and G. M. Haarberg, Cuihua Xuebao/Chinese J. Catal., 2010, 31, 12-17.

140. M. A. Fraga, E. Jordão, M. J. Mendes, M. M. A. Freitas, J. L. Faria and J. L. Figueiredo, J. Catal., 2002, 209, 355-364.

141. S. Pérez-Rodríguez, E. Pastor and M. J. Lázaro, Int. J. Hydrogen Energy, 2018, 43, 7911-7922.

142. H. D. Nguyen, T. T. L. Nguyen, K. M. Nguyen, T. H. Ha and Q. H. Nguyen, Adv. Nat. Sci.: Nanosci. Nanotechnol., 2015, 6, 025011-025016.

143. Y. Cho, W. H. Lee and H. Kim, J. Mater. Chem. A, 2014, 2, 11635-11641.

144. P. Sonstroem and M. Baeumer, Phys. Chem. Chem. Phys., 2011, 13, 19270-19284.

145. A. Capelo, M. A. Esteves, A. I. de Sá, R. A. Silva, L. Cangueiro, A. Almeida, R. Vilar and C. M. Rangel, Int. J. Hydrogen Energy, 2016, 41, 12962-12975.

146. V. A. Golovin, N. V. Maltseva, E. N. Gribov and A. G. Okunev, Int. J. Hydrogen Energy, 2017, 42, 11159-11165.

147. Q. Zhang, Y. Zhang, W. Cai, X. Yu, Y. Ling and Z. Yang, Int. J. Hydrogen Energy, 2017, 42, 16773-16781.

148. L. Liu, D. W. Zha, Y. Wang and J. B. He, Int. J. Hydrogen Energy, 2014, 39, 14712-14719.

149. M. M. Najafpour, F. Rahimi, M. Fathollahzadeh, B. Haghighi, M. HołyŃska, T. Tomo and S. I. Allakhverdiev, J. Chem. Soc.. Dalton Transactions, 2014, 43, 10866-10876.

150. J. L. G. de la Fuente, M. V. Martínez-Huerta, S. Rojas, P. Terreros, J. L. G. Fierro and M. A. Peña, Catal. Today, 2006, 116, 422-432.

151. J. L. G. de la Fuente, S. Rojas, M. V. Martínez-Huerta, P. Terreros, M. A. Peña and J. L. G. Fierro, Carbon, 2006, 44, 1919-1929.

152. J. L. Figueiredo and M. F. R. Pereira, J. Energy Chem., 2013, 22, 195-201.

153. J. L. Figueiredo, M. F. R. Pereira, P. Serp, P. Kalck, P. V. Samant and J. B. Fernandes, Carbon, 2006, 44, 2516-2522.

154. M. J. Bleda-Martínez, J. M. Pérez, A. Linares-Solano, E. Morallón and D. Cazorla-Amorós, Carbon, 2008, 46, 1053-1059.

155. H. S. Oh, K. Kim, Y. J. Ko and H. Kim, Int. J. Hydrogen Energy, 2010, 35, 701-708.

156. S. S. Barton, M. J. B. Evans, E. Halliop and J. A. F. MacDonald, Carbon, 1997, 35, 1361-1366.

157. J. B. Donnet, Carbon, 1968, 6, 161-176.

Chapter 2: Experimental

2.1. Materials

The details of all chemicals used in this work are detailed below.

Materials for catalyst preparation	
Material	**Supplier**
Polyvinylalcohol (PVA)	Sigma Aldrich UK
$NaBH_4$ (98 %)	Sigma Aldrich UK
Cabot Vulcan XC72R	Cabot Corporation
TiO_2 (P25)	Degussa
$H_2PtCl_6 \cdot 3H_2O$	Alfa Aesar
Ethanol absolute	VWR
$Zn(NO_3)_2 \cdot 6H_2O$ (98 %)	Sigma Aldrich UK
$AlCl_3$ (99.99 %)	Sigma Aldrich UK
H_2SO_4 (>95 %)	Fisher
$BiCl_3$ (99.9 %)	STREM
$SnCl_4 \cdot 5H_2O$	General purpose reagent
$PbCl_2$ (98 %)	Sigma Aldrich UK
HCl (~ 37 %)	Fisher
NaOH	Fisher
Reactants and Products	
Material	**Supplier**
1-Butanol (99.8 %)	Sigma Aldrich UK
2-Butanol (99.5 %)	Sigma Aldrich UK
Butyraldehyde (≥99 %)	Sigma Aldrich UK
Butyric acid	Sigma Aldrich UK

2.2. Catalyst preparation

Several catalysts were prepared and tested for oxidation of *n*-butanol. This Chapter covers detail preparation methods/procedures employed for the synthesis of various catalysts tested for oxidation of *n*-butanol.

2.2.1. Preparation of supported catalyst

Supported metal catalysts (1 wt.%metal loading) were prepared using a sol-immobilisation method. In the case of bimetallic catalysts the ratio of 0.5:0.5,1:0.5 and 1:1 metals were used.

2.2.1.1. Sol-immobilisation

In this study, all the catalyst were prepared by one method, which is sol-immobilisation (SI). This method involves the preparation of metal nanoparticles in solution followed by their subsequent immobilisation on a support.[1] The steps to prepare the catalyst are as follows: (1) A metal salt was dissolved in a large excess of solution and a stabilising agent – usually a polymer – was added (2). A reducing agent was then used to generate metallic nanoparticles, the growth of which has been studied by Turkevic and co-workers.[2] (3) Once the nanoparticles are generated, the support is added and the nanoparticles were immobilised onto the surface by altering the charge of the support through addition of an acid or base. The electrochemical double layer surrounding the metal nanoparticles causes them to be attracted to the support. Because metallic nanoparticles are laid onto the support surface, there is seldom need for subsequent reduction treatment when SI is used for catalyst preparation. The advantage of SI is that it is applicable to any type of support.

Analysis of the catalyst before the reaction was carried out with Raman spectroscopy in order to see whether PVA is remained on the catalyst surface. The Raman analysis show no traces of any PVA on the surface.

2.2.1.1.1. Preparation of Pt/support

Various Pt/X catalysts; X= TiO_2: Degussa P25 and Carbon (C: Cabot Vulcan XC-72R) were prepared by the sol-immobilisation. The procedure for synthesizing 1 g of 1 wt.%Pt/TiO_2 (P25) by sol-immobilisation was as follows: an aqueous solution of $H_2PtCl_6 \cdot 6H_2O$ (0.051 mmol of Pt, concentration: 36.4 mg mL^{-1}) was prepared and added under stirring to a 1 L glass beaker containing 400 mL of water. After 5 min, to this solution polyvinyl alcohol (PVA) (weight-average molecular mass = 9,000-10,000 g/mol; 80 % hydolysed, Sigma-Aldrich) was added such that the PVA to metal ratio was 1 : 1.20 by mass. After 15 minute of stirring, a freshly prepared 0.2 M (2 mmol) solution of $NaBH_4$ (>96 % purity, $NaBH_4$/Metal mole fraction = 7.5, Sigma Aldrich) was added to

form a dark-brown solution. After 45 minute of sol-generation, the colloid was immobilised by adding TiO_2 (P25) (0.99 g) and acidifying to pH 2 by concentrated H_2SO_4 (>95 %). The catalyst was prepared at room temperature. The catalyst was filtered and washed thoroughly with 2 L of distilled water to remove the excess of PVA, H_2SO_4 and chlorides, then dried (110 °C, 16 h). Catalysts were ground in a pestle and mortar prior to testing. This catalyst was designated as Pt/TiO_2.

2.2.1.1.2. Preparation of Pt-X/Support (where X = Al, Zn, Sn, Bi and Pb)

Bimetallic Pt-X catalysts were also prepared by the sol-immobilisation method. The total metal loadings of Pt-X catalysts was varied. For each bimetallic catalyst three different metal loadings were used; 0.5:0.5, 1:0.5 and 1:1.

Pt–X catalysts supported on carbon or TiO_2 were prepared using a sol-immobilisation method. Aqueous solutions of $H_2PtCl_6{\cdot}6H_2O$ (Alfa Aesar) and X (where X = $Zn(NO_3)_2{\cdot}6H_2O$, $AlCl_3$, $BiCl_3$, $SnCl_4{\cdot}5H_2O$ and $PbCl_2$) were used as the precursors. For a given preparation, desired quantities $H_2PtCl_6{\cdot}6H_2O$ and X were added to 800 mL of H_2O. To this solution, polyvinyl alcohol (PVA) (1 wt%solution, Aldrich, weight averaged molecular weight M_W = 9000–10 000 g mol^{-1}, 80% hydrolysed) was added (PVA/X (wt/wt) = 1.2). Subsequently, a freshly prepared 0.2 M (2 mmol) solution of $NaBH_4$ (>96 % purity, $NaBH_4$/Metal mole fraction = 7.5, Sigma Aldrich) as then added to form a sol. After 30 min of sol generation, the colloid was immobilised by adding activated carbon (acidified to pH 1 by sulfuric acid) under vigorous stirring conditions. The support (1.98 g) was then added to the solution and after 2 h of vigerous stirring, the slurry was filtered, washed thoroughly with distilled water and dried at 110 °C for 16 h. Bimetallic catalysts containing Pt and X were denoted as $Pt\text{-}Zn/TiO_2$, $Pt\text{-}Al/TiO_2$, $Pt\text{-}Bi/TiO_2$, $Pt\text{-}Sn/TiO_2$, $Pt\text{-}Pb/TiO_2$, Pt-Zn/C, Pt-Al/ C, Pt-Bi/ C, Pt-Sn/ C and Pt-Pb/ C, respectively.

2.2.2. High temperature activations

Some of the catalysts used in this research were subjected to heat treatments prior to catalytic testing. In these cases, the catalyst was loaded into a ceramic calcination boat and reduced and/or oxidised at 200 °C for 2 h under a flow of 5 vol.%H_2/Ar or air (5 mL min^{-1}) respectively. These catalysts are abbreviated to $Pt/Support^{RED}$, $Pt/Support^{OXI}$, $Pt\text{-}X/Support^{RED}$ and $Pt\text{-}X/Support^{OXI}$.

2.2.3. Catalyst testing

The catalyst testing were performed in a 50 mL Colaver glass reactor (**Figure 2.1**). The reactor was charged with 10 mL *n*-butanol (5.4 mmol of 4 wt.%*n*-butanol, 0.54 M) and

catalyst added (typically) 15 mg. The glass reactor was sealed, purged three times with oxygen and then pressurised with oxygen to 3 bar.

Figure 2.1. Catalyst testing using a Colaver reactor.

This pressure was maintained throughout the experiment; hence as the oxygen was consumed in the reaction it was continuously replenished. Upon heating to reaction temperature; typically 100 °C, the reaction solution was stirred continuously with a magnetic stirrer at 750 rpm. The reactor was then cooled in an iced bath for 10 minutes and the reaction mixture separated by centrifugation. Samples were prepared for analysis by mixing 0.5 mL of reaction mixture with 0.5 mL of 2-butanol standard solution (external standard, [2-butanol] = 0.55 M). A gas chromatograph (GC) is used to analyse the data.

Conversion, selectivity, and carbon balance were calculated using Equations 2.1, 2.2 and 2.3 respectively:

$$\text{Conversion of R \%} = \frac{[R]_0 - [R]_1}{[R]_0} \; X \; 100 \qquad \text{Equation 2.1}$$

where R = reactant; $[R]_0$ = initial concentration of reactant; $[R]_1$ = final concentration of reactant determined by GC analysis.

$$\text{Selectivity to Pi (\%)} = \frac{[P]_i}{[P]_0} \; X \; 100 \qquad \text{Equation 2.2}$$

where P = product ; $[P]_i$ = concentration of P_i determined GC analysis; $[P]_0$ = total concentration of all products determined by GC.

$$\text{Carbon balance (\%)} = \frac{[C]_1}{[C]_0} X\ 100 \qquad \text{Equation 2.3}$$

where $[C]_0$ = carbon concentration of reactants; $[C]_1$ = carbon concentration of residual reactant and products determined by GC analysis.

Each experiment presented in this thesis was repeated at least twice or more, to ensure a good reproducibility was observed. Typically, the error for the conversion of *n*-butanol was *ca.* ± 4 %.

2.3. Reaction analysis

2.3.1. Gas chromatography

Chromatography is the collective term for a family of techniques capable of producing data for the composition of chemical mixtures. Gas chromatography is one of the most extensively used techniques amongst the analytical methods. This technique specifically involves a sample being vaporized and injected into the head of the chromatographic column. The sample is transported through the column by the flow of an inert, gaseous mobile phase. The column itself contains a stationary phase, which is adsorbed onto the surface of an inert solid. The instrument mainly consists of carrier gas flow control, sample injector port, columns, detectors and data acquisition system. In this study a gas chromatograph (Agilent Technologies 7820 A), fitted with a CPwax 52 CB capillary column, Helium carrier gas and a flame ionization detector was used to analyse the data.

The reaction solution (0.2 µL) was injected into a split/splitless injector at 200 °C with a split ratio of 10:1 with an average column velocity of (5.92 cm sec^{-1}). The initial oven temperature was held at 40 °C for 10 minutes. The temperature of the oven was then raised at 15 °C/min to 250 °C and held for a further 10 minutes (**Figure 2.2**).

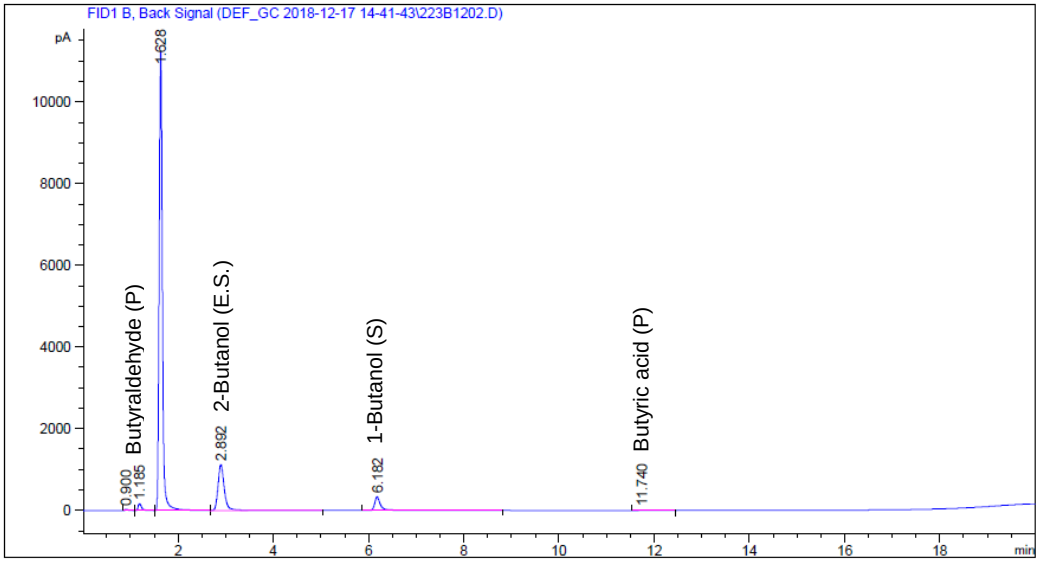

Figure 2.2. The gas chromatogram of the product of a typical *n*-butanol oxidation (where; S = Substrate, P = Product and E.S. = External Standard).

The catalytic oxidation of *n*-butanol was monitored using gas chromatography (GC) and substrate disappearance and product formation was quantified using an external calibration method. For this, four aqueous solutions of each known compound with known concentrations were prepared and combined with a known mass of 2-Butanol (external standard); typically 0.55 M. Each solution was subsequently injected into the GC and the corresponding areas were normalised to the area of the standard in order to construct a calibration plot. An example of calibration curve for 1-butanol is shown below (**Figure 2.3**).

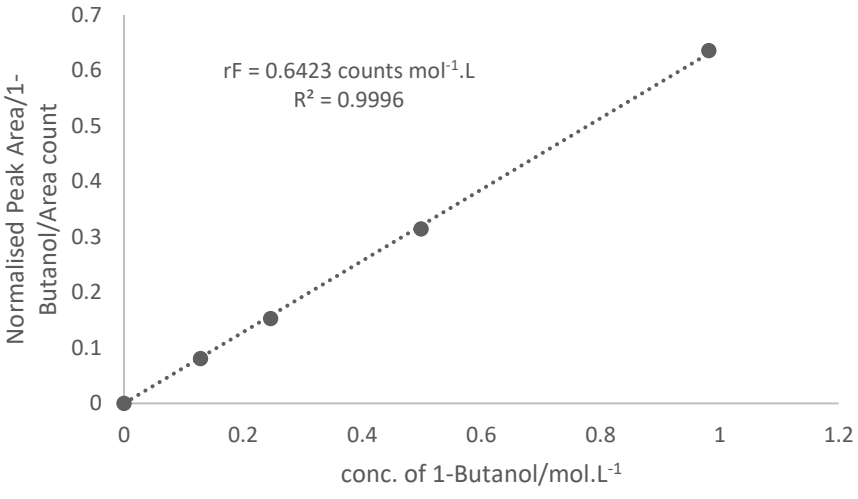

Figure 2.3. Calibration curve of *n*-Butanol at different concentration.

The gradient of the calibration line is regarded as the response factor and can be used to quantify a known compound in a post reaction solution. Response factors for all the reaction components were calculated in the same way; all the response factors are displayed in Table 2.1. The response factors for 1-butanol, butyraldehyde and Butyric acid rate were determined to be 0.64, 0.50 and 0.87 respectively.

Table 2.1. Response factor of 1-Butanol, Butyraldehyde and Butyric acid.

Chemicals	Response factor
1-Butanol	0.64
Butyraldehyde	0.50
Butyric acid	0.87

2.4. Characterisation

2.4.1. X-ray Photoelectron spectroscopy

X-ray photoelectron spectroscopy (XPS) is a commonly used surface sensitive technique in catalytic research for the analysis of elemental composition, elemental oxidation state and metal dispersion.[3]

The basis of XPS is the photoelectric effect, where an atom absorbs a photon of energy ($h\upsilon$) and ejects a photoelectron with a kinetic energy defined by Einstein equation (equation 1). The kinetic energy measured by XPS is used to determine the binding energy of the photoelectron, which is characteristic for each element and its associated orbitals. As the binding energy is characteristic of the elemental orbital from which it was ejected, it is affected by any changes in the initial chemical state of the emitting atom, therefore chemical information can be obtained. AlthoughX-rays penetrate many microns in to a sample, the small inelastic mean free path (IMFP, λ) of the ejected photoelectrons means that *ca.* 95% of the signal comes from a depth of 3 λ meaning that the majority of the signal comes from the surface or near-surface region (up to 10 nm total depth) and it is this phenomena which is responsible for the inherent surface sensitivity in XPS

$$E_k = h\upsilon - E_b - \varphi \qquad \text{Equation 2.4}$$

where E_k = kinetic energy of the ejected photoelectron; $h\upsilon$ = energy of the incident X-ray photon; E_b = binding energy of the photoelectron with respect to the fermi level; φ = work function of the spectrometer.

Data for XPS analysis presented in this work were collected on a Kratos Axis Ultra DLD X-ray photoelectron spectrometer using a monochromatic Al Kα X-ray source operating at 140 W (**Figure 2. 4**). Survey scans and high resolution scans were acquired at pass energies of 160 eV and 40 eV, respectively. Charge neutralization was achieved using a low energy electrons , and spectra were subsequently calibrated to the C(1s) signal for adventitious carbon, taken to have a binding energy of 284.8 eV; all experimental binding energies are quoted ±0.2 eV.

Figure *2*.4. The Kratos Axis Ultra DLD X-ray photoelectron spectrometer used in this study.

2.4.2. Transmission electron microscopy

Transmission electron microscopy (TEM) is based on the detection of transmitted and diffracted electrons (**Figure *2*.5**). Bright field images represent a 2D projection of the transmitted electrons, which depends on the mass distribution; the density and thickness of the sample. Dark field images represent the diffracted electrons, which

have a slightly different angle than those of the transmitted beam. Contrast in the images is caused by attenuation of the electron beam, dependent on the density and thickness of the sample, and also by diffraction and interference.[3] TEM instruments operate in a similar way to an optical microscope, with electromagnetic lenses and an electron beam instead of optical lenses and light. Typically, a TEM instrument has superior magnification and resolution to a SEM instrument.[4]

Figure *2*.5. JEOL JEM2100 Transmission electron microscope (TEM).

TEM is widely used in catalysis to determinate the dispersion, particle size and morphology of supported particles and to investigate metal support interactions.

Scanning Transmission Electron Microscopy (STEM) combines both TEM and SEM operation modes. It is possible to select specific regions of the sample that are irradiated with the primary electron beam and obtain either bright or dark field images. Dark field images are obtained based on the electrons that are diffracted by the metal particles and thus, images of supported metal particles with improved contrast are obtained.

Transmission electron microscopy (TEM) and scanning transmission electron microscopy (STEM) were performed on a JEOL JEM-2100 microscope operating at 200

kV. Energy dispersive X-ray analysis (EDX) was done using an Oxford Instruments X-Max^N 80 detector and the data analysed using the Aztec software. Samples were prepared by dispersion in ethanol by sonication and deposited on 300 mesh copper grids coated with holey carbon film.

2.4.3. Scanning electron microscopy (SEM)

Scanning electron microscopy (SEM) is very similar to TEM. The main differences between TEM and SEM are: TEM uses a broad static beam as opposed to the focused fine point that scans in a rectangular raster pattern in SEM; the accelerating voltages used for SEM are much lower than used for TEM; and the samples do not need to be thin for SEM, simplifying sample preparation.

Microscopy was performed on a Tescan MAIA3 field emission gun scanning electron microscope (FEG-SEM) operating at 15 kV. Images were acquired using the backscattered electron detector. The samples were dispersed as a powder onto 300 mesh copper grids coated with a holey carbon film.

2.4.4. Inductively coupled plasma mass spectrometry (ICP-MS)

ICP-MS is a technique that utilizes the methods of mass spectroscopy which is capable of detecting elements at low concentration PPB parts per billion. The instrument used was an Agilent 7900 ICP-MS with argon plasma. This is achieved by the plasma dissociating compounds into their constituent elements which are ionised and can quantify those ions.

The torch itself is quartz. The plasma is formed by a combination of the RF coil and the Argon gas forming a superheated gas (the plasma) which consists of free electrons and ions, when the sample enters the plasma (from the nebulizer and ultimately the spray chamber) it is 'dried' and any molecules are dissociated and electrons removed, forming the ions we can detect in the mass analyser. ICP uses argon for the plasma gas, Helium is used in the collision/reaction cell. The plasma itself is initiated and maintained by an RF coil wrapped around the torch.

Compared to atomic absorption techniques, ICP-MS has greater speed, precision, sensitivity and is a sequential technique able to analyse multiple elements whereas older atomic spectroscopy methods generally can't do this. Only reaction solutions were run with ICP-MS as they required a higher sensitivity that this technique can provide.

The calibration was made from 0 to 1 PPM (5 calibration points). The matrix for standards matches the samples. If samples are diluted then the matrix would also be diluted the same to ensure consistency.

2.4.5. Thermogravimetric analysis (TGA)

Thermogravimetric analysis determines the weight loss of a material as a function of temperature in a controlled atmosphere (**Figure 2.6**). This technique is used to identify the temperature at which chemical changes occur including redox reactions, decompositions, phase transformations and desorption of adsorbed species. TGA curves are the representation of the weight loss, given as a percentage of the initial sample weight, versus temperature.

Figure *2*.6. PerkinElmer Thermogravimetric (TGA 4000) analyser.

TGA analysis was conducted using a PerkinElmer TGA 4000 instrument. A 6 mg of the sample was placed in a crucible. After ~ 2 minutes stabilisation, TGA was conducted in air (20 mL/min) by heating the sample from 30 °C to 800 °C (15 °C/min).

2.4.6. Powder X-ray diffraction

Powder X-ray Diffraction (PXRD) is a non-destructive technique that can provide detailed information about the crystallographic structure of heterogeneous catalysts.

Diffraction occurs when electromagnetic radiation strikes on a material with a comparable length scale to the wavelength of radiation.

X-rays are electromagnetic radiation with wavelengths in the region of 10^{-10} m (1 Å). X-Rays are generated in a vacuum tube when high energy electrons, released by the cathode (a tungsten filament), collide with the atoms and nuclei of the anode or metal target (typically copper).[5] When electrons have enough energy, the metal target's inner orbital electrons are ejected and electrons from higher energy levels fill the vacancies. As a result, X-rays of specific wavelength are emitted. Generated X-rays are filtered, collimated and concentrated to produce monochromatic radiation, which is directed towards the sample.

Crystalline materials are formed by repetition of ordered arrangements of atoms. X-ray wavelengths are about the same order of magnitude as atomic distances in solids (*ca.* 1 Å). Hence, XRD techniques require long-range order. Interaction of the incident X-Rays with the sample results in a constructive interference when Bragg's law is satisfied. Hence, X-ray diffraction is dictated by the Bragg equation (Equation 2.5):[6]

$$n\lambda = 2\,d\sin\theta \qquad \text{Equation 2.5}$$

Where:

n is the order of reflection, an integer number (n = 1,2,3 …)

λ is the incident X-ray wavelength

d is the distance between two lattice planes

θ is the angle of incidence

The diffracted X-Rays are detected, processed and counted with a movable detector that scans the radiation intensity as a function of the angle 2θ.

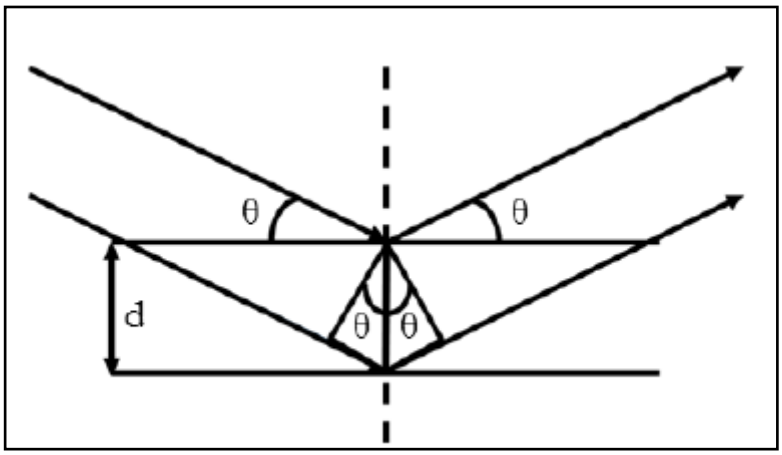

Figure 2.7. Illustration of X-ray beams on a crystal from which Bragg's Law is derived.

Each crystalline material possesses a unique characteristic X-Ray pattern used as a "fingerprint". Thus, identification of crystalline phases present in a sample is possible through comparison with a database of XRD patterns. Structure determination is achieved by conversion of the diffraction peaks to d-spacings.

It is possible to calculate the crystallite size of a given phase using the diffraction peak's width via the Debye-Scherrer equation (Equation 2.6):[7, 8]

$$D_{hkl} = \frac{\kappa \lambda}{B_{hkl} \cos\theta} \qquad \text{Equation 2.6}$$

Where:

D_{hkl} is the crystallite size in the direction perpendicular to the lattice planes, hkl are the Miller indices of the planes being analysed.

κ is a numerical factor frequently referred to as the crystallite-shape factor.[9]

λ is the wavelength of the X-rays.

B_{hkl} is the width (full-width at half-maximum) of the X-ray diffraction peak in radians.

θ is the Bragg angle.

The main limitation of this technique is that samples require sufficient long range order to observe clear diffraction peaks and that its application is restricted to compounds with particle sizes of greater than 4 nm. The rotation of the powdered sample maximises the chance that particles are orientated such that a certain crystal plane is at the θ right angle defined by the Bragg's law, contributing to the diffraction pattern.

Powder X-ray diffraction patterns were obtained on a PANalytical X'Pert Pro diffractometer using Cu Kα ray source operating at 40 kV and 40 mA. The signal was recorded for 2θ comprised between 10^0 and 80^0 with a step of 0.02^0. The XRD patterns were analysed by matching measured patterns against the JCPDS database.

2.4.7. BET surface area analysis

The Brunauer–Emmett–Teller (BET) theory uses amount of gas physisorbed on to the surface of a catalyst to calculate physical properties, such as surface area and pore volume. BET is based on the Langmuir theory, which calculates the monolayer coverage of an adsorbate that is bound to a surface. The Langmuir equation is:

$$\theta = \frac{\alpha P}{1+\alpha P} \qquad \text{Equation 2.7}$$

Where θ is the fractional surface coverage, P is the gas pressure and α is the Langmuir adsorption constant, which is dependent on binding energy and temperature.

BET theory measures multi layer adsorption. It adopts non-corrosive (inert gases) like nitrogen and helium as the adsorbate to determine the surface area data. Quantachrome surface area analysers use both gases for both: analysis and calibration.

This technique is therefore an extension of the Langmuir equation, and takes into account that a multilayer can be represented as stacked monolayers.

There are five assumptions made when using the BET method, which are:[10]

1. Adsorption occur only on well-defined sites of the sample surface (one per molecule)
2. The only molecular interaction considered is the following one: a molecule can act as a single adsorption site for a molecule of the upper layer.
3. The uppermost molecule layer is in equilibrium with the gas phase
4. The desorption is a kinetically-limited process.
5. At the saturation pressure, the number of molecular layers tends to infinity.

Taking these into account a modified Langmuir equation can be written in the linear form:[11]

$$\frac{1}{v[(p_0/p)-1]} = \frac{c-1}{v_m c}\left(\frac{p}{p_0}\right) + \frac{1}{v_m c} \qquad \text{Equation 2.8}$$

Where p and p_0 are the equilibrium and saturation pressures of adorbates at the temperature of adsorption, v is the adsorbed gas quantity and v_m is the monolayer adsorbed gas quantity. c is the BET constant which calculated by:

$$c = \exp\left(\frac{E_1 - E_L}{RT}\right) \qquad \text{Equation 2.9}$$

Where E_1 is the heat of adsorption for the first layer, E_L is for the second and higher layers, and is equal to the heat of liquefaction, R is the gas constant and T is the absolute temperature.

The BET equation describing the adsorption isotherm can be plotted as a straight line with $\frac{1}{v\left[\left(\frac{p_0}{p}\right)-1\right]}$ on the y-axis and $\frac{p}{p_0}$ on the x-axis. This is know as the 'BET plot'. From this plot v_m and c can be calculated from the extrapolation of the y intercept and the gradient, respectively. Once these have been obtained the surface area of the material can be found using the following equations:

$$S_{Total} = \frac{V_m N s}{V} \qquad \text{Equation 2.10}$$

$$S_{BET} = \frac{S_{total}}{a} \qquad \text{Equation 2.11}$$

Where v_m is the monolayer adsorbed gas quantity, N is Avogadro's number, s is the adsorption cross section of the adsorbing species, V is the molar volume of adsorbate gas and a is the mass of the solid sample. Analysis was carried out using a Quantachrome Quadrosorb instrument.

Before N_2 adsorption at 77 K, the samples (0.36 g) was placed in a glass sample bulb and degassed at 120 °C for 3 h under vacuum. Analysis was performed through a five-point BET method using adsorption data in the standard pressure range 0.05-0.3 P/P_0.

2.4.8. Infrared Fourier Transform Spectroscopy

Fourier Transform Infrared spectroscopy (FTIR) is considered one of the most powerful techniques for chemical analysis and in several applications in biological analysis (e.g. food). FT-IR can analyse solids and liquids without sample preparation. Fourier transform (FT) is a mathematical procedure that allows polychromatic radiation to be

used in IR experiments, which dramatically decreases the time it takes to obtain a spectrum, FT breaks down the interferogram provided by the interferometer into sine waves for each wavelength in the light and reconstructs the information to form the final IR spectrum.[12] The important components of an FTIR spectrometer are the interferometer, source, beam splitter, detector, and laser. The function of the detector is to transduce the light intensity received by it to electrical signal. The MCT detector is one of the most commonly used detectors. It is a semiconductor and the electrons present absorb IR light and move from the valence band to conduction band. These electrons in the conduction band generate an electrical current proportional to the IR intensity. MCT detectors are more sensitive, faster and provide a spectrum with higher signal to noise ratio (SNR). The MCT must be cooled, typically using liquid N_2.

The sample is simply placed on top of the attenuated total reflection (ATR) crystal. In case of solids, pressure must be applied (in form of a clamp) to ensure optimal contact between the sample and the ATR crystal. In case of liquids, a cover lid may be used to protect the sample from evaporation under vacuum conditions inside the spectrometer. The incident lights angle is set so that at the interface of the high refraction ATR crystal and the sample an evanescent wave is created that penetrates into the sample and interacts with it. This interaction results in absorption at wavelengths / energies that are informative of the chemical functional groups building up the sample. The penetration depth is dependent on the sample, the wavelength of the light and the ATR crystal material, as well as the quality of contact between them. The ATR accessories (Bruker) are mounted in a vacuum bench spectrometer (Vertex 70), operating spectral range of 4500 – 400 cm^{-1}, spectral resolution 4 cm^{-1}, scanning time 32 scan and scanner velocity is 10 kHz.

2.5. References

1. L. Prati and A. Villa, Catal., 2012, 2, 24-37.

2. J. Turkevich, Gold Bull., 1985, 18, 86-91.

3. J. W. Niemantsverdriet and Editor, Spectroscopy in Catalysis: An Introduction; Third, Completely Revised and Enlarged Edition, Wiley-VCH Verlag GmbH & Co. KGaA, 2007.

4. J. C. Yang, M. W. Small, R. V. Grieshaber and R. G. Nuzzo, Chem. Soc. Rev., 2012, 41, 8179-8194.

5. A. K. Cheetham and P. Day, 1987.

6. G. E. Jauncey, Proc. Natl. Acad. Sci., U S A, 1924, 10, 57-60.

7. A. L. Patterson, Phys. Rev., 1939, 56, 978-982.

8. U. Holzwarth and N. Gibson, Nat. Nanotechnol., 2011, 6, 534.

9. H. P. Klug and L. E. Alexander, X-Ray Diffraction Procedures for Polycrystalline and Amorphous Materials. 2nd ed, Wiley-Interscience, 1974.

10. K. S. W. Sing, Adv. Colloid Interface Sci., 1998, 76-77, 3-11.

11. S. Brunauer, P. H. Emmett and E. Teller, J. Am. Chem. Soc., 1938, 60, 309-319.

12. A. Subramanian and L. Rodriguez-Saona, in Infrared Spectroscopy for Food Quality Analysis and Control, ed. D.-W. Sun, Academic Press, San Diego, 2009, DOI: https://doi.org/10.1016/B978-0-12-374136-3.00007-9, pp. 145-178.

Chapter 3: Oxidation of *n*-Butanol over Pt/TiO_2 based catalysts

3.1. Introduction

Oxidation is an important method for the synthesis of chemical intermediates used for the manufacture of high-tonnage commodities, high-value fine chemicals, agrochemicals and pharmaceuticals.[1] The selective oxidation of alcohols is widely recognized as one of the most fundamental transformations in both laboratory and industrial synthetic chemistry, because the resulting compounds serve as important and versatile intermediates for the synthesis of fine chemicals. It is possible to use chromate or permanganate as stoichiometric oxygen donors, but these reagents are expensive, toxic and pose environmental issues.[2] Therefore, there is a need to replace stoichiometric oxidants with cheaper, readily available and environmentally friendly oxidants, *e.g.* O_2 and air.

Catalytic oxidation involving the use of molecular oxygen as oxidant has attracted great interest, as it is a clean alternative to conventional oxidants, offering environmental and economic benefits, and is a desired green process for selective oxidation of alcohols.[2] Thus, the goal has been directed towards the development of promising catalytic protocols employing O_2 as a primary oxidant, which is readily available and produces only water as a by-product in the selective oxidation of alcohols.[3] Alcohol oxidation is predominantly carried out in water, where the primary alcohols are oxidized to aldehydes and carboxylic acids (Scheme 3.1).[4]

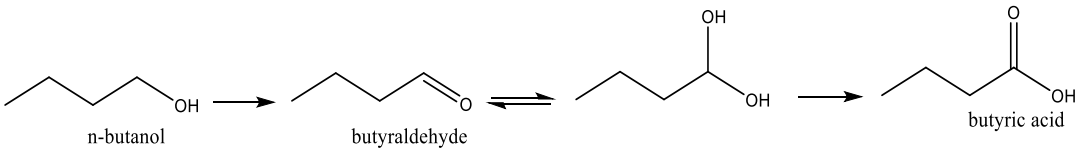

Scheme 3.1. Selective oxidation of *n*-butanol to butyraldehyde and butyric acid

It was previously reported that a 1 wt.%Pt/TiO_2 catalyst gives a high selectivity toward butyraldehyde (78.8 %) with a total *n*-butanol conversion of 31.4 %.[5] The goal of the present Chapter is to start with this catalyst and to study the effect of different parameters, such as the catalyst mass, Pt loading, effect of products of the reaction, temperature, pH, stirring rate on the activity of the catalyst. The previous study has shown that some Pt was leaching from the catalyst during the reaction, therefore the

effect of this leaching on the reaction has been carried out. The stability of the catalyst is an important parameter to make the process viable for industrial application and therefore, the reusability of the catalyst was investigated. The catalyst preparation and the catalyst testing protocol are described in detail in the experimental Chapter 2.

3.2. Mass transfer study

3.2.1. Effect of the catalyst mass

To determine if the oxidation of *n*-butanol is diffusion limited, differing masses of the 1 wt.%Pt/TiO_2 catalysts were tested at 100 °C, 3 bar O_2 for 2 h. A reaction time of 2 h was used for these experiments to ensure that the experiments were conducted at low conversion, to ensure that the conversion was not limited by the quantity of substrate available. The initial concentration of *n*-butanol was 0.54 M. The data is reported in Figure 3.1.

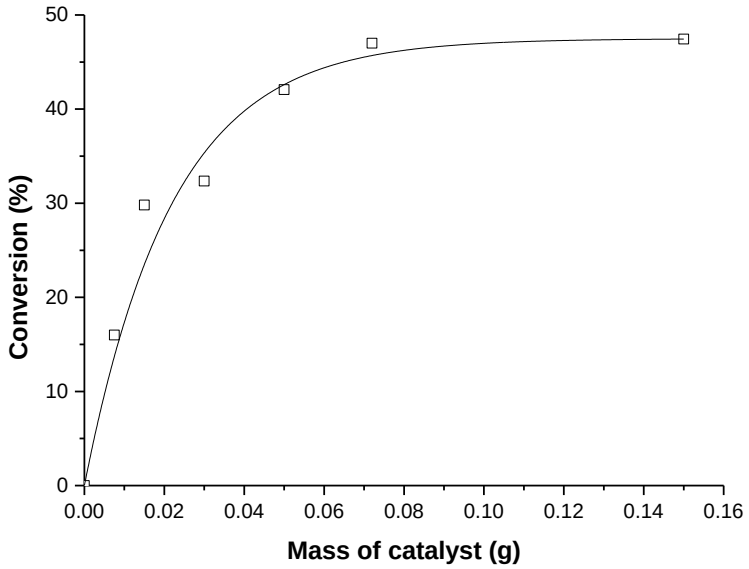

Figure 3.1. Conversion as a function of varying mass of 1 wt.%Pt/TiO_2 catalyst for selective oxidation of *n*-butanol. ***Reaction conditions*:** 100 °C, 3 bar O_2, 2 h, *n*-butanol (10 mL, 0.54 M), 750 rpm.

The data shows that the conversion of *n*-butanol increases from 30 % for 15 mg of catalyst to 42 % for 50 mg. After 50 mg up to 150 mg there was only a slight increase of the conversion to 47 %, despite the amount of catalyst used being 3 times higher. These results indicate that below 15 mg the reaction is under a kinetic regime and above 15 mg the reaction is under a diffusion regime.[6] Transport of reactant to the catalyst is the physical process, whereby the reactants are transported through liquid

phase surrounding the solid catalyst to the active sites on the catalyst's surface. This is a diffusion process, and the phenomenon is called mass transport.[6] The diffusion regime indicates that the observed activity of the catalyst is decreased by either the transfer of *n*-butanol or O_2 to the catalyst, or the removal of products, which becomes the limiting-step during the reaction. Therefore, it is more suitable to use a catalyst mass, which is below 15 mg to avoid the effect of this mass transfer limitation. Based on this result all the following experiments in this Chapter have been performed with a catalyst mass of 15 mg.

3.2.2. Effect of the stirring rate

A variation of reaction stirring speed was performed using 1 wt.%Pt/TiO_2 catalyst under standard reaction conditions, and the activity data are presented in Figure 3.2. The aim is to observe the effect of the stirring speed on the reaction and its an additional way to ensure that there are no mass transfer limitations and the reaction is operating within the kinetic regime.

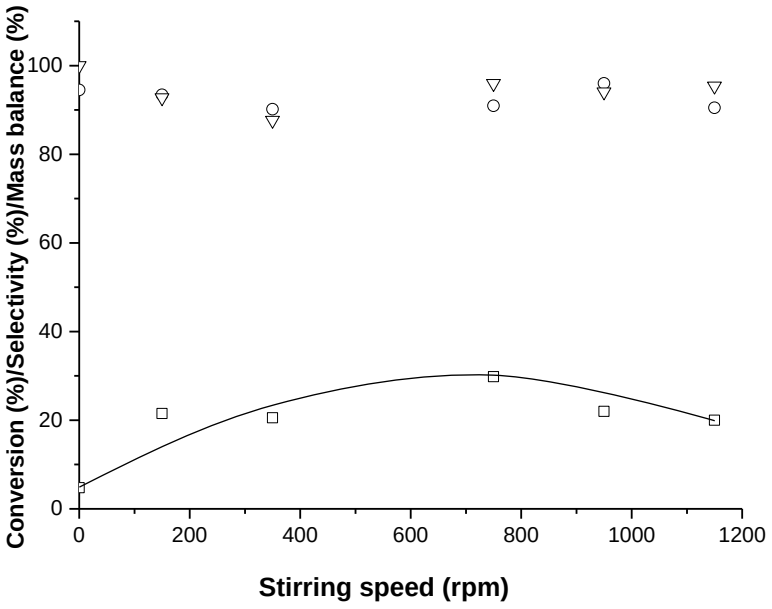

Figure 3.2. Influence of varied reaction stirring speed using 1 wt.%Pt/TiO_2 catalyst for selective oxidation of *n*-Butanol. ***Reaction conditions*****:** 3 bar O_2, 120 min, *n*-butanol (10 mL, 0.54 M), catalyst (15 mg). □ Conversion of *n*-butanol, ○ Butyraldehyde Selectivity, ▽ Carbon Mass balance.

The effect of stirring speed on the conversion was investigated by increasing from 0 to 1150 rpm with the magnetic stirrer as shown in Figure 3.2. This plot illustrates how the

conversion was influenced by the stirring speed. Selectivity of butyraldehyde slightly increased with stirring speed, up to a maximum of 96 % at 950 rpm. The results show that when the stirring speed increased from 0 to 1150 rpm, the conversion of *n*-butanol shows a volcano shape, with a maximum at 750 rpm, where the conversion of *n*-butanol reaches 30 %. Although increasing the stirring speed should be beneficial for enhancing *n*-butanol oxidation as it improves the mass transfer,[7] a decrease in activity at stirring speed > 750 rpm was observed. The reason could be addressed to non-homogeneous stirring that forces the catalyst onto the internal wall of the colavor reactor vessel avoiding a homogeneous mixing. The possibility of the catalyst contacting with reactants would decrease. This would result in the decrease of reaction conversion.[8]

3.3. Effect of reaction conditions

3.3.1. Effect of reaction temperature

Variation of reaction temperature was performed using the 1 wt.%Pt/TiO_2 catalyst under standard reaction conditions and the activity data are presented in Figure 3.3. The aim was to observe the effect of the temperature on the reaction.

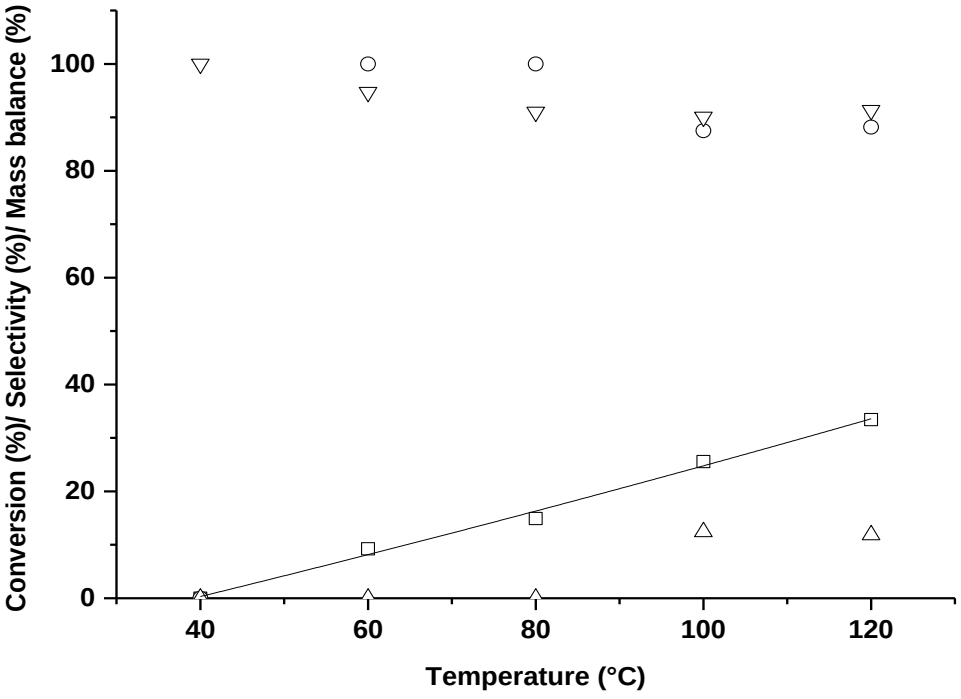

Figure 3.3. Influence of varying reaction temperatures using 1 wt.%Pt/TiO_2 catalyst for selective oxidation of *n*-butanol. ***Reaction conditions*****:** 3 bar O_2, 120 min, *n*-butanol (10 mL, 0.54 M), catalyst (15 mg), 750 rpm. □ Conversion of *n*-Butanol, ○ Butyraldehyde Selectivity, △ Butyric Acid Selectivity, ▽ Carbon Mass balance.

From Figure 3.3 no activity was observed at 40 °C. Above 40 °C, the *n*-butanol conversion increased and butyraldehyde was produced. Further Increase in temperature up to 60 °C showed 9 % conversion with full selectivity to butyraldehyde. At 80 °C the conversion was 15 % again with full selectivity to butyraldehyde. A much higher conversion was observed at 100 °C (30 %) with selectivity towards butyraldehyde and butyric acid of 91 and 9 % respectively, with a mass balance of 96 %. Between 100 and 120 °C there is no further increase in the conversion of *n*-butanol and selectivity of butyraldehyde and butyric acid, which is possibly due to leaching and sintering.

3.3.2. Effect of the pH

A previous study has reported the effect of pH on the platinum-catalyse oxidation of glucose to gluconic acid.[9] Poisoning of the catalyst by the reaction products in neutral and acidic medium was observed, and the degree of the inhibition of the catalytic activity was pH dependent. D-Gluconic acid in its 'free' form is considered to be the main inhibiting species of the platinum catalyst during the oxidation of glucose in acidic medium.[9] Based on this it has been decided to study the effect of pH on the reaction rate.

The pH before reaction when no base is added is 6.20. This pH drops down to 2.7 after two hours reaction. It has been reported in the literature review Chapter that alkaline pH prevents the catalyst from leaching, but the product distribution is affected and more acid is produced at the expense of the aldehyde. In this section the influence of pH, above 6.20, has been tested and the data are reported in Figure 3.4.

To perform these experiments the pH at t = 0 is adjusted with a solution of 0.05 M NaOH (strong base) and 0.06 M HCl (strong acid), with fresh catalysts prepared and then tested.

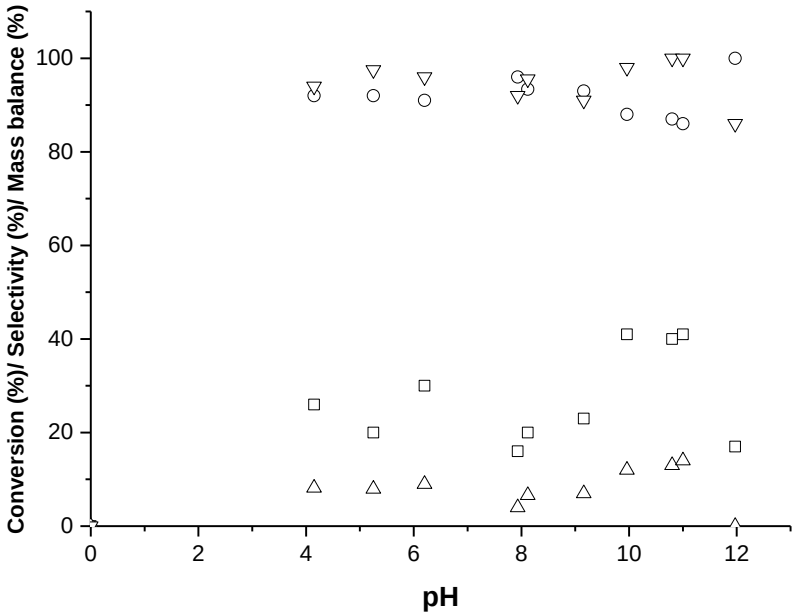

Figure 3.4. Effect of the pH (the pH at t = 0 adjusted) on the oxidation of *n*-butanol over 1 wt.%Pt/TiO_2.***Reaction conditions*:** 100 °C, 2h, 3 bar O_2, *n*-butanol (0.54 M), NaOH (0.05 M), HCl (0.06 M), 750 rpm. □ Conversion of *n*-Butanol, ○ Butyraldehyde Selectivity, △ Butyric Acid Selectivity, ▽ Carbon Mass balance.

The results reported in Figure 3.4 show a significant increase in the rate of alcohol oxidation at pH > 6.20, the selectivity toward butyraldehyde decreases in favour of butyric acid. A previous study showed that during alcohol oxidation the rise of the pH promotes the *n*-butanol conversion and the selectivity toward the acid.[10] Another study indicated that alcohol oxidation over supported catalysts (Au, Pt, and Pd) proceeds by dehydrogenation to an aldehyde or ketone intermediate, followed by oxidation to acid product. In an aqueous environment, the initial deprotonation of the alcohol to form an alkoxy intermediate occurs in basic solution, and the extent of the reaction is related to the system pH [the pK_a (where Ka is the acid dissociation constant) of alcohol is approximately 16].[11] The initial activation of the alcohol can also occur on the catalyst surface. The presence of surface bound hydroxide intermediates, however, can facilitate O-H bond activation via proton transfer in much the same way as it occurs in solution. The presence of adsorb hydroxide intermediates also lowers the barrier for the subsequent activation of C-H bond of ensuing alkoxide intermediate to form aldehyde.[10] This helps to explain the overall increase in catalytic activity of the noble metal at high pH. During the oxidation reaction several roles for O_2 in water at high pH have been proposed, including direct participation of atomic O during dehydrogenation reactions, the reduction of atomic O to water through H atoms adsorbed on the surface, the direct

oxidation of the intermediate aldehyde with atomic O to form the O-insertion acid product, and the removal of strongly bound organic adsorbates such as CO through oxidation.[10] At pH = 12 the conversion of *n*-butanol drops down to 17 % and only butyraldehyde is detected in the solution (selectivity = 100 %). The selectivity to aldehyde generally decreased at the expense of the acid as the pH increased. However, at pH 12, no acid is observed, which coincides with a significant drop in the carbon mass balance (86 %). There is no clear correlation between pH and conversion/ selectivity in Figure 3.4. This phenomenon is not clearly understood yet.

3.4. Effect of the Pt weight loading

The aim of this section is to show first the effect of different percentage of Pt loading on TiO_2 on the conversion of *n*-butanol and on the selectivity toward the different products. A series of wt.%Pt/TiO_2 catalysts with Pt weight loadings of 0.1 wt.%, 0.25 wt.%, 0.5 wt.% and 1 wt.% were prepared and tested for the oxidation of *n*-butanol at 100 °C, 3 bar O_2 for 6 h, Appendix A. The results are reported in Figure 3.5.

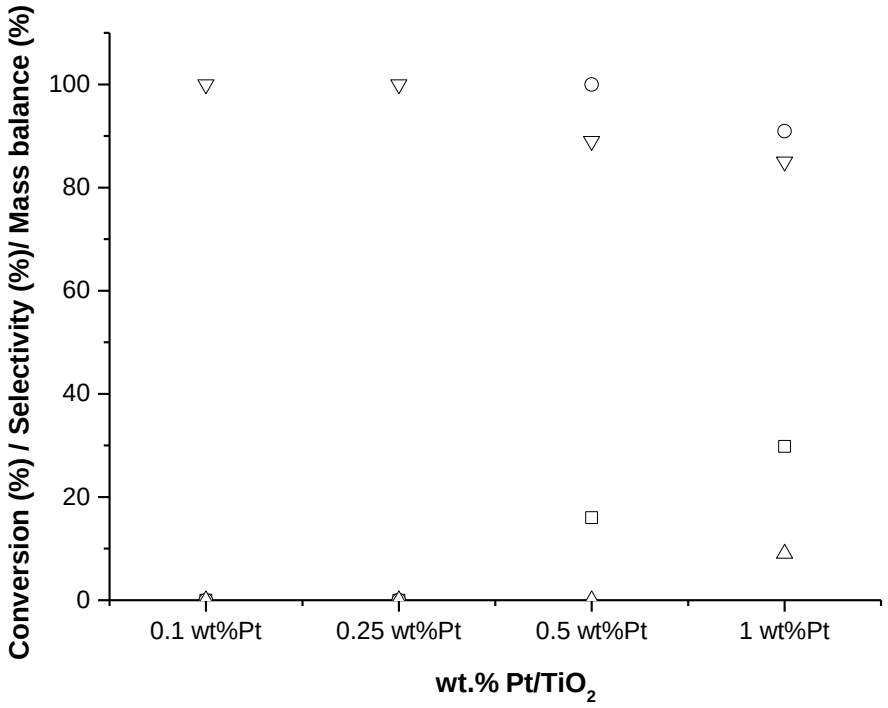

Figure 3.5. Effect of variation of Pt loading on TiO_2 catalyst for selective oxidation of *n*-butanol. ***Reaction conditions*****:** 100 °C, 3 bar O_2, 6 h, *n*-butanol (10 mL, 0.54 M), catalyst (15 mg), 750 rpm. □ Conversion of *n*-Butanol, ○ Butyraldehyde Selectivity, △ Butyric Acid Selectivity, ▽ Carbon Mass balance.

The data shows that after 6 h there was no conversion of *n*-butanol with 0.1 and 0.25 wt.%Pt/TiO_2 catalyst, increasing the Pt loading from 0.25 wt.% to 1 wt.% enhanced the *n*-butanol conversion.[12] The conversion of *n*-butanol becomes 16 % when 0.5 wt.% catalyst was used, then the conversion increased to 30 % when 1 wt.%Pt/TiO_2 was used, these data are consistent with the amount of metal being doubled.

It can be noted, that by increasing the Platinum metal loading from 0.5 wt.% to 1 wt.% the selectivity, of butyraldehyde, decreased from 100 % to 90 % and the selectivity towards butyric acid increased from 0 % to 9 %. Furthermore, for 0.1 wt.% and 0.25 wt.%Pt/TiO_2 the mass balance was 100 %, however, the mass balance increased to 89 % and 96 % for 0.5 and 1 wt.%Pt/TiO_2 respectively. The decrease in selectivity to butyraldehyde is predominantly due to the sequential oxidation of the aldehyde to butyric acid, however, a previous study reported that carbon dioxide can be formed from the decarboxylation of butyric acid (Scheme 3.2).[4, 5, 13-15]

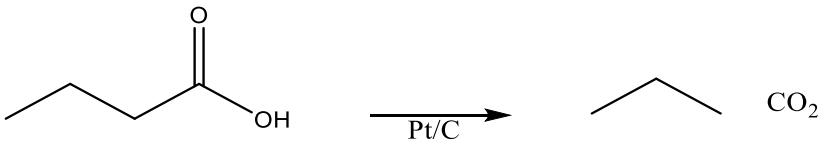

Scheme 3.2. Butyric acid decarboxylation.[13]

In order to establish whether the loss in carbon was attributed to the decarboxylation of butyric acid, an additional experiment was conducted in a stainless steel Parr autoclave over the 1 wt.%Pt/TiO_2 catalyst (reaction conditions: 100 °C, 6h, 3 bar O_2). Organic keto acids can undergo oxidative decarboxylation reactions, which can result in the formation of CO_2 (Scheme 3.3). Given that butyric acid is not a keto acid, it was unsurprising to observe than only traces of CO_2 were measured in the gas phase and no corresponding C_3 species were detected in the liquid phase.[16-18]

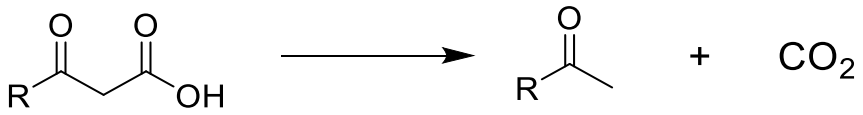

Scheme 3.3. The decarboxylation of a keto-acid resulting in the formation of CO_2.

An alternative explanation could be that butyric acid reacts stoichiometrically with butanol, the reactivity of which would likely be enhanced in the presence of an acid

catalyst and would result in the formation of the corresponding C_8 ester (Scheme 3.4).[19-29]

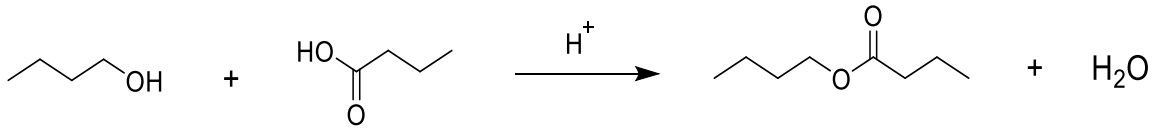

Scheme 3.4. Acid catalysed reaction of *n*-butanol and butyric acid producing the corresponding ester.

In order to determine how the catalytic performance proceeded over time some additional experiments were conducted. Therefore, time on-line studies on 0.5 wt.%Pt/TiO_2 and 1 wt.%Pt/TiO_2 catalysts were performed. The data for 0.5 wt.%Pt/TiO_2 and 1 wt.%Pt/TiO_2 are shown in Figures 3.6 and 3.7 respectively.

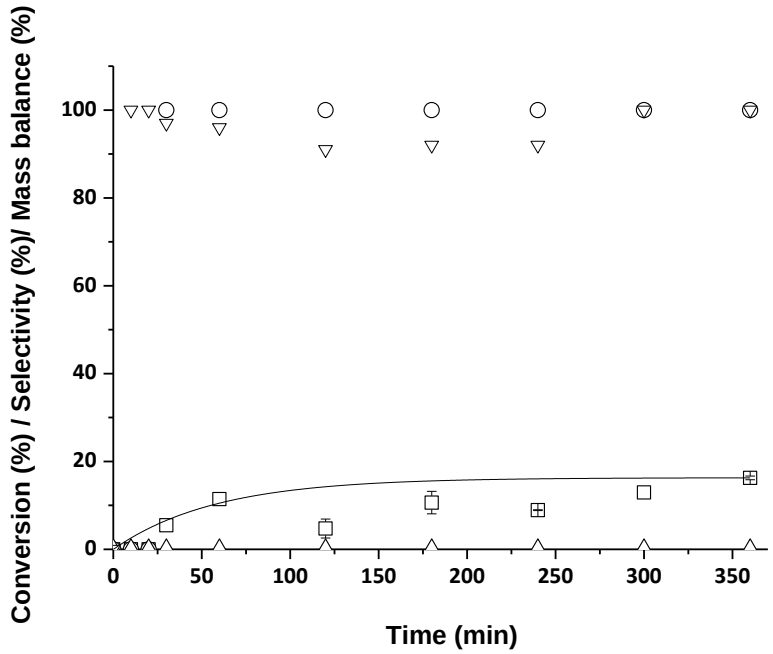

Figure 3.6. Time on-line data for 0.5 wt.%Pt/TiO_2 catalyst for selective oxidation of *n*- butanol. ***Reaction conditions*****:** 100 °C, 3 bar O_2, *n*-butanol (10 mL, 0.54 M), catalyst (15 mg), 750 rpm. □ Conversion of *n*-Butanol, ○ Butyraldehyde Selectivity, △ Butyric Acid Selectivity, ▽ Carbon Mass balance.

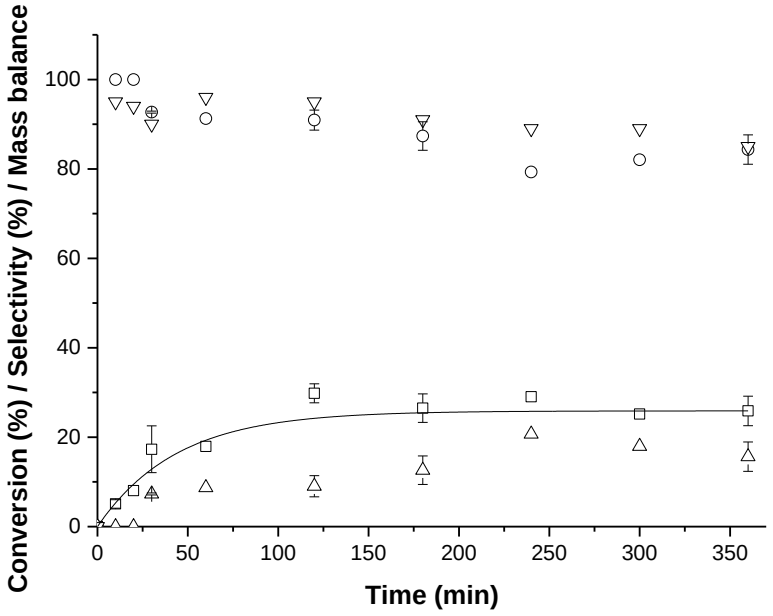

Figure 3.7. Time on-line data for 1 wt.%Pt/TiO_2 catalyst for selective oxidation of *n*- butanol. ***Reaction conditions*****:** 100 °C, 3 bar O_2, *n*-butanol (10 mL, 0.54 M), catalyst (15 mg), 750 rpm. □ Conversion of *n*-Butanol, ○ Butyraldehyde Selectivity, △ Butyric Acid Selectivity, ▽ Carbon Mass balance.

For 0.5 wt.% Pt/TiO_2 the conversion reached 11 % after 1 h and butyraldehyde is the main primary product, Figure 3.6. After 2 h the conversion of *n*-butanol and the selectivity toward butyraldehyde remains almost the same until the end of the 6 h reaction time.

In the case of 1 wt.%Pt/TiO_2 the conversion of *n*-butanol increased up to 30 % after 2 h and remains the same until the end of the 6 h reaction period. The selectivity toward butyraldehyde undergoes different regimes during this time. Indeed, after 2 h the selectivity decreased from 100 % to 91 %, then after 4 h the selectivity of butyraldehyde remained the same until the end of the time on-line. Butyric acid is the secondary product, which appears when the selectivity of butyraldehyde starts to decrease.

From this result it can be observed that the two catalysts, 0.5 and 1 wt.%Pt/TiO_2, over a 6 h reaction period show different behaviour. First for the 0.5 wt.%Pt/TiO_2, the conversion of *n*-butanol remained almost the same after 2 h and the selectivity toward butyraldehyde remained the same after 6 h. This observation seems to indicate that the catalyst is totally deactivated after 2 h of reaction. In the case of the 1 wt.%Pt/TiO_2 catalyst, the conversion of *n*-butanol stops after 2 h and the selectivity of butyraldehyde decreases and butyric acid is formed. In this case the catalyst is still active and it seems

to promote the conversion of butyraldehyde into butyric acid. But after 4 h there was no more conversion of butyraldehyde into butyric acid, which seems to indicate that the catalyst is totally deactivated.

Previous studies show that when carbon is used as a support, 1 wt.%Pt/C shows a higher conversion (85.9 %) of *n*-butanol compared to the 1 wt.%Pt/TiO_2 (31.4 %) prepared under the same conditions.[5] This study also revealed that the selectivity toward butyraldehyde is higher when TiO_2 (78.8 %) is used as a support instead of C (21.2 %). Carbon is considered to reduce the rate of oxidation of Pt, by an electronic effect.[30-31] However, according to the results of Bogotski and Snudkin the electron density on platinum is increased due to the catalyst support.[30, 32]

Brunauer–Emmett–Teller (BET) surface area of TiO_2 catalysts with the variation of platinum loading are shown in Table 3.1.

Table 3.1. BET surface areas of TiO_2 catalysts with the variation of Pt loading.

Sample	BET Surface Area (m^2/g)
TiO_2	49
0.1 wt.%Pt/TiO_2	53
0.25 wt.%Pt/TiO_2	55
0.5 wt.%Pt/TiO_2	52
1 wt.%Pt/TiO_2	55

From data in Table 3.1 it can be seen that compared to TiO_2 (49 m^2/g), surface area of a series of wt.% Pt/TiO_2 catalysts with Pt weight loadings of 0.1 wt.%, 0.25 wt.%, 0.5 wt.% and 1 wt.% are similar, there is approximately a 10 % error on these measurements. Hence, deposition of small Pt nanoparticles on TiO_2 show no significant difference from the TiO_2 support after different loadings of metal, as all are within experimental error.

The X-Ray Diffraction (XRD) patterns of the supported catalysts are shown in Figure 3.8.

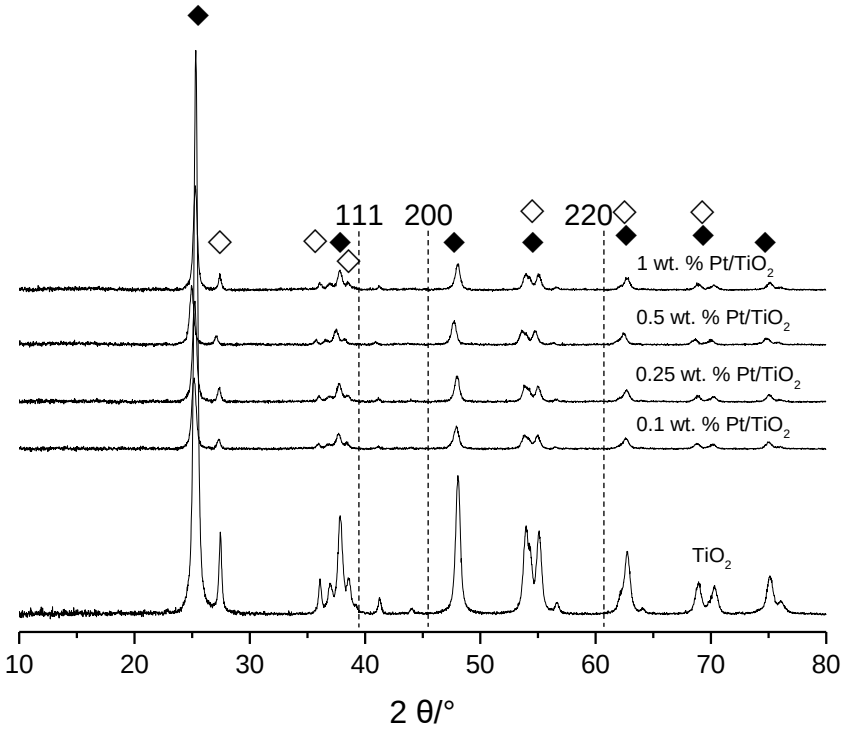

Figure 3.8. X-ray diffraction patterns of supported TiO_2 catalysts with varying Pt loadings. ◆ Anatase ◇ Rutile ¦ Pt.

Figure 3.8 shows that the XRD pattern of the Pt loadings of 0.1 wt.%, 0.25 wt.%, 0.5 wt.% and 1 wt.% are essentially the same as that of the TiO_2. However, as reported in previous studies,[12] the absence of diffraction lines corresponding to platinum within the XRDs of the supported platinum catalysts (2Θ/°of 39^0 (111), 46^0 (200) and 67^0 (220)), indicating that the relatively low loading of platinum is highly dispersed, with a small average particle size. However, XPS analysis (see section 3.6.1) does reveal that all samples contain Pt that is metallic in nature with a binding energy of 70.8 eV.

To study the catalyst deactivation, an investigation into product inhibition was made. This was to see if there was an inhibiting effect of butyraldehyde or butyric acid on the conversion of *n*-butanol. The effect of products on the activity of the catalyst has been studied and the results are introduced in the next section.

3.5. Effect of products on the activity of the catalyst 1 wt.%Pt/TiO_2

The main motivation for running these experiments is based on the observation of catalyst deactivation that has been shown in Figure 3.7. Butyraldehyde and butyric acid are the main products of the reaction of *n*-butanol oxidation. With the aim to understand their effect on the activity of the 1 wt.%Pt/TiO_2, three kinds of experiments have been performed: Firstly, a solution containing only butyraldehyde was tested over the

catalyst. Secondly, a solution containing 4 wt.% *n*-butanol and 1 wt.% butyraldehyde have been prepared and tested using the catalyst. Thirdly, a solution containing 4 wt.% *n*-butanol and 1 wt.% butyric acid has been prepared and tested over the catalyst.
It was important to consider first how these substrates were affected by reaction conditions. The data without catalyst are reported in Table 3.2.

Table 3.2. Conversion of solutions containing 4 wt.%*n*-butanol, 1 wt.% butyraldehyde **without** catalyst.

Substrate	Conv. BuALD (%)	Sel. BuAC (%)	Mass balance (%)	
			***n*-BuOH**	**BuALD**
4 wt.% BuALD (0.55 M)	83	100	-	79
4 wt.% n-BuOH + 1 wt.% BuALD (0.14 M)	0	0	100	100
4 wt.% n-BuOH + 0.8 wt.% BuALD (0.11 M)	0	0	100	100
4 wt.% n-BuOH + 0.5 wt.% BuALD (0.07 M)	0	0	100	100
4 wt.% n-BuOH + 0.1 wt.% BuALD (0.01 M)	0	0	100	100

Conversion (Conv.), Selectivity (Sel.), *n*-Butanol (*n*-BuOH), Butyraldehyde (BuALD), Butyric Acid (BuAC). ***Reaction conditions*:** 100 °C, 2h, 3 bar O_2, *n*-butanol (0.54 M), 750 rpm.

Table 3.2 shows that when *n*-butanol and butyraldehyde are put in solution without catalyst, there is no conversion of either *n*-butanol or butyraldehyde. Accordingly, it seems that in solution without catalyst the auto-oxidation of butyraldehyde is also inhibited by the presence of *n*-butanol. The same effect was reported by Inaki *et al.*[5] Their results demonstrate that in an aqueous phase the oxidation of butyraldehyde to butyric acid in the presence of *n*-butanol is inhibited for this uncatalysed oxidation reaction. It was determined that the alcohol inhibit the formation of the acids by intercepting the peroxy radicals, which play a key role in the aldehyde uncatalysed oxidation reaction (Scheme 3.5). Also Meenakshisundaram *et al.*[33] confirmed that benzyl alcohol (and a number of other alcohols), even at low concentrations in benzaldehyde, inhibits the autoxidation of benzaldehyde.

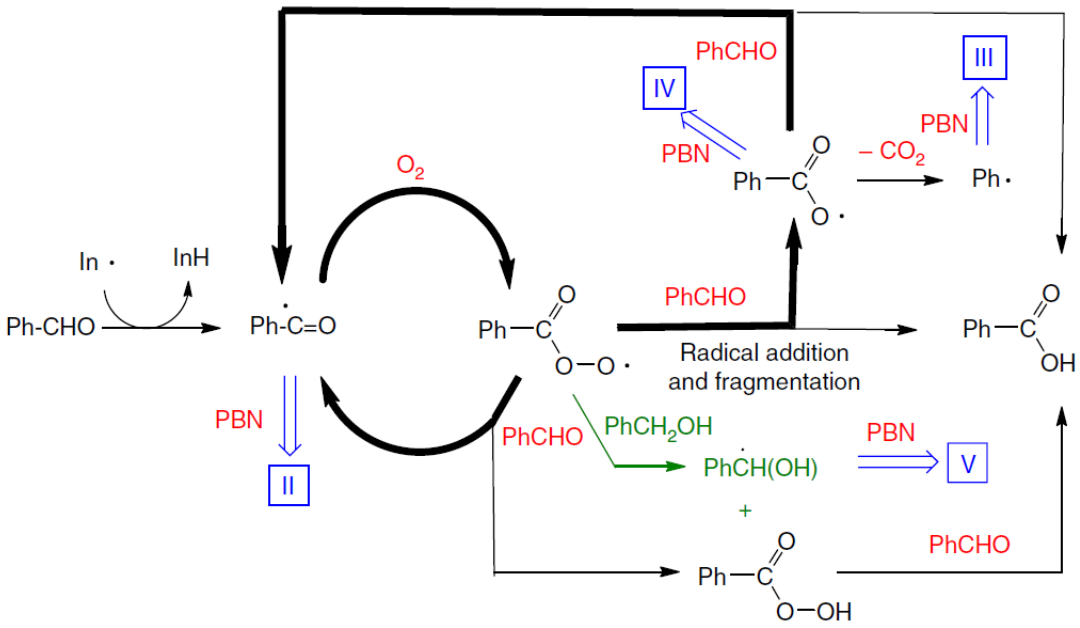

Scheme 3.5. Proposed reaction scheme for benzaldehyde autoxidation. Bold arrows indicate the main radical chain processes, while blue arrows represent the formation of the PBN-spin adducts II, III, IV and V. Key: In • : radical initiator. [33]

The inhibitory effect of benzyl alcohol on benzaldehyde autoxidation is associated with the low bond dissociation energy of C–H bonds in the α-position relative to the hydroxyl group, and is enhanced since the α-Hs are also benzylic. In wholly aliphatic systems, a hydroxyl group lowers the bond strength of an α-C–H bond substantially, compared with the parent hydrocarbon, but a C–H bond adjacent to a –CHO group is even weaker, which may be the case here. In Table 3.3, the conversion of butyraldehyde with catalyst is reported, with the aim to measure the effect of the auto-oxidation contribution. In all cases there is no prior pre-treatment of the catalyst.

Table 3.3. Conversion of solutions containing 4 wt.%*n*-butanol, 1 wt.%butyraldehyde or 1 wt.%butyric acid over fresh (as-obatined) 1 wt.%Pt/TiO_2 catalyst.

Entry	Substrate	Conv. *n*-BuOH (%)	Conv. BuALD (%)	Sel. (%)			Mass balance (%)	
				n-BuOH source		BuALD source		
				BuALD	BuAC	BuAC	*n*-BuOH	BuALD
1	**4 wt.%*n*-BuOH**	30	-	90	9	0	96	-
2	**4 wt.% BuALD (0.55 M)**	0	91	-	-	100	-	90
3	**4 wt.%*n*-BuOH + 1 wt.%BuALD (0.14 M)**	0	19	-	-	100	100	85
4	**4 wt.%*n*-BuOH + 1 wt.%BuAC (0.11 M)**	24	0	100	-	-	90	-

Conversion (Conv.), Selectivity (Sel.), *n*-Butanol (*n*-BuOH), Butyraldehyde (BuALD), Butyric Acid (BuAC). ***Reaction conditions*:** 100 °C, 2h, 3 bar O_2, *n*-Butanol (0.54 M), 15 mg of catalyst, 750 rpm.

Entry 1 of Table 3.3 reports the conversion of *n*-butanol and the selectivity towards butyraldehyde and butyric acid when only *n*-butanol is in the solution with the catalyst. After 2 h, 30 % of *n*-butanol is converted into 91 % butyraldehyde and 9 % butyric acid. Entry 2 of the table reports the conversion of butyraldehyde and the selectivity towards butyric acid when 4 wt.% butyraldehyde is in solution with the catalyst. After 2 h, 91% of butyraldehyde is converted into butyric acid. Butyraldehyde is rapidly oxidised into butyric acid. The non-catalytic oxidation of butyraldehyde into butyric acid, which is reported in Table 3.2, shows that the contribution of the catalyst to the oxidation of butyraldehyde into butyric acid is only 9 %. This information means that the catalyst can hinder the butyraldehyde conversion into butyric acid, and the catalyst plays an important role in this step.

Entry 3 of Table 3.3 reports the conversion of *n*-butanol and butyraldehyde and the selectivity toward butyric acid, when 4 wt.%*n*-butanol is mixed with 1 wt.% butyraldehyde. It can be noticed there is no conversion of *n*-butanol and 19 % of butyraldehyde is converted into 100 % butyric acid. This data supports the fact that butyraldehyde inhibits the conversion of *n*-butanol, which has been reported already in

the literature.[34] One of the hypothesis proposed is that butyraldehyde occupied the same active site as *n*-butanol, suppressing oxidation of alcohol. Then butyraldehyde is preferentially converted into butyric acid.[15]

Entry 4 of Table 3.3 reports the conversion of *n*-butanol and butyraldehyde and the selectivity toward butyraldehyde, when 4 wt.% *n*-butanol is mixed with 1 wt.%butyric acid. Considering the calculated margin of error, the conversion of *n*-butanol is almost the same as when 4 wt.%*n*-butanol is present alone in the solution. It is clear from these data, that butyric acid does not inhibit the conversion of *n*-butanol. Since addition of simple acids to the oxidation reaction did not inhibit the reaction rate, carboxylic acids do not compete with alcohol substrates for the catalyst surface sites.[34] However, the selectivity toward butyraldehyde was 100 % when butyric acid was present in the initial solution.

The addition of butyric acid to the catalyst may promote the leaching of Pt.[5,35] The pH of the solution when 1 wt. % butyric acid was added to the solution was 2.9 before the reaction, and after the reaction the pH was 2.9. This hypothesis will be further investigated in the next sections.

With the aim to see what the minimum concentration of *n*-butanol is needed to avoid the conversion of butyraldehyde, in the presence of catalyst, different ratios of n-butanol/butyraldehyde have been tested and the results are reported on Table 3.4.

Table 3.4. Conversion of solutions containing 4 wt.%*n*-butanol and different concentration of butyraldehyde over 1 wt.%Pt/TiO_2.

Substrate	Conv. *n*-BuOH (%)	Conv. BuALD (%)	Sel. (%)			Mass balance (%)	
			n-BuOH source		BuALD source	*n*-BuOH	BuALD
			BuALD	BuAC	BuAC		
4 wt.%*n*-BuOH	30	0	91	9	0	94	-
4 wt.%BuALD (0.55 M)	0	91	0	0	100	-	90
4 wt.% *n*-BuOH + 1 wt.%BuALD (0.14 M)	0	19	0	0	100	100	85
4 wt.% *n*-BuOH + 0.8 wt.%BuALD (0.11 M)	10	-	-	-	-	90	-
4 wt.% *n*-BuOH + 0.5 wt.%BuALD (0.07 M)	21	-	-	-	-	93	-
4 wt.%*n*-BuOH + 0.1 wt.%BuALD (0.01M)	20	-	-	-	-	100	-

Conversion (Conv.), Selectivity (Sel.), *n*-Butanol (*n*-BuOH), Butyraldehyde (BuALD), Butyric Acid (BuAC). ***Reaction conditions*:** 100 °C, 2h, 3 bar O_2, *n*-Butanol (0.54 M), 15 mg of catalyst, 750 rpm.

In Table 3.4 the conversion of *n*-butanol and butyraldehyde is reported when different concentrations of butyraldehyde are introduced into a solution of *n*-butanol. It can be noticed that when the concentration of butyraldehyde is lowered to 0.5 wt.% and 0.1 wt.%, the conversion of *n*-butanol was enhanced. The calculated conversion for *n*-butanol is of *ca.* 20 % in both cases. The difference between the two systems relies on the mass balance, which is 93 % for the 0.5 wt.%Butyraldehyde addition and 100 % for the 0.1 wt.%. The former mass balance being lower means that some products may be formed in the gas phase, it may be carbon dioxide as it has also been measured in the previous experiments reported in the previous section.

The calculation of the conversion and selectivity of butyraldehyde and butyric acid is very complex, therefore the results are not reported, as butyraldehyde is present in the initial solution. These results indicate that there is a maximum concentration of butyraldehyde in the solution for which the *n*-Butanol is not converted anymore.

In Table 3.5 the catalyst has been calcined at 200 °C (5 °C/min) for 2 h under air and the effect of the addition of butyraldehyde and butyric acid on the conversion of *n*-butanol and on the product distribution are reported.

Table 3.5. Conversion of *n*-butanol and selectivity toward butyraldehyde and butyric acid, with solutions containing 4 wt.% *n*-butanol, 1 wt.%butyraldehyde or 1 wt.% butyric acid over **calcined** 1 wt.%Pt/TiO_2.

Entry	Substrate	Conv. *n*-BuOH (%)	Conv. BuALD (%)	Sel. (%)			Mass balance (%)	Leaching (%)
				n-BuOH source		BuALD source		
				BuALD	BuAC	BuAC		
1	**4 wt.% *n*-BuOH**	24	-	94	5	-	100	3.3
2	**4 wt.%BuALD (0.55 M)**	-	54	0	0	100	82	2.8
3	**4 wt.%*n*-BuOH + 1 wt.%BuALD (0.14 M)**	-	-	-	-	-	100	1.5
4	**4 wt.% *n*-BuOH + 1wt.%BuAC (0.11 M)**	7	-	25	-	-	100	0.9

Conversion (Conv.), *n*-Butanol (*n*-BuOH), Selectivity (Sel.), Butyraldehyde (BuALD), Butyric Acid (BuAC). ***Reaction conditions*****:** 100 °C, 2h, 3 bar O_2, *n*-butanol (0.54 M), 15 mg of catalyst, 750 rpm. ***Catalysts pre-treated by:*** Calcined under air for 2 h at 200 °C (5 °C/min).

Entry 1 of Table 3.5 shows the conversion of *n*-butanol and the selectivity towards butyraldehyde and butyric acid, when 4 wt.%*n*-butanol is used, over an calcined 1 wt.%Pt/TiO_2 catalyst. The results showed that the conversion of *n*-butanol increases slightly when the catalyst was not calcined (*i.e.* 30 *%)*. The selectivity toward butyraldehyde shows no improvement (94 %), compared to when the catalyst is not calcined (91 %), which is within ± 4% experimental error.

Entry 2 reports the conversion of butyraldehyde and the selectivity toward butyric acid when a solution of 4 wt.% butyraldehyde is used.

Entry 3 of the Table shows that when the 4 wt.%*n*-butanol and 1 wt.% butyraldehyde are mixed together and tested over the calcined Pt catalyst, there is no conversion of *n*-butanol and neither is there conversion of butyraldehyde. When the catalyst was not calcined, 19 % of butyraldehyde was converted into butyric acid. All these results suggest that butyraldehyde may bind quickly to the calcined platinum and is strongly bound to the active site suppressing any conversion of either *n*-butanol and butyraldehyde.

Entry 4 shows the conversion of *n*-butanol when butyric acid is added to the solution. The results are different from those obtained on the non-calcined catalyst. Indeed here, the conversion of *n*-butanol is 7 % when it was of 24 % with the non-calcined catalyst. Furthermore, the experiments have shown that the initial amount of butyric acid introduced into the solution remains the same at the end of the reaction. Therefore, the aldehyde formed is not converted into acid.

From these results several observations can be made when the catalyst is calcined: Firstly, when *n*-butanol is present alone in the initial solution, it can be converted on the calcined platinum and the conversion is close to the catalyst prepared by sol- immobilisation and dried at 110 °C under air for 16 h. However, the mass balance and the selectivity toward butyraldehyde are higher. Second, when butyraldehyde is present alone in the solution, only 54 % of it is converted into butyric acid, and the mass balance is 82 % which is likely to be due to decarboxylation of butyric acid (as shown previously in Scheme 3.2). Secondly, the addition of 1 wt.%butyraldehyde to *n*-butanol in the initial solution inhibits the conversion of both *n*-butanol and butyraldehyde.[5] Thirdly, the addition of butyric acid to the initial solution of *n*-butanol decreases the conversion of *n*-butanol to 7 %.

In Table 3.6 the same experiments performed this time on the reduced catalyst are reported. For all the experiments the catalyst is heat treated in 5 vol.%H_2/Ar at 200 °C for 2 h.

Table 3.6. Conversion of solutions containing 4 wt.%*n*-butanol, 1 wt.% butyraldehyde or 1 wt.%butyric acid over **5 vol.%H_2/Ar** heat treatment 1 wt.%Pt/TiO_2 catalyst.

Entry	Substrate	Conv. *n*-BuOH (%)	Conv. BuALD (%)	Sel. (%)			Mass balance (%)	Leaching (%)
				n-BuOH Source		BuALD Source		
				BuALD	BuAC	BuAC		
1	**4 wt.% *n*-BuOH**	43	-	93	7	-	100	3.1
2	**4 wt.% BuALD (0.55 M)**	-	83	-	-	100	47	2.7
3	**4 wt.% *n*-BuOH + 1 wt. % BuALD (0.14 M)**	12	-	-	-	-	94	4.7
4	**4 wt.% *n*-BuOH + 1 wt.% BuAC (0.11 M)**	14	-	37	-	-	97	1.0

Conversion (Conv.), Selectivity (Sel.), *n*-Butanol (*n*-BuOH), Butyraldehyde (BuALD), Butyric Acid (BuAC). ***Reaction conditions*****:** 100 °C, 2h, 3 bar O_2, *n*-butanol (0.54 M), 15 mg of catalyst. ***Catalysts pre-treated by:*** 5 vol.%H_2/Ar for 2 h at 200 °C (5 °C/min).

Entry 1 reports the conversion of *n*-butanol over the catalyst heat treated in 5 vol.% H_2/Ar. As has been reported in the previous section, the conversion of *n*-butanol is increased to 43 % and the selectivity toward butyraldehyde and butyric acid are 93 and 7 % respectively, and the mass balance is 100 %.

Entry 2 reports the conversion of butyraldehyde. It is noticed here that 83 % of butyraldehyde is converted and the mass balance is only of 47 %. In the liquid phase, only butyric acid is detected, therefore there are unidentified products, one of which is likely to be carbon dioxide. one hypotheses that may explain this low mass balance is that the butyraldehyde is strongly bound to the catalyst surface and that promotes the decarboxylation of butyraldehyde. Therefore another product coming from this route should be formed, but the liquid phase does not show any other products present under analysis conditions used. Further investigation should be done to identify all the products present in the gas phase, but this would require access to a different type of sealed reactor and this was not possible.

Entry 3 reports the results after reaction using the heat treated catalyst (5 vol.%H_2/Ar) for 4 wt. %*n*-butanol mixed with 1wt.%butyraldehyde. It is noticed here that 12 % of

n- butanol was converted. It has been observed in the previous section that when the catalyst is calcined there was no conversion of *n*-butanol.

Entry 4 of the Table reports the results obtained when 4 wt.%*n*-butanol was mixed with 1 wt.% butyric acid. It can be observed that 14 % of *n*-butanol is converted to butyraldehyde with a selectivity of 37 %, compared to the fresh catalyst (dried in air at 110 °C) which gave a 24 % *n*-butanol conversion and butyraldehyde selectivity of 100 %.

FT-IR has been used to verify the vibrational bands for both the catalyst and reaction products that may be retained on the catalyst. As discussed in Chapter 1, aldehydes can bind strongly to Pt surface sites through their carbonyl group and thereby, inhibit interactions between the metal and the alcohol by occupying the same active site. The aim of these experiments was to understand the effect of product inhibition on 1 wt.%Pt/TiO_2. FT-IR of the as-received substrate (*n*-butanol) and products (butyraldehyde and butyric acid) were performed and illustrated in Figure 3.9.

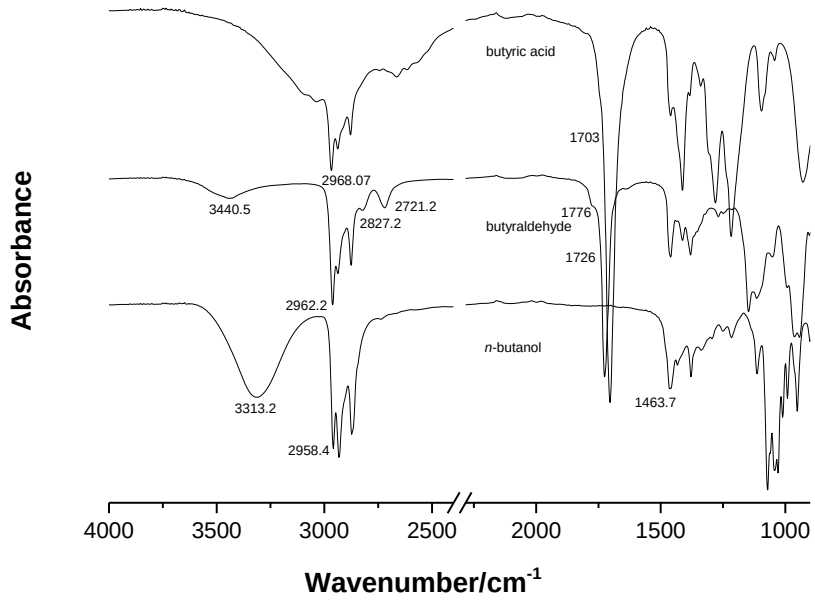

Figure 3.9. Infrared spectra of Substrate (*n*-butanol) and Products (butyraldehyde and butyric acid).

According to the spectra obtained with *n*-butanol a broad peak at 3313 cm^{-1} is characteristic of a O-H stretching modes indicative of hydrogen bonding between hydroxyl groups (Figure 3.9). Furthermore, peaks characteristic of C-H stretching (sp^3) and CH_2 bending modes are observed at 2958 and 1464 cm^{-1}, respectively.[36] In

addition, there is a strong C-O stretching mode near 1070 cm^{-1}. For comparative purposes, ATR-IR measurements were also carried out on the reaction product, butyraldehyde (Figure 3.9).[36] The peak at 2962 cm^{-1} is characteristic of an alkyl C-H stretch. There are two unique peaks corresponding to C-H stretching of the aldehyde moiety, clearly visible at 2827 and 2721 cm^{-1}. The carbonyl stretch C=O of the aldehyde can be assigned to the peak at 1726 cm^{-1}. A further ATR-IR experiment was conducted on butyric acid (Figure 3.9), and peaks characteristic of -OH H-bonding *ca.* 3050 cm^{-1}, C-H alkyl stretching at 2968 cm^{-1} and C=O stretching at 1703 cm^{-1} are observable.[36]

FTIR (Figure 3.10) characterisation was also conducted on the catalyst before and after catalysts were tested for the oxidation reaction (reaction conditions: 100 °C, 2 h, 3 bar O_2, *n*-butanol (0.54 M), 15 mg of catalyst) in order to establish whether any substrate or reaction products remained on the surface. The fresh catalyst has been retreated under the same conditions (100 °C, 2 h and dried at room temperature) as stated previously as the used catalyst, however, with the addition of 10 mL water in place of *n*-butanol.

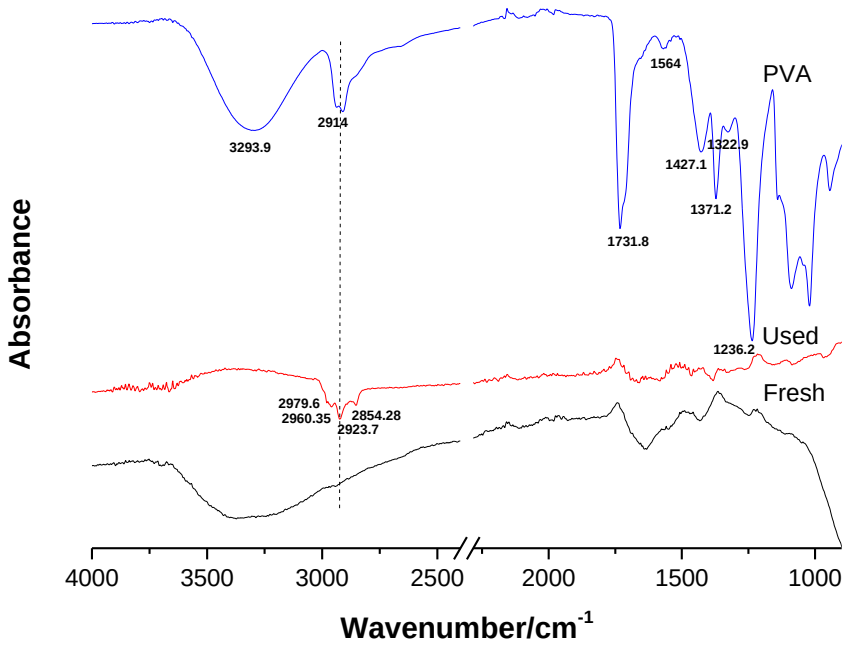

Figure 3.10. Infrared spectra of fresh (as-obtained), Used 1 wt.%Pt/TiO_2 catalyst and polyvinyl alcohol (PVA).

Distinct changes can be observed in the regions between 3250-2500 cm^{-1} and 2200-900 cm^{-1} in the FTIR spectra of the catalyst before and after a standard butanol

oxidation reaction (100 °C, 2h, 3 bar O_2) (Figure 3.10). The change in IR spectrum at *ca*. 2900 cm^{-1} is highlighted in Figure 3.9 for the 1 wt.% Pt/TiO_2 catalyst following exposure to *n*-butanol. In the spectrum of the used catalyst, clear bands at 2980, 2960, 2924 and 2854 cm^{-1} are observed. The bands at 2980, 2960, 2924 and 2854 cm^{-1} are characteristic of C-H stretching (asymmetric CH_2 stretch).

The spectra of the as-received polyvinyl alcohol (PVA) are presented in Figure 3.10. A strong and broad peak at 3294 cm^{-1}, which indicates an O-H stretching vibration typically found with carboxy groups and adsorbed water in the spectrum of PVA.[37] Moreover, a broad stretching vibration band at 2800–3000 cm^{-1} belonging to $C-H_2$ is observed. The characteristic peak for a C-O stretching vibration is present and appears at 1732 cm^{-1} and the peak at 1564 cm^{-1} correspond to C-C skeletal stretching vibration. The peaks at 1371 and 1323 correspond to the skeletal vibrations of C-OH and C-O-C. In the spectrum of the used catalyst (after a 2 h reaction at 100 °C) there is one clear band at 2960 cm^{-1} (Figure 3.10). The peak at 2960 cm^{-1} in Figure 3.10 corresponds to characteristic alkyl C-H stretches in butyraldehyde (Figure 3.9). This data supports that there is evidence to suggest that C-H on the used catalyst is unlikey to be from PVA,[38] because nothing was observed on the fresh catalyst (as-obtained). This may suggest that there are some C-Hs formed on the catalyst surface following a 2 h reaction at 100 °C. This may support the time on-line reactivity data in Figure 3.7.

Analysis of the catalyst before and after reaction was carried out with FTIR (reaction conditions: room temperature (RT), 1h, butyraldehyde (0.55 M), 15 mg of catalyst) in order to establish whether any butyraldehyde remained on the surface (Figure 3.11). The fresh catalyst has been retreated under the same conditions (1 h and dried at room temperature) as stated previously in the case of the used catalyst, however, with the addition of 10 mL water in place of butyraldehyde.

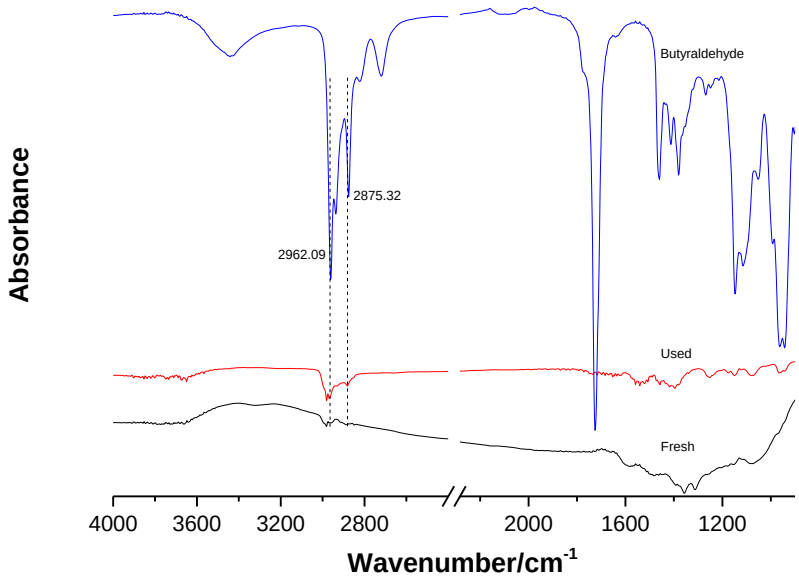

Figure 3.11. Infrared spectra of 1 wt.%Pt/TiO_2 before (fresh) and after reaction (used). ***Reaction conditions*****:** RT, 1h, butyraldehyde (10 mL, 0.55 M), 15 mg of catalyst, 750 rpm.

The spectra of the as-received butyraldehyde are presented in Figure 3.11, in addition to the spectra of the 1 wt.% Pt/TiO_2 catalyst following exposure to butyraldehyde and the differences at *ca*. 3000 cm^{-1} are highlighted. In the spectrum of 1 wt.% Pt/TiO_2 used catalyst a number of bands are observed after exposure to butyraldehyde. Bands characteristic of -C-H stretching and bending are observed at 2875 cm^{-1}. In the CH_3 asymmetric stretching region one band appears at 2962 cm^{-1}, it also can be seen in Figure 3.10. It can be noted from the spectrum that the addition of butyraldehyde to the catalyst suggests aldehydes can bind strongly to a Pt surface through their carbonyl group and it is this interaction which inhibits the interaction between the metal and the alcohol by occupying the same active site.[15]

3.6. Investigation into the catalyst deactivation

3.6.1. Role of catalyst pre-treatment

In order to understand the effect of the different Pt oxidation states in this reaction, some additional experiments were conducted. The first consisted of calcining the two catalysts under air and then testing under the optimal reaction conditions, whilst the second consisted of a heat treatment in 5 vol.%H_2/Ar at 200 °C of the 1 wt.%Pt/TiO_2 catalyst. The reason of this pre-treatment is that during the preparation step of the

catalyst by sol-immobilisation, a drying step of the catalyst under air is performed at 110 °C.

The time of pre-treatments under air or hydrogen were kept constant, *i.e.* 2 h at 200 °C, at a ramp rate of 5 °C/min.

The effect of surface treatments on activity towards *n*-butanol oxidation has been studied for 0.5 and 1 wt.%Pt/TiO_2, Appendix B. The results of this first set of experiments are reported in Table 3.

Table 3.7. Conversion of *n*-butanol over 0.5 and 1 wt.%Pt/TiO_2 catalysts following different pre-treatments.

Catalyst	Conv. *n*-BuOH (%)	Sel. (%)		Mass balance (%)	Leaching (%)
		BuALD	BuAC		
0.5 wt.%Pt/TiO_2	16	100	-	89	0.10
0.5 wt.%Pt/TiO_2 (Calcined)	15	100	0	88	0.02
0.5 wt.%Pt/TiO_2 (5 vol.% H_2/Ar)	29	92	8	79	0.04
1 wt.%Pt/TiO_2	30	91	9	96	5.20
1 wt.%Pt/TiO_2 (Calcined)	23	93	7	100	3.30
1 wt.%Pt/TiO_2 (5 vol.% H_2/Ar)	43	93	7	89	3.10

Conversion (Conv.), Selectivity (Sel.), *n*-Butanol (*n*-BuOH), Butyraldehyde (BuALD), Butyric Acid (BuAC). ***Reaction Conditions:*** 100 °C, 2 h, 3 bar O_2, *n*-butanol (0.54 M), 15 mg of catalyst. ***Catalysts pre-treated:*** Calcined under air or A flow of 5 vol.%H_2/Ar for 2 h at 200 °C (5 °C/min).

Table 3.7 shows that when the catalysts are calcined under air for 2 h, the conversion of the *n*-butanol is 16%. Furthermore, when the catalysts are heat treated in 5 vol.%H_2/Ar at 200 °C and tested, the conversion of *n*-butanol increases. All the pre-treatments are performed at 200 °C and for 2 h. It can be seen that there are increased conversion of *n*-butanol for heat treated catalyst under 5 vol.%H_2/Ar, for 0.5 wt.% and 1 wt.%Pt/TiO_2 conversion is 29 % and 43 %, respectively.

Considering the time on-line results, it has been observed that the 0.5 wt.%Pt/TiO_2 catalyst quickly deactivates, Figure 3.6. Indeed, no further conversion of the *n*-butanol is observed. As discussed in section 1.6.3.1 aldehydes can bind strongly to Pt active site through their carbonyl group and inhibit the interaction between the metal and the alcohol by occupying the same active site, as shown in FT-IR (Figure 3.11).[15]In an attempt to understand further the nature of the catalyst surface X-ray Photoelectron Spectroscopy characterisation was carried out.

Table 3.8 reports the XPS data of fresh (as-obtained), used catalyst (after 2 h reaction), calcined and 5 vol.%H_2/Ar at 200 °C treatment for 0.5 and 1 wt.%Pt/TiO_2.

Table 3.8. XPS of 0.5 and 1 wt.%Pt/TiO_2 under different pre-treatments catalysts.

Catalyst and pre-treatment	Pt($4f_{7/2}$)Binding Energy / eV	Pt Oxidation State
0.5 wt.%Pt/TiO_2 (Fresh)	70.4	Pt^0
0.5 wt.%Pt/TiO_2 (Used)	70.4	Pt^0
0.5 wt.%Pt/TiO_2 (Calcined)	70.4	Pt^0
0.5 wt.%Pt/TiO_2 (5%H_2/Ar at 200 °C)	70.5	Pt^0
1 wt.%Pt/TiO_2 (Fresh)	70.4	Pt^0
1 wt.%Pt/TiO_2 (Used)	70.4	Pt^0
1 wt.%Pt/TiO_2 (Calcined)	70.4	Pt^0
1 wt.%Pt/TiO_2 (5 vol.%H_2/Ar at 200 °C)	70.4	Pt^0

***Catalysts pre-treated*:** Calcined under air or A flow of 5 vol.%H_2/Ar for 2 h at 200 °C (5 °C/min).

Analysis of the Pt(4f) signal must be performed with caution due to the overlap of a portion of the Pt(4f) doublet with a titania loss feature. However with careful analysis, using a bare titania sample as a reference, the loss feature can be modelled, resolving the chemical state of the Pt is possible. Regardless of loading or treatment, the Pt for all sample is found to be metallic.

Of note is the oxygen content for all samples, the concentration of which is reported in Table 3.9, together with all other elemental concentrations derived by XPS. For the 0.5 % catalysts, three oxygen species are found, specifically 529.6 (Ti-O), 531.5 (OH) and 533.0 eV (water/organic species). A similar trend is found for the 1 wt. % samples.

Table 3.9. XPS derived at % for 0.5 and 1 wt.%Pt/TiO_2 Catalysts.

Sample	Concentration / at%					
	O 1s (529.6 eV)	**O 1s (531 eV)**	**O 1s (533 eV)**	**Ti 2p**	**C 1s**	**Pt 4f**
0.5 wt.%Pt/TiO_2 (5%H_2/Ar at 200 °C)	33.6	7.3	2.6	17.2	39.3	0.02
0.5 wt.%Pt/TiO_2 (Calcined)	22.5	8.2	4.8	11.4	53.1	0.02
0.5 wt.%Pt/TiO_2 (Fresh)	24.8	8.5	4.5	12.8	49.3	0.02
1 wt.%Pt/TiO_2 (5 vol.%H_2/Ar at 200 °C)	30.8	7.7	2.7	15.9	42.8	0.09
1 wt.%Pt/TiO_2 (Calcined)	30.3	7.8	3.4	15.4	42.9	0.10
1 wt.%Pt/TiO_2 (Fresh)	32.9	8.0	2.6	16.8	39.6	0.12
1 wt.%Pt/TiO_2 (Used/2 h)	35.5	7.2	1.0	18.9	37.3	0.09
1 wt.%Pt/TiO_2 (Used/4 h)	31.4	7.9	3.5	16.1	41.0	0.08

***Catalysts pre-treated*:** Calcined under air or A flow of 5 vol.%H_2/Ar for 2 h at 200 °C (5 °C/min).

Analysis of samples taken after 2 and 4 hour reaction times (Table 3.9), indicate no change in the oxidation state of the Pt, remaining as Pt^0, and again with little change in the overall Pt concentration, with values similar to that of the fresh and treated catalysts. The small changes in the Pt concentration, could indicate sintering or leeching of metal, but with such low concentrations of metal and the Ti loss structure, this is within experimental error. With respect to the O(1s) spectra, the oxygen species are significantly different.

After 2h reaction the oxygen speciation has changed, with the high binding energy species almost being eliminated from the system, only to return to similar levels to the oxidised catalysts after 4 h reaction. There is no significant change in the C(1s) spectra which may account for this change, so at present we assign this to strongly bound water or a possibly a surface carbonate from exposure to the atmosphere during preparation for XPS analysis. In the case of the 0.5 wt.%Pt/TiO_2, when the catalyst is calcined, the conversion of *n*-butanol is 15 % and only butyraldehyde was detected and butyric acid was not detected. When the catalyst was treated under 5 vol.%H_2/Ar at 200 °C the selectivity to butyric acid is 8 %.

The catalyst pre-treatment plays an important role in *n*-butanol oxidation. From a previous study it has been shown that when carbon is used as a support, XPS analysis of 1 wt.%Pt/C reveal that exclusively metallic Pt^0 was formed.[5] Many previous

publications have suggested that the interaction between Pt/C is attributed to electron transfer from the platinum to carbon support, this interaction leads to change of catalyst properties and enhance the catalytic properties and stability.[30, 31, 39-41] This may promote the conversion of *n*-butanol (85.9 %) in the same paper. Remarkably, the pre-treatment of Pt/C under 5 vol.% H_2/Ar show active and stable Pt nanoparticles, in term of stability, less than 1 % leaching was observed for Pt/C catalyst.[5]

Thermogravimetric (TGA) experiments have been performed on the catalysts to identify whether there are remaining species adsorbed on the catalyst surface. Figure 3.12 show the difference between the fresh and used (after reaction) catalyst. A 6.12 mg sample of 1 wt.%Pt/TiO_2 was analysed.

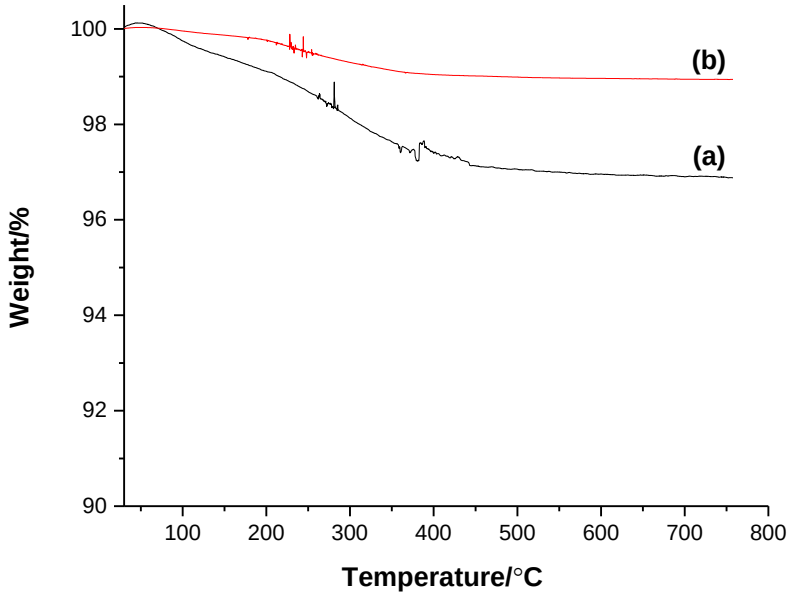

Figure 3.12. TGA analysis of the samples (a) Fresh 1 wt.%Pt/TiO_2 catalyst (b) Used catalyst (after reaction). ***Reaction conditions:*** 100 °C, 3 bar O_2, 2 h. Temperature program = heat from 30 °C to 800 °C at 15 °C/min in air with a purge rate of 20 ml/min.

TGA analysis of 1 wt.%Pt/TiO_2 fresh catalyst shows 3.15 % weight loss between 30 and 800 °C, which may correspond to removal of adsorbed water, this is in good agreement with XPS analysis (section 3.6.1). The TGA of 1 wt.%Pt/TiO_2 after the reaction (100 °C, 3 bar O_2, 2 h) shows a total mass loss of 1.06 %, lower than the fresh catalyst. A mass loss of 1.06 % appears in the range of 200-250 °C. There is no evidence of coking or of product. There may be some organics formed on the catalyst surface but it is below the detection limits.

3.6.2. Particle size effects

Figure 3.13 shows a SEM image of 1 wt.%Pt/TiO_2 fresh (as-obtained), calcined, 5 vol.%H_2/Ar at 200 °C treatment and used catalyst (after 2 h reaction).

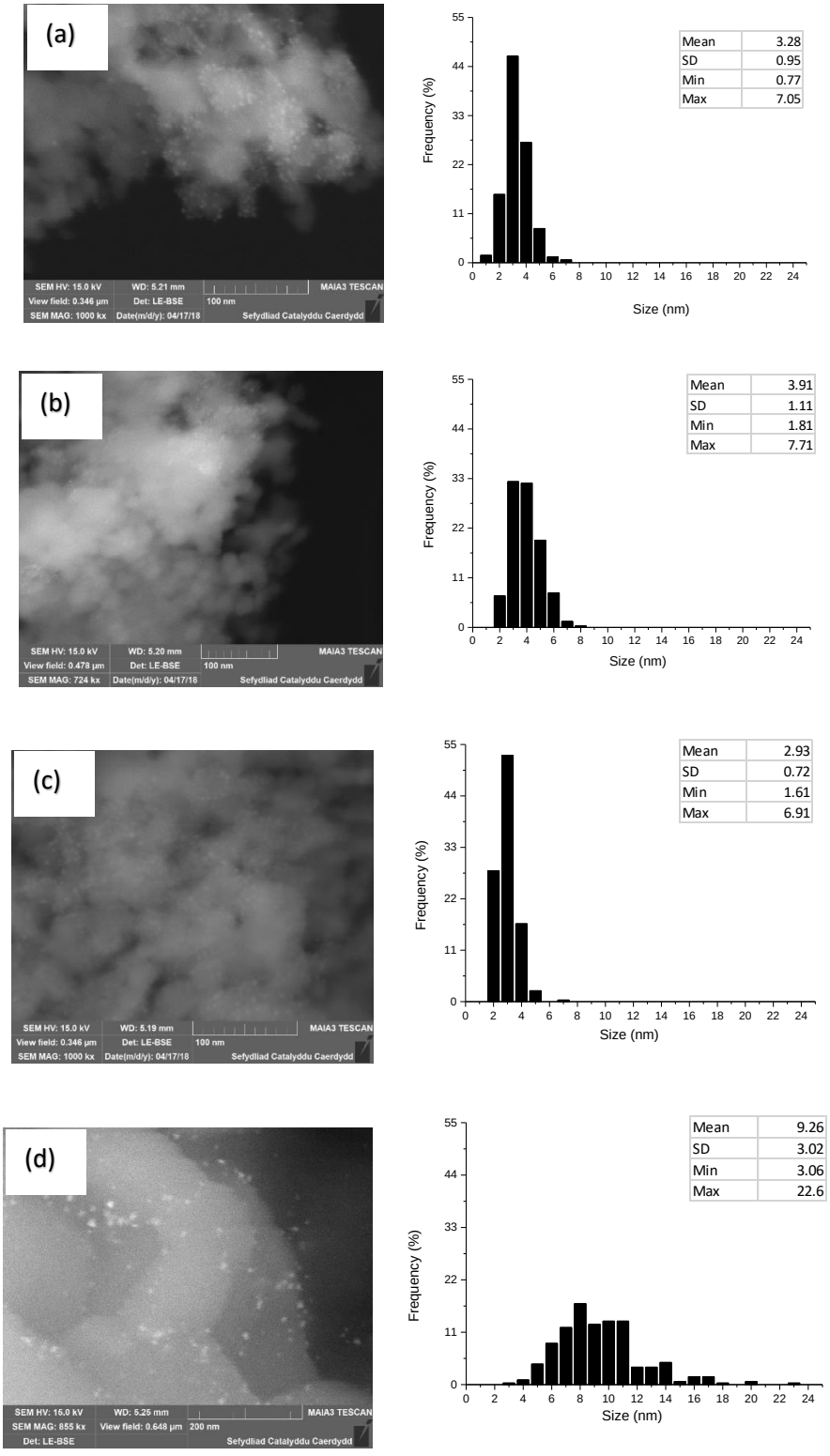

Figure 3.13. Representative SEM images and particle size distribution of the 1 wt.%Pt/TiO_2 (a) Fresh (as-obtained) (b) Calcined (c) 5 vol.%H_2/Ar at 200 °C treatment (d) Used catalyst (after 2 h reaction). ***Reaction conditions:*** 100 °C, 2 h, 3 bar O_2, *n*-butanol (0.54 M), 15 mg of catalyst, 750 rpm. ***Catalysts pre-treated:*** Calcined under air or A flow of 5 vol.%H_2/Ar for 2 h at 200 °C (5 °C/min).

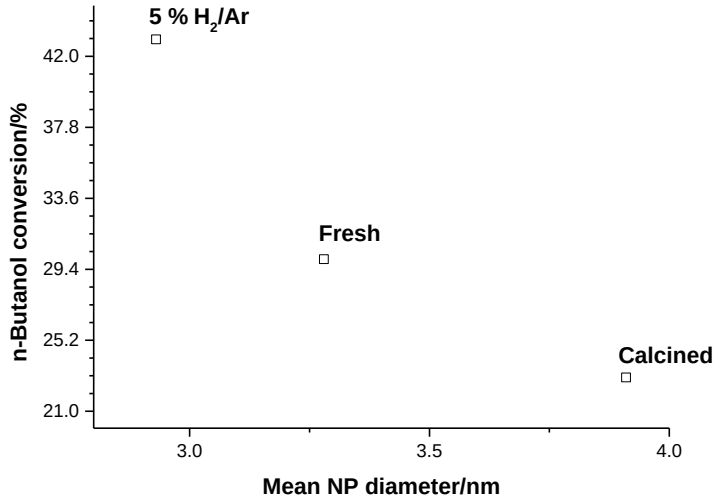

Figure 3.14. Relationship between mean nanoparticle (NP) size and substrate conversion at 2h of the Fresh (as-obtained), calcined and 5 vol.%H_2/Ar at 200 °C treatment of 1 wt.%Pt/TiO_2. ***Catalysts pre-treated:*** Calcined under air or a flow of 5 vol.%H_2/Ar for 2 h at 200 °C (5 °C/min).

SEM analysis was carried out on fresh (as-obtained), calcined, 5 vol.%H_2/Ar at 200 °C treatment and used (after 2 h reaction) catalysts. The 5 vol.%H_2/Ar at 200 °C treatment, calcined and fresh (as-obtained) catalysts do not have comparable mean particle size as shown in Table 3.10.

Table 3.10. Mean NP diameter of 1 wt.%Pt/TiO_2 under different pre-treatments catalysts.

Catalyst and pre-treatment	Mean NP diameter	SD
1 wt.%Pt/TiO_2 (Fresh)	3.28	0.95
1 wt.%Pt/TiO_2 (Used)	9.26	3.02
1 wt.%Pt/TiO_2 (Calcined)	3.91	1.11
1 wt.%Pt/TiO_2 (5 vol.%H_2/Ar at 200 °C)	2.93	0.72

Nanoparticles (NP), Standard Deviation (SD). ***Catalysts pre-treated*:** Calcined under air or A flow of 5 vol.%H_2/Ar for 2 h at 200 °C (5 °C/min).

From results described in Table 3.7 and 3.10 the catalyst activity is greatly affected by the mean nanoparticle size, which are 3.28, 3.91 and 2.93 nm for fresh, calcined, 5 vol.%H_2/Ar at 200 °C treatment, respectively. The different activities observed could therefore likely be attributed to either the physicochemical properties of the different

catalysts after different pre-treatment under air or 5 vol.%H_2/Ar for 2h at 200 °C (5 °C/min). The pre-treatment conditions increase the metal support interaction for example, making it more stable and less susceptible to sintering in-situ.[5] The mean nanoparticle size of fresh catalyst increased to 9.26 nm after 2 h reaction. These observations suggest that exposure to reaction conditions resulted in particles sintering, and therefore lower rates of activity with the time of use. The catalyst was initially more active, this may explain the dramatic increase in Pt sintering rate, suggesting a potential deactivation mechanism, after 2 h process (Time on-line study, Figure 3.7). For the 5 vol.%H_2/Ar at 200 °C treatment catalyst the mean nanoparticles size was 2.93 nm and in the case of calcined catalyst the mean diameter size 3.91 nm, implying that nanoparticle size is the reason for the difference in catalyst activities, Figure 3.14. If there are very few small nanoparticles in the calcined catalyst (conversion = 23 %), this would explain why it is significantly less active than the fresh (conversion = 30 %) and the 5 vol.%H_2/Ar at 200 °C treatment (conversion = 43 %) catalyst. For various applications, sintering of metal particles has been a major cause for catalyst deactivation.[42, 43]

The hypothesis advanced previously regarding the importance of the pre-treatment of the catalyst activity, seems to be confirmed here. Indeed, there is a strong correlation between the mean diameter of the nanoparticles of the pre-treated catalyst and the rate of *n*-butanol conversion.

3.6.3. Metal leaching

Sets of experiments have been carried out to investigate the effect of leaching on the *n*-butanol conversion. The potential role of leached Pt on the reaction is reported in Table 3.11.

Two sets of experiments have been designed and performed: The first experiment (Table 3.11, Entry 1) consisted of testing in a first step the oxidation of 4 wt.%*n*-butanol with 15 mg catalyst at 100 °C, 3 bar O_2, for two hours. Then in Table 3.11, Entry 2, collecting the solution after filtration and in a third step performing the reaction with the collected solution without catalyst at 100 °C, 3 bars O_2, for two hours. Table 3.11, Entry 3 consisted of measuring how much Pt was leached after 2 h reaction, and then use a solution of $H_2PtCl_6 \cdot 3H_2O$ containing the same amount of Pt leached and perform the reaction at 100 °C and 3 bar O_2, for two hours.

Table 3.11. Study on the effect of Pt leaching on *n*-butanol conversion.

Entry		Conv. *n*-BuOH (%)	Sel. (%)	
			BuALD	BuAC
1	**With catalyst**	30	91	9
2	**After filtration Without catalyst**	26	67	33
3	**$H_2PtCl_6 \cdot H_2O$**	13	100	-

***Reaction conditions*:** 100 °C, 2h, 3 bar O_2, *n*-butanol (10 mL, 0.54 M), 15 mg of catalyst, 750 rpm.

From the presented data, the amount of 1 wt.%Pt/TiO_2 leaching has been found to be 5.2 %. Entry 1 of Table 3.11 reports the conversion of *n*-butanol and the selectivity of butyraldehyde and butyric acid when 4 wt.%*n*-butanol is put in solution with 1 wt.%Pt/TiO_2.

Entry 2 reports the conversion of *n*-butanol and the selectivity of butyraldehyde and butyric acid after filtration and reaction, without addition of the catalyst.

The third row reports the conversion of *n*-butanol and the selectivity of butyraldehyde and butyric acid when $H_2PtCl_6 \cdot H_2O$ is put in solution with 4 wt.%*n*-butanol (experiment 2).

The conversion and the selectivity based on Entry 1 have been calculated by using the initial concentration of *n*-butanol (4 wt.%). It means that the conversion of *n*-butanol before and after filtration (without addition of the catalyst), remains the same and the selectivity of butyraldehyde and butyric acid after filtration (without addition of the catalyst) is 24 % less for butyraldehyde and 14 % more for butyric acid.

This result indicates that the oxidation of butyraldehyde is carried out after filtration (without addition of the catalyst, Entry 2), which suggests that there was some leached Pt in the solution.

The ICP has shown that 5.2 % of Pt leaches from the catalyst after 2 h of reaction, which corresponds to a concentration of 17 mg/L of Pt (36.4 mg/L of $H_2PtCl_6 \cdot H_2O$). For this reason, 14.27 µL of $H_2PtCl_6 \cdot H_2O$ (36.4 mg/L) was added to a reaction with *n*-butanol

(Table 3.11, Entry 3) and the results shows that 13% of *n*-butanol is converted to butyraldehyde.

From these data, two main points can be emphasized. The first one is that the reaction of *n*-butanol with 1 wt.%Pt/TiO_2 can promote the leaching of the catalyst. The Pt leached can promote the oxidation of butyraldehyde into butyric acid and the conversion of *n*-butanol is stopped because of the presence of butyraldehyde. The second point is that $H_2PtCl_6 \cdot 3H_2O$ promotes the conversion of *n*-butanol into butyraldehyde, there is no trace of butyric acid. Several hypotheses can be proposed here to explain the difference of behaviour between the two experiments. The first hypothesis is that the Pt that has leached has a different oxidation state than the one in $H_2PtCl_6 \cdot 3H_2O$ added into the solution. This Pt in the leaching promotes the oxidation of butyraldehyde into butyric acid. The Pt (Pt^{4+}) in $H_2PtCl_6 \cdot 3H_2O$ may promote the oxidation of *n*-butanol into butyraldehyde, which doesn't oxidise further to butyric acid. Pt^{4+} seems also to allow the conversion of *n*-butanol.

3.6.4. Reusability tests of 1 wt.%Pt/TiO_2

With the aim to demonstrate the stability of the 1 wt.%Pt/TiO_2 catalyst, the catalyst has been tested, recovered and retested under the standard conditions (100 °C, 2 h and 3 bar O_2), the results are reported in Table 3.12. Reusability studies, shown in Table 3.12 show the conversion of *n*-butanol and the selectivity toward butyraldehyde and butyric acid.

Table 3.12. Reusability of 1 wt.%Pt/TiO_2 for 3 cycles.

Test cycle	Conv. *n*-BuOH (%)	Sel. (%)		Leaching (%)	Mass Balance (%)
		BuALD	BuAC		
1st	30	91	9	5.2	96
2nd	24	94	6	1.4	100
3rd	26	100	0	2.6	92

Conversion (Conv.), Selectivity (Sel.), *n*-Butanol (n-BuOH), Butyraldehyde (BuALD), Butyric Acid (BuAC). ***Reaction conditions:*** 100 °C, 2 h, 3 bar O_2, *n*-Butanol (10 mL, 0.54 M), 15 mg of catalyst.

The data shows that after 3 repeated experiments the conversion of *n*-butanol remained unchanged. However, the selectivity toward butyraldehyde increased with subsequent repeat experiments from 91 % from the first test to 100 % to the third reusability experiment. In parallel the selectivity to butyric acid decreases with the reusability test, from 9 % from the first test to 0 % for the third test.

It was found that after each test the catalyst is still converting *n*-butanol and the conversion reaches the same level after 2 h reaction. It is clear that when butyraldehyde is not initially in the solution the catalyst can convert *n*-butanol into butyraldehyde. As soon as the concentration of butyraldehyde reaches a certain level in the solution there is no more conversion of *n*-butanol (see section 3.5).

During the tests the selectivity toward butyraldehyde and butyric acid changes. The catalyst present here is still active toward the conversion of *n*-butanol at the same level along cycles. The reusability test shows that the selectivity towards the products is affected after every reuse.

XPS analysis was performed on the used catalyst. XPS of the Pt(4f) region is shown in Figure 3.15.

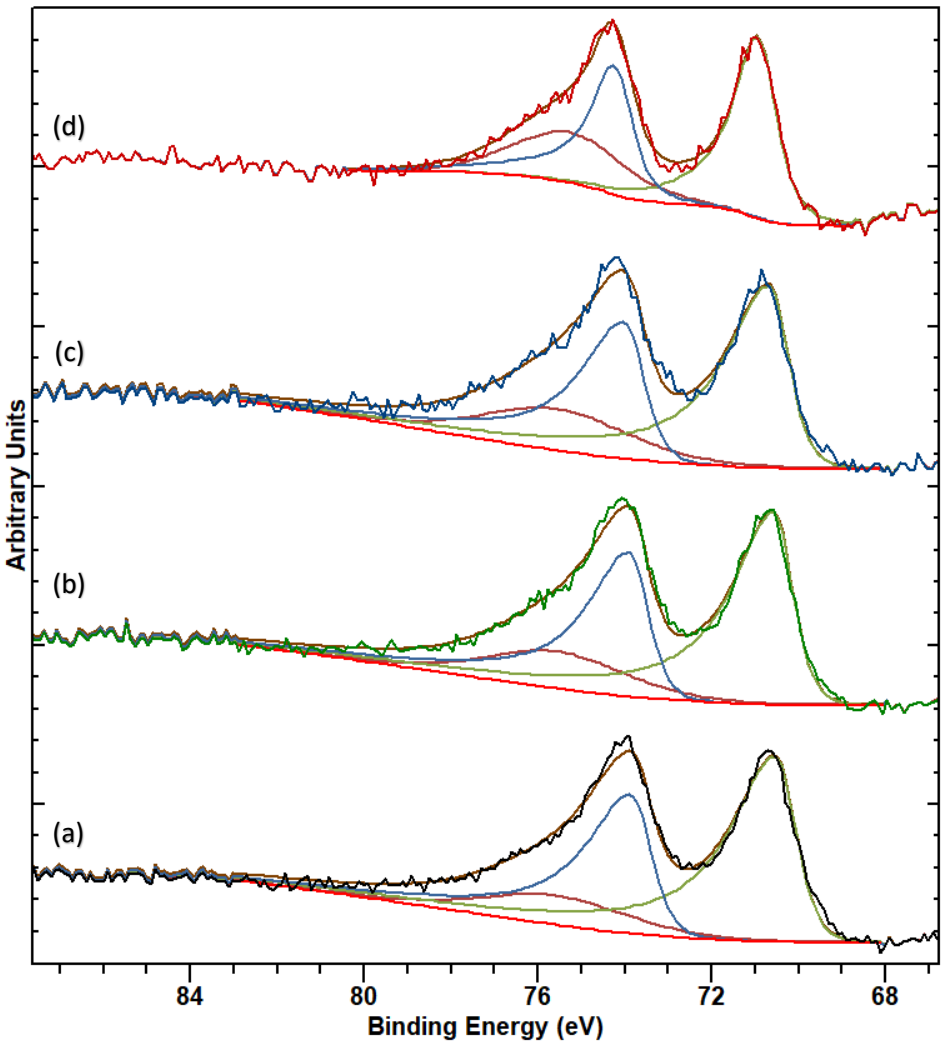

Figure 3.15. Pt(4f) core-level spectra for (a) Fresh (as-obtained), (b) 1st reuse, (c) 2nd reuse, (d) 3rd reuse. Spectra are fitted with a constrained doublet for Pt and a peak for a Ti loss structure as modelled from a reference P25 sample.

In respect of the XPS analysis, on reuse negligible change is noted for the overall spectral shape although an increase in binding energy of *ca.* 0.4 eV is observed which is above the experimental uncertainty of ±0.2 eV. This shift upward in binding energy is mirrored by an apparent decrease in the concentration of Pt detectable by XPS and consequently we attribute this to loss of Pt resulting in smaller particles size as a function of reuse, since sintering would typically shift the binding energy to more bulk like values (i.e. lower binding energies).

3.7. Conclusion

The *n*-Butanol oxidation has been performed with a Pt/TiO_2 catalyst. A study of the effect of different percentage loadings of platinum on TiO_2 has shown that 1 wt.%Pt/TiO_2 presents the highest activity towards the conversion of *n*-butanol. The study of the effect of catalyst mass has shown that below 50 mg catalyst used the reaction is under a kinetic regime, and above it is under a diffusion limited regime. From these data 15 mg catalysts have been used for all the catalytic tests. The time on-line data has shown that different steps are occurring during the oxidation of *n*-butanol at different times of the reaction. It has been suggested that the inhibition of the reaction by the presence of butyraldehyde affect the conversion of *n*-butanol and the selectivity toward the different products of the reaction. The effect of the temperature has shown that measurable activity is obtained above 40 °C. The leaching tests have shown that the catalyst is leaching and sintering can affect the conversion of the reaction. The effect of surface treatments on activity towards *n*-butanol oxidation has been studied on Pt/TiO_2. The Pt/TiO_2 showed significant sensitivity to such treatment and it has been concluded that there is a strong correlation between the pre-treated catalyst and the rate of *n*- butanol conversion. XPS analysis of Pt/TiO_2 samples reveal exclusively it is in the metallic state. SEM characterisation of the Pt/TiO_2 catalyst shows that catalyst pre- treatment affects the average particle size. The reusability of the catalyst has been tested over 3 cycles and the results have shown that the catalyst is still active toward the conversion of *n*-butanol at the same level along all cycles, the selectivity toward butyraldehyde increased with the 3rd experiments to 100 % and butyraldehyde was the main product.

3.8. References

1. M. D. Hughes, Y.-J. Xu, P. Jenkins, P. McMorn, P. Landon, D. I. Enache, A. F. Carley, G. A. Attard, G. J. Hutchings, F. King, E. H. Stitt, P. Johnston, K. Griffin and C. J. Kiely, Nature (London, U. K.), 2005, 437, 1132-1135.

2. L. Prati and A. Villa, Catal., 2012, 2, 24-37.

3. N. Mizuno and Editor, Modern Heterogeneous Oxidation Catalysis: Design, Reactions and Characterization, Wiley-VCH Veralg GmbH & Co. KGaA, 2009.

4. T. Mallat and A. Baiker, Catal. Today, 1994, 19, 247-283.

5. I. Gandarias, E. Nowicka, B. J. May, S. Alghareed, R. D. Armstrong, P. J. Miedziak and S. H. Taylor, Catal. Sci. Technol., 2016, 6, 4201-4209.

6. G. C. Bond, Heterogeneous Catalysis: Principles and Applications. 2nd Ed, Clarendon Press, 1987.

7. R. H. Perry, D. W. Green and J. O. Maloney, Perry's chemical engineers' handbook, McGraw-Hill, New York, 1999.

8. Y.-W. Chen and T.-Y. Hsieh, J. Nanopart. Res., 2002, 4, 455-461.

9. A. Abbadi and H. van Bekkum, J. Mol. Catal. A: Chem., 1995, 97, 111-118.

10. B. N. Zope, D. D. Hibbitts, M. Neurock and R. J. Davis, Science (Washington, DC, U. S.), 2010, 330, 74-78.

11. P. Ballinger and F. A. Long, J. Am. Chem. Soc., 1960, 82, 795-798.

12. C. Zhang, H. He and K.-i. Tanaka, Appl. Catal., B, 2006, 65, 37-43.

13. T. Yeh, S. Linic and P. E. Savage, ACS. Sustainable Chem. Eng., 2014, 2, 2399-2406.

14. S. E. Davis, M. S. Ide and R. J. Davis, Green Chem., 2013, 15, 17-45.

15. M. Besson and P. Gallezot, Catal. Today, 2000, 57, 127-141.

16. B. R. Brown, Quart. Revs. (London), 1951, 5, 131-146.

17. R. W. Hanson, J. Chem. Educ., 1987, 64, 591.

18. E. S. Gould, Mechanism and Structure in Organic Chemistry, Holt, Rinehart and Winston, london, 1959.

19. I. B. Ju, H.-W. Lim, W. Jeon, D. J. Suh, M.-J. Park and Y.-W. Suh, Chem. Eng. J. (Amsterdam, Neth.), 2011, 168, 293-302.

20. S. H. Ali, A. Tarakmah, S. Q. Merchant and T. Al-Sahhaf, Chem. Eng. Sci., 2007, 62, 3197-3217.

21. W. T. Liu and C. S. Tan, Ind. Eng. Chem. Res., 2001, 40, 3281-3286.

22. T. Pöpken, L. Götze and J. Gmehling, Ind. Eng. Chem. Res., 2000, 39, 2601-2611.

23. H. Y. Lee, L. T. Yen, I. L. Chien and H. P. Huang, Ind. Eng. Chem. Res., 2009, 48, 7186-7204.

24. K. Vahteristo, S. Maury, A. Laari, A. Solonen, H. Haario and S. Koskimies, Ind. Eng. Chem. Res., 2009, 48, 6237-6247.

25. M. Schmitt, S. Blagov and H. Hasse, Ind. Eng. Chem. Res., 2008, 47, 6014-6024.

26. A. K. Kolah, N. S. Asthana, D. T. Vu, C. T. Lira and D. J. Miller, Ind. Eng. Chem. Res., 2008, 47, 5313-5317.

27. A. K. Kolah, N. S. Asthana, D. T. Vu, C. T. Lira and D. J. Miller, Ind. Eng. Chem. Res., 2007, 46, 3180-3187.

28. R. Kumar and S. M. Mahajani, Ind. Eng. Chem. Res., 2007, 46, 6873-6882.

29. J. Lilja, D. Y. Murzin, T. Salmi, J. Aumo, P. Maäki-Arvela and M. Sundell, J. Mol. Catal. A Chem., 2002, 182, 555-563.

30. X. Yu and S. Ye, J. Power Sources, 2007, 172, 133-144.

31. L. J. Hillenbrand and J. W. Lacksonen, J. Electrochem. Soc., 1965, 112, 249-252.

32. V. S. Bagotzky and A. M. Skundin, Electrochemica. Acta., 1984, 29, 757-765.

33. M. Sankar, E. Nowicka, E. Carter, D. M. Murphy, D. W. Knight, G. J. Hutchings and D. Bethell, Nat Commun, 2014, 5, 3332.

34. B. N. Zope and R. J. Davis, Green Chem., 2011, 13, 3484-3491.

35. I. Bakos, T. Mallat and A. Baiker, Catal. Lett., 1997, 43, 201-207.

36. https://www.nist.gov/.

37. T. Wang, Y. Li, S. Geng, C. Zhou, X. Jia, F. Yang, L. Zhang, X. Ren and H. Yang, RSC Advances, 2015, 5, 88958-88964.

38. J. A. Lopez-Sanchez, N. Dimitratos, C. Hammond, G. L. Brett, L. Kesavan, S. White, P. Miedziak, R. Tiruvalam, R. L. Jenkins, A. F. Carley, D. Knight, C. J. Kiely and G. J. Hutchings, Nat. Chem., 2011, 3, 551-556.

39. A. L. Dicks, J. Power Sources, 2006, 156, 128-141.

40. M. Kim, J.-N. Park, H. Kim, S. Song and W.-H. Lee, J. Power Sources, 2006, 163, 93-97.

41. J. A. S. Bett, K. Kinoshita and P. Stonehart, J. Catal., 1976, 41, 124-133.

42. Z. C. Zhang and B. C. Beard, Appl. Catal., A, 1999, 188, 229-240.

43. S. F. Adler and J. J. Keavney, J. Phys. Chem., 1960, 64, 208-212.

Chapter 4: Investigation of the mechanism of deactivation and reactivation of 1 wt.%Pt/TiO_2 for *n*- butanol oxidation

4.1. Introduction

In the previous Chapter it was shown that the 1 wt.%Pt/TiO_2 catalyst displayed the highest conversion of *n*-butanol. However, after two hours of reaction deactivation of the catalyst was observed.

The mechanism of deactivation has not been totally elucidated. Several hypotheses have been proposed to investigate the reason for deactivation. One such hypothesis was that the poisoning of Pt^0 by the products is responsible for reduction the conversion of *n*- butanol. It has been proposed in the previous Chapter that during *n*-butanol oxidation, butyraldehyde strongly binds to the active site which prevents the further adsorption and conversion of *n*-butanol. Another hypothesis is that catalyst leaching and sintering can affect the conversion of *n*-butanol. Also, the platinum surface oxidation state of the catalyst is believed to have an effect.

In order to investigate the surface oxidation of the catalyst, two approaches have been examined based on the literature. The first approach is to study the effect of the concentration of oxygen on the performance of the catalyst; the effects of this have been observed by several authors.[1-3] The second approach, also used by other groups, is to combine Pt with another metal. Bi and Pb are metals which are commonly used. Based on this approach 5 metals have been selected, namely Sn, Al, Bi, Zn and Pb, to be combined with Pt.

The aim of this study is to investigate the effect of these changes on the stability of the catalysts towards leaching, and also towards the conversion of *n*-butanol. The different results obtained from these approaches are disclosed in the following sections of this Chapter.

4.2. Effect of Oxygen

Several studies in the literature on alcohol oxidation have found out that alternating steps of oxidation followed by a purge with an inert gas help to avoid/slow down the deactivation of the catalyst.[3]

The effect of this on the performance of the 1 wt.%Pt/TiO_2 catalysts has been investigated, and the results obtained are given below in Table 4.1.

In Table 4.1, Entry 1 represents the 1 wt.%Pt/TiO_2 without any cycling of nitrogen and purging by air. For Entry 2, the reaction was performed for 1 hour under 3 bar oxygen at 100 °C, before the reactor was cooled down with an ice bath for 10 min under the same pressure of oxygen. Then the reactor was vented to air to remove the oxygen and nitrogen was introduced. The reactor was then maintained at 100 °C for 10 min under 3 bar of nitrogen. Following this, the reactor was again cooled down under 3 bar nitrogen for 10 min. Oxygen under 3 bar was reintroduced and the reaction was performed again for 1 hour. This cycle was repeated 2 more times.

Second experiment (Entry 3), in order to be sure that in the first experiment it is nitrogen that has an effect on the reaction, and not the stages of cooling and venting, the same stages of cooling and venting were performed under pure oxygen (3 bar O_2). Therefore, the protocol for Entry 3 is the same as Entry 2, except that the steps involving purging and pressurising with nitrogen have been omitted. The reasons for introducing cooling stages in the protocol is for safety when the oxygen and nitrogen are switched. Their action was quenched, by reducing temperature, to prevent any further reaction and prevent loss of water of reactants/products.

Table 4.1. Conversion of 4 wt.%*n*-butanol and selectivity towards butyraldehyde and butyric acid over 1 wt.%Pt/TiO_2 with and without N_2 treatment under **Oxygen**.

Entry	Conv. *n*-BuOH (%)	Sel. (%)		Mass Balance (%)
		BuALD	BuAC	
1	30	90	9	96
2	63	77	11	67
3	51	79	16	87

Conversion (Conv.), *n*-Butanol (*n*-BuOH), Butyraldehyde (BuALD), Butyric Acid (BuAC), Selectivity (Sel.).

***Reaction conditions*:** 100 °C, *n*-butanol (10 mL, 0.54 M), 2h, 3bar O_2 and catalyst (0.015 g). [2] 3 bars O_2 for total of 3 h the reaction every 1 h flow N_2 (3 bar) for 10 min.[3] 3 bars O_2 for total of 3 h the reaction every 1 h purging by air for 10 min.

The data show that alternating cycles, *i.e.* experiments Entry 2 and 3, increase the conversion of *n*-butanol from 30 % (Chapter 3, Figure 3.7) when compared to the reaction without cycles (Entry 1), to 63 % and 51 % for Entries 2 and 3 respectively.
As shown previously in Chapter 3, Section 3.4, carbon dioxide is present in the gas phase, this can lead to a decrease in the mass balance observed for experiments Entry 2 and 3. Secondly, *n*-butanol is volatile and it is possible that some of the alcohol is lost when the colaver is vented, this would lead to both increased conversion and also decreases in the mass balance observed for the experiments Entry 2 and 3.

From these Entry 2 and 3 experiments it seems that the performance of the catalyst in term of *n*-butanol conversion is more active compared to the non-cyclic one (Entry 1). It should be noted that the utilisation of nitrogen (Entry 2) gives a higher conversion of *n*-butanol (*i.e.* 63 %), compared to when purging by air (Entry 3), is used instead (*i.e.* 51 %). It was also shown in the previous Chapter that during *n*-butanol oxidation the butyraldehyde binds strongly to active surface Pt sites. The hypothesis that the concentration of oxygen in the solution during the 10 min “purge” by air or by nitrogen cycles allows the Pt active sites to return to their initial state by removal of adsorbed butyraldehyde.

XPS was performed on fresh (as-obtained) and used catalyst after purging by air and nitrogen Figure 4.1, under reaction conditions (100 °C, 2h, 3bar O_2).

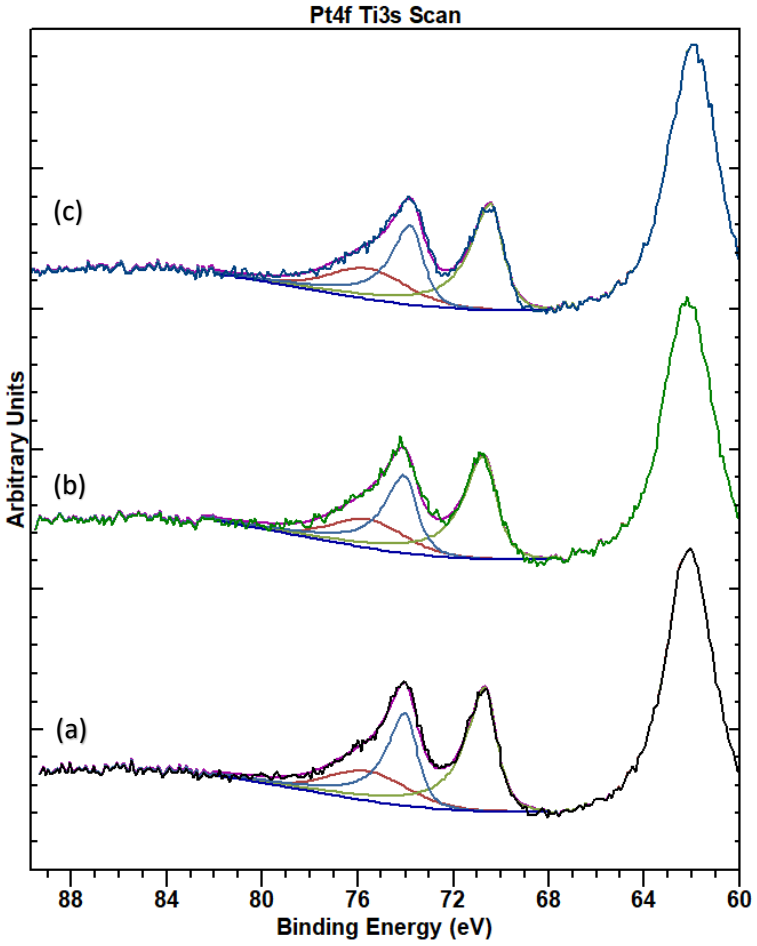

Figure 4.1. XPS analysis of 1 wt.%Pt/TiO_2 catalyst (a) Fresh, (b) After N_2 cycle, (c) Air venting.

XPS showed no significant change in Pt oxidation state or concentration, with the Pt remaining metallic, and *ca.* 0.3 at% concentration of the total elemental concentration did not change.

In previous studies it has been reported that the dynamic balance of competitive adsorption of organic substrate and oxygen controls the initial reaction rate and the equilibrium tends to shift towards predominant oxygen coverage as the substrate concentration decreases.[4] The activity was usually regenerated by alternating cycles of air and nitrogen. Because of the progressive loss of reactivation efficiency, it was suggested that oxygen atoms penetrate more and more deeply into the subsurface or the platinum bulk causing deactivation of the catalyst surface.[4]

A study by Djikgraaf *et al.*[4] showed that adsorbed oxygen atoms on the platinum active metal sites slowly penetrate the upper lattice of the platinum metal and form a subsurface atomic species leading to platinum oxide formation, which in this case is not

consistent with Pt XPS, which eventually leads to catalyst deactivation. This step is considered reversible. The simplest way for reduction or reactivation of the catalyst is to use exposure to an inert gas, and then the alcohol reactant inside the solution reduces the Pt surface. Indeed, alcohols are widely used in catalyst synthesis as soft reductants.[5-11]

In the case of the experiment (Entry 3) a step of cooling under oxygen and venting under air was introduced in the protocol. The concentration of oxygen and *n*-butanol inside the solution is decreased as a result of this venting (*i.e.* the solubility of oxygen is decreased when the pressure of oxygen decreases). This phenomenon may explain the increase in the conversion of *n*-butanol (though the mass balance does decrease as mentioned previously), but it is lower compared to when nitrogen is used. Obviously, the utilisation of nitrogen has removed molecular oxygen dissolved in the water and then the reduction of the Pt surface is more rapid. These data can be correlated with the paper published previously,[12] which shows a higher conversion of *n*-butanol on Pt supported on C. This has been already discussed in the previous Chapter. It has been suggested, based on the literature review, that Pt supported on C is protected from oxidation by the electronic properties of carbon and for this reason shows a high conversion of *n*-butanol compare to when other supports are used. So, it seems that when Pt is protected, either by the support, or by reduction using anaerobic conditions, or by lowering the concentration of oxygen, a higher conversion of *n*-butanol is promoted. The lower mass balance may be attributed to either CO_2 formation or losing some of the volatile substrate during the venting process. Lower mass balances can lead to artificial high conversions due to the loss of substrate, rather than actual conversion.

This first set of experiments have helped to gain a better understanding of the mechanism of deactivation and reactivation of the Pt catalyst. Oxygen at higher pressure (*i.e.* 3 bar) is one factor contributing to deactivation. Based on this It has been observed that purging the reaction by air or nitrogen helps to also recover the catalytic activity.

Based on these observations, another set of reactions was designed and performed to see the effect of lowering the concentration of oxygen in the system by using air instead of pure oxygen.

4.3. Effect of Air

The first experiment consisted of using air at 3 bar at the same operating conditions as pure oxygen, as the experiment in Entry 1. The results of this experiment are reported in Table 4.2, and compared to results obtained when pure oxygen was used.

Table 4.2. Conversion of 4 wt.% *n*-butanol and selectivity towards butyraldehyde and butyric acid over 1 wt.%Pt/TiO_2 under Air and O_2.

Oxidant	Conv. (%)	Sel. (%)		BuALD Yield (%)	Mass Balance (%)
		BuALD	BuAC		
Air	25	100	-	23	91
O_2	30	90	9	26	96

Conversion (Conv.), Selectivity (Sel.), Butyraldehyde (BuALD), Butyric Acid (BuAC).
***Reaction conditions*:** 100 °C, 3 bars O_2, 2 h, *n*-butanol (10 mL, 0.54 M), and catalyst (0.015 g).

The data show that under air and pure oxygen, after 2 hours reaction, the *n*-butanol conversion is almost the same (25-30 %). However, in the case of the air there is only butyraldehyde detected in the solution, but the mass balance was 5 % lower compared to when oxygen is used. It seems that when more oxygen is provided to the reaction, butyraldehyde is oxidised into butyric acid in the solution (9 %). Although the conversion using air gives high selectivity to butyraldehyde, the yield when using oxygen is better. From the previous observations it can be proposed that the lower concentration of oxygen, in the case of air, hinders the oxidation of butyraldehyde into butyric acid, because less oxygen is supplied to the reaction.

As the utilisation of air gives a better selectivity to butyraldehyde, and with the aim to increase the conversion of *n*-butanol, the same alternating cycles with nitrogen were performed under the same conditions as the ones used for the pure oxygen. The results are reported in Table 4.3.

Table 4.3. Conversion of 4 wt.%*n*-butanol and selectivity towards butyraldehyde and butyric acid over 1 wt.%Pt/TiO_2 with and without N_2 under **Air**.

Entry	Conv. (%)	Sel. (%)		BuALD Yield (%)	Mass Balance (%)
		BuALD	BuAC		
1	25	100	-	23	91
2	29	100	-	26	88
3	23	93	7	23	100

Conversion (Conv.), Selectivity (Sel.), *n*-Butanol (*n*-BuOH), Butyraldehyde (BuALD), Butyric Acid (BuAC).

***Reaction conditions*:** 100 °C, *n*-butanol (10 mL, 0.54 M), and catalyst (0.015 g).[2] 3 bar air for 3 h cool down every 1 h under N_2 for 10 min. [3] 3 bars air for total of 3 h the reaction every 1 h venting to air for 10 min.

In Table 4.3, Entry 1 corresponds to the reaction at 100 °C for 2 hours under 3 bar air without any cycle. Entry 2 corresponds to the same nitrogen cycling protocol as in Section 4.2, except that air is used instead of oxygen. Entry 3 represents an air cycling protocol.

When nitrogen was introduced into the reaction (Entry 2) the conversion of *n*-butanol is slightly increased when compared to Entry 1 (without cycling), to 29 %. Furthermore, it is important to notice here that butyric acid is not detected in the solution.

In the case of reaction Entry 3, there was no effect on the conversion of *n*-butanol compared with the Entry 1 experiment. However, it is noticed that only two products were generated in the solution, *i.e.* butyraldehyde and butyric acid, the mass balance being 100%. This last point is not yet clearly understood.

From this second set of experiments it appears that when the concentration of oxygen is lowered by using air, it doesn't have a positive effect on the conversion of *n*-butanol, even with the cooling down and the venting. The use of nitrogen has a slight promoting effect on the conversion of *n*-butanol under 3 bar air, but it is very minor, and it has a negative effect on the mass balance.

The statement that can be made from these two sets of experiments is that it is important to keep a concentration of oxygen which allows the oxidation of *n*-butanol into

butyraldehyde, but at the same time does not deactivate the catalyst, by catalyst poisoning.

4.4. Effects of pressure

Based on the observation in Section 4.3, the effect of the pressure of pure oxygen has been investigated. Indeed, the solubility of oxygen increases with increasing pressure. Figure 4.2 reports the results when the pressure of oxygen is lowered from 3 to 1 bar.

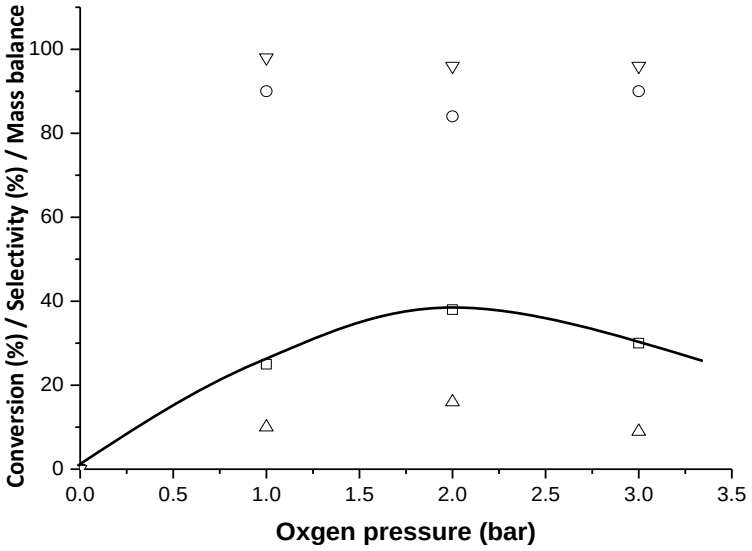

Figure 4.2. Conversion of 4 wt.% *n*-butanol and selectivity towards butyraldehyde and butyric acid over 1 wt.%Pt/TiO_2 at different O_2 pressures. □ Conversion of *n*-butanol, ○ Butyraldehyde Selectivity, △ Butyric Acid Selectivity, ▽ Carbon Mass balance. ***Reaction conditions*****:** 100 °C, 2 h, *n*-butanol (10 mL, 0.54 M), catalyst (15 mg), 750 rpm.

Figure 4.2 reports the experiment when pure oxygen under 3, 2 and 1 bar is used for 2 hours at 100 °C. The results show that when the pressure is increased from 1 to 3 bar, the conversion of *n*-butanol shows a volcano shape relationship, with a maximum for 2 bar O_2, where the conversion of *n*-butanol reaches 38 %. Another point is that the calculated mass balance, based on *n*-butanol, butyraldehyde and butyric acid, is increased as the pressure decreases.

The same kind of experiments have been performed with air. Figure 4.3 reports the effect of decreasing the pressure of air on the reaction.

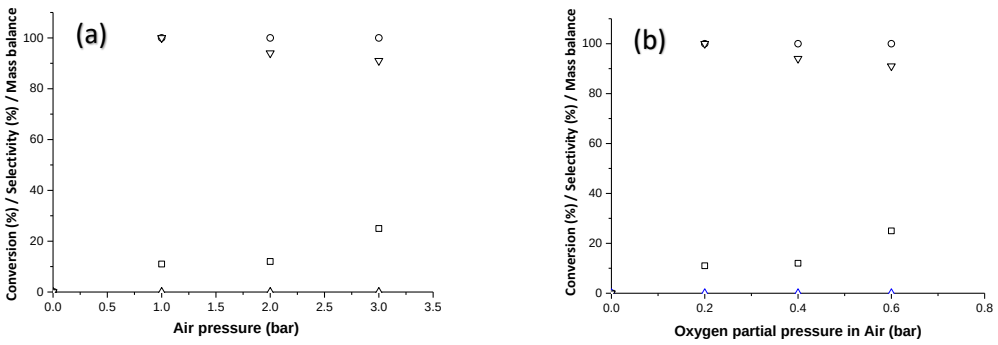

Figure 4.3. Conversion of 4 wt.%*n*-butanol and selectivity towards butyraldehyde and butyric acid over 1 wt.%Pt/TiO_2 (a) At different pressures of air (b) Different oxygen partial pressure. ☐ Conversion of *n*-butanol, ○ Butyraldehyde Selectivity, △ Butyric Acid Selectivity, ▽ Carbon Mass balance.

As the pressure of air decreased the conversion of *n*-butanol goes down from 25 % at 3 bar to 11 % at 1 bar. Furthermore, only butyraldehyde was detected in the solution for all pressures. Indeed, the concentration of oxygen is too low to oxidise butyraldehyde into butyric acid. Though the mass balance decreases linearly with increasing pressure, this suggest that oxidation may be occurring. It is important to note that in the previous Chapter it has been observed that butyraldehyde at 3 bar oxygen was undergoing auto-oxidation and this is not the case here. The mass balance increases when the pressure decreases, as observed with pure oxygen.

All these experiments have given a better understanding of how the concentration of oxygen in the solution, either by using pure oxygen or air, and by varying the pressure, can affect the final conversion of *n*-butanol. A compromise has to be found between the concentration of oxygen to be used in the solution to improve the performance of the catalyst. A low concentration of oxygen doesn't allow the sufficient oxidation of *n*-butanol, whilst a higher concentration of oxygen contributes to the catalyst deactivation. It has been found that using 2 bar of pure oxygen is a good compromise to reach a high conversion of *n*-butanol, *i.e.* 38 %, and a relatively high selectivity toward butyraldehyde *i.e.* 84 %.

4.5. Time on-line studies under 2 bar O_2

Based on the results of the previous section, and with the aim to determine the effect of a lower concentration of oxygen on the deactivation of the catalyst, the next step of the study was to perform a time-on line (TOL) reaction, for 6 hours under 2 bar O_2 at 100 °C. The results of the study are reported in Figure 4.4, Appendix C.

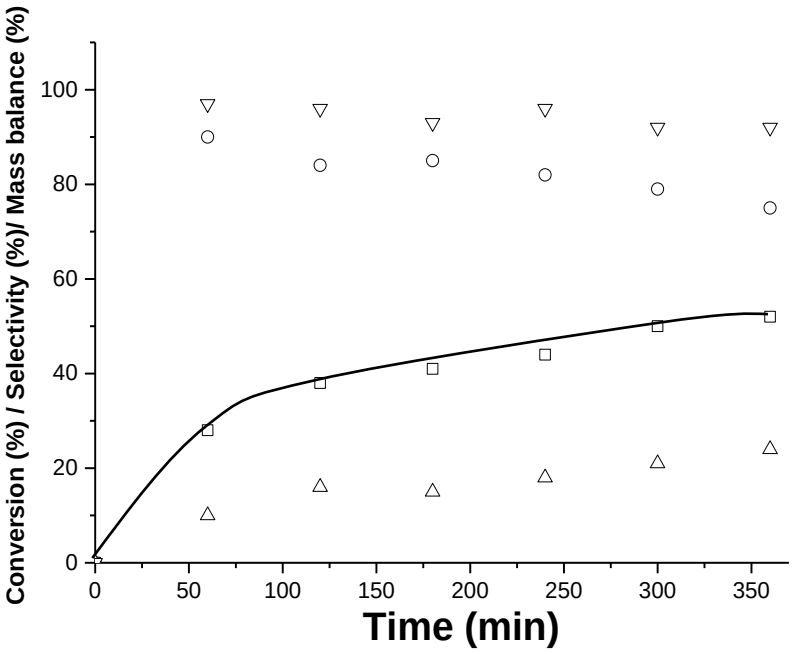

Figure 4.4. Time on-line data with 1 wt.%Pt/TiO_2 catalyst for selective oxidation of *n*-butanol. ***Reaction conditions*****:** 100 °C, 2 bar O_2, *n*-butanol (10 mL, 0.54 M), catalyst (15 mg), 750 rpm. □ Conversion of *n*-butanol, ○ Butyraldehyde Selectivity, △ Butyric Acid Selectivity,▽ Carbon Mass balance.

The results show that after 6 hours the conversion of *n*-butanol reached 54 % under 2 bar oxygen. This value is 2 times higher than when the 3 bar oxygen was used, *i.e.* 30 % (see Section 3.4, Figure 3.7). After 2 hours the selectivity towards butyraldehyde decreased slightly from 90 to 84 %, then after 4 hours the selectivity of butyraldehyde remained the same until the end of the time on-line. Butyric acid is the secondary product, which appears when the selectivity of butyraldehyde starts to decrease.

In addition, an important point to emphasize is that after 2 hours reaction the catalyst is still active, which was not the case when the reaction was performed under 3 bar oxygen (Chapter 3, Figure 3.7). It seems that after 5 hours the catalyst was still active.

4.6. Effect of promoters

As has been reported in the literature review (Chapter 1, Section 1.6.3.3.1), promoters are generally used to increase the activity during the alcohol oxidation process.[13, 14] Their role is not clearly understood. Among these promoters Bi and Pb are commonly used and help to increase the performances of Pt. They suppress the irreversible adsorption of alcohols (self-poisoning) on Pt and form new active site centres, which adsorb OH better than Pt in the potential range where the oxidation reaction occurs.[15]

The promoter metals such as Bi, Pb, Te, Sn, and others, have generated the most interest.[16-20] The promoter metals alone are inactive towards alcohol oxidation under the mild conditions applied; still, they induce sometimes spectacular rate enhancement [21, 22] or a shift in the product distribution. [23-25] Despite the intensive effort by several research groups, the real nature of the promoter effect is still debated, and there are no studies using *n*-butanol. Based on these studies bimetallic catalysts PtM (M=second metal) supported on TiO_2 have been prepared. The elements Al, Zn, Sn, Bi and Pb were selected and added to the Pt to study their effect on the Pt activity for the selective oxidation of *n*-butanol.

To improve the performance of platinum catalyst, the preparation of a Pt-base bimetallic is an effective route. It has been found that the use of a second element with Pt yield significant improvements relative to pure Pt. With respect to the nature of metallic components, it must be indicated that Pt has been intensively used as the active metal, catalysing several reactions such as the hydrogenation, isomerisation, dehydrogenation, oxidation of hydrocarbons, etc.[26, 27] The performance of the Pt metallic phase could be enhanced by addition of inactive metals of Group 14, such as Sn, Pb and Ge.[28-30] Previous studies show the influence of Pb on dehydrogenation performance.[31, 32] Other studies have demonstrated previously that Pt-based intermetallics containing less expensive metals, for instance Pb, show enhanced catalytic activities compared to pure Pt for the oxidation of methanol, formic acid, and hence can be used as efficient anode materials for fuel cell applications.[33-35]

The aim of this section is to compare the effect of promoters on catalytic properties of PtM supported catalysts, and to study the influence of different amounts of M added to Pt on the characteristics of the metallic phase, and on the catalytic performance in *n*-butanol oxidation. The catalysts have been prepared by sol-immobilisation, following the same protocol described in Chapter 2, Section 2.2.1.1.

4.6.1. 0.5 wt. % Pt – 0.5 wt. % M/TiO_2

In Table 4.4 the conversion of *n*-butanol, the selectivity toward butyraldehyde and butyric acid are reported, along with the mass balance and the leaching of Pt and the second added metal. The experiments have been performed using 0.5 wt.%Pt/TiO_2 and 0.5 wt.% of metal promoter added to the catalyst.

Table 4.4. Conversion of 4 wt.%*n*-butanol and selectivity towards butyraldehyde and butyric acid over 0.5 wt.%Pt/TiO_2 and 0.5 wt.%Pt 0.5 wt.%M/TiO_2 (M= Bi, Pb, Al, Zn, Sn).

Catalysts Supported on TiO_2	Conv. (%)	Sel. (%)		Mass Balance	Leaching (%)	
		BuALD	BuAC		Pt	M
0.5 wt.%Pt	8	96	4	98	0.1	-
0.5 wt.%Pt -0.5 wt. %Bi	14	95	5	100	0.1	0.1
0.5 wt.%Pt b-0.5 wt. %Pb	43	94	6	96	0.6	0.4
0.5 wt.%Pt -0.5 wt. %Sn	34	91	9	100	1.9	0.1
0.5 wt.%Pt -0.5 wt. %Al	25	93	8	100	2.0	4.1
0.5 wt.%Pt -0.5 wt. %Zn	35	94	6	93	0.6	2.3

Conversion (Conv.), Selectivity (Sel.), *n*-Butanol (*n*-BuOH), Butyraldehyde (BuALD), Butyric Acid (BuAC).

Reaction conditions: 100 °C, 2 Bar O_2, 2 h, *n*-butanol (10 mL, 0.54 M), 0.015g of catalyst, 750 rpm.

The conversion of *n*-butanol and the selectivity towards butyraldehyde and butyric acid using 0.5 wt. Pt/TiO_2 were 8, 96 and 4 % respectively.

The addition of the second metal had an effect mainly on the conversion of *n*-butanol. The activity was increased, with the following order established:

$$Bi < Al < Zn \approx Sn < Pb$$

The addition of Pb showed the best activity, as has been found by several groups.[13, 14]

XPS was performed on the used catalyst. XPS of the Pt(4f) region is shown in Figure 4.5.

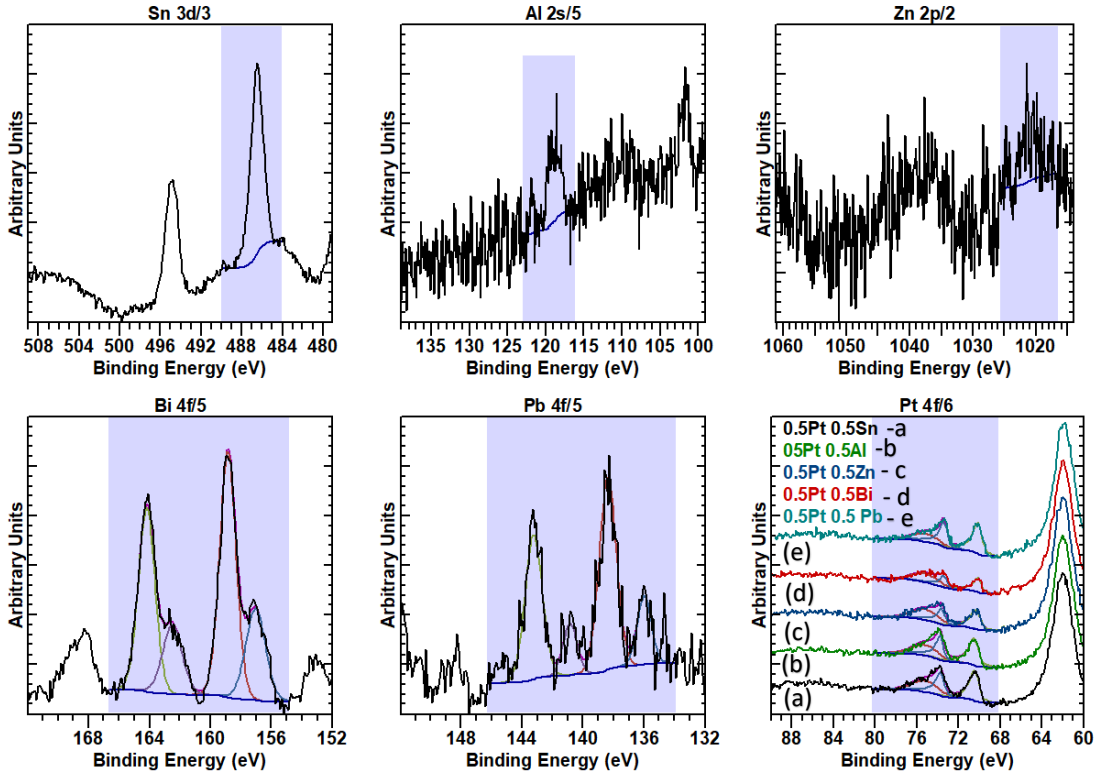

Figure 4.5. Core levels spectra for 0.5 wt.%Pt/TiO_2 and 0.5 wt.%Pt 0.5-wt.%M/TiO_2 catalysts. Each bi-metallic component is shown together with a labelled stack of the Pt(4f) spectra.

From the XPS spectra of the bimetallic species, it is clear that the second metal typically is in a cationic form, whilst some (Bi and Pb) typically reveal both oxidic and elemental states. This may be a thin oxide 'skin' on the elemental species, as both oxide and elemental species would not necessarily be expected. As explored in the following tables, it can be seen that regardless of loading, the oxidation states of the metals discussed did not differ significantly from those of the 0.5Pt-0.5M samples. Of note is the shift to lower values of binding energy for the Pt species, from 70.8 eV, typical of bulk metallic species, to around 70.2 eV, suggesting the Pt particles have become smaller due to the inclusion of the second metal, or electron transfer between the metals is occurring making the Pt more electron-rich.

TEM was used to characterise the 0.5 wt. % Pt and 0.5 wt.% Pt-0.5 wt.%Sn colloids that were used to prepare the catalysts (Figure 4.6).

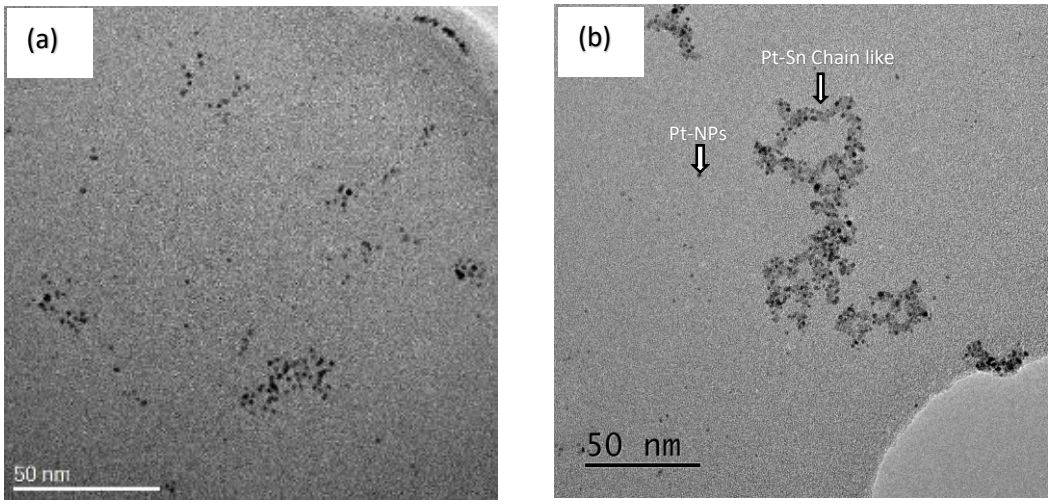

Figure 4.6. TEM image of Pt and Pt-Sn sol immobilisation colloids dispersed on the TEM grid (a) 0.5 wt. % Pt sol (PVA, $NaBH_4$) and (b) 0.5 wt. % Pt-0.5 wt. %Sn (PVA, $NaBH_4$).

The Pt prepared by sol immobilisation is well dispersed (Figure 4.6 (a)). However, Pt-Sn sol-immobilised colloidal catalysts display chain-like structures as shown in Figure 4.6 (b). By looking to Figure 4.6 (a) one can see that there are discrete Pt nanoparticles, whereas in (b) it can be seen that Pt nanoparticles are attached together with Sn species; the presence of SnOx was confirmed by XPS in Figure 4.5.

Figure 4.7 shows TEM images of 0.5 wt. % Pt and 0.5 wt. % Pt-0.5 wt. %Sn on the TiO_2 support.

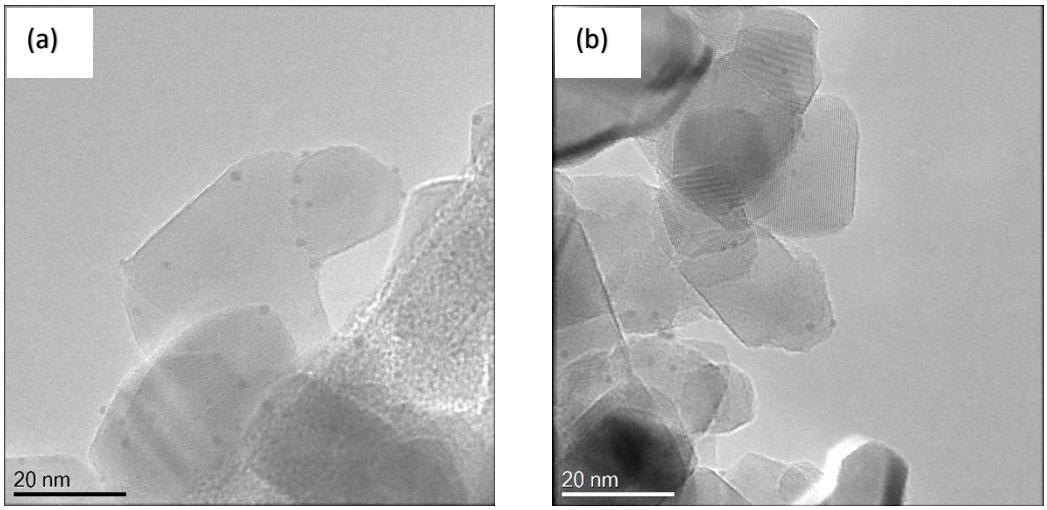

Figure 4.7. TEM image of (a) 0.5 wt.%Pt/TiO_2 and (b) 0.5 wt.%Pt-0.5 wt.%Sn/TiO_2 catalysts.

From Figure 4.7 we do not see the chain like structures (as seen in colloid Figure 4.6 (b)) when the Pt-Sn is supported on TiO_2.

Due to the results shown in Chapter 3 it was decided that work would be continued using 1 wt.%Pt /M and this catalyst would be used in a study of different promoters and their loadings.

4.6.2. 1 wt.%Pt – 0.5 wt.%M/TiO_2

Table 4.5 displays the *n*-butanol conversion, the selectivity toward butyraldehyde and butyric acid, the mass balance and the leaching when the monometallic 1 wt.%Pt/TiO_2 and the bimetallic catalysts 1 wt.%Pt - 0.5 wt.%M/TiO_2 are used, Appendix D.

Table 4.5. Conversion of 4 wt.%*n*-butanol and selectivity towards butyraldehyde and butyric acid over 1 wt.%Pt/TiO_2 and 1 wt.%Pt-0.5 wt.%M/TiO_2 (M= Bi, Pb, Al, Zn, Sn).

Catalysts Supported on TiO_2	Conv. (%)	Sel. (%)		Mass balance	Leaching (%)	
		BuALD	BuAC		Pt	M
1 wt.% Pt	38	84	16	96	3.10	-
1 wt.%Pt-0.5 wt.%Al	12	99	2	96	0.01	0.3
1 wt.%Pt-0.5 wt.%Sn	40	89	11	98	3.70	0.9
1 wt.%Pt-0.5 wt.%Bi	26	85	15	99	1.00	0.6
1 wt.% Pt-0.5 wt.% Zn	23	94	7	98	0.30	5.3
1 wt.% Pt-0.5 wt.% Pb	41	85	15	89	1.20	0.6

Conversion (Conv.), Selectivity (Sel.), Butyraldehyde (BuALD), Butyric Acid (BuAC).
Reaction Conditions: 100 °C, 2h, 2 bar O_2, *n*-butanol (10 mL, 0.54 M), 15 mg of catalyst.

The addition of a second metal to Pt shows lower conversion of *n*-butanol compared to the 1 wt.% Pt/TiO_2, except for 1 wt.%Pt-0.5 wt.%Sn/TiO_2 and 1 wt.%Pt-0.5 wt.%Pb/TiO_2. However, for all the bimetallic catalysts the leaching of Pt decreased, compare to the monometallic one, except for the catalyst with Sn (3.7 %). The addition of a second metal in some case appears to reduce the extent of Pt leaching in the reaction. With the PtPb catalyst for example, the activity is comparable to the monometallic Pt catalyst, though the mass balance is 7 % lower, but the quantity of Pt leached is decreased (from 3.1 % to 1.2 %). This suggests that the addition of a second metal may be a method for stabilising the catalyst. In some cases however, the addition

of the secondary metal appears to reduce the performance of the catalyst, as shown in Table 4.5.

The 1 wt.%Pt-0.5 wt.%Pb/TiO_2 has higher activity for *n*-butanol than the other catalysts. Accordingly, it was decided to carry on the work focussing on the 1 wt.%Pt- 0.5 wt.%Pb/TiO_2 from Table 4.5.

4.6.2.1. 1 wt.%Pt–0.5 wt.%Pb/TiO_2

Platinum based catalysts can be greatly improved in performance by alloying Pt with p-block elements, such as Pb, which is widely utilised for fuel cell applications and in the petrochemical industry.[33, 34, 36-41] Alloying can enhance the activity which attributes to the bi-functional mechanism, electronic effects, crystal orientations, or a favourable interatomic distance between Pt and the counter atoms.[42] A previous study showed that the two types of catalysts, Pt-based and Pb-based, exhibit activity towards HCOOH electrooxidation.[43] In comparison with Pt-based and Pb-based, the pure Pt is easily poisoned by adsorbed CO (CO_{ad}), a reaction intermediate,[44, 45] whereas Pb-based exhibits a very high initial activity due to being free of CO poisoning, but their long-term stability is not satisfactory.[46-48] By modifying the Pt surface with sub-monolayer foreign metal adatoms such as Pb can enhance the activity significantly.[49-51]

The catalytic activity of the 1 wt.%Pt-0.5 wt.%Pb/TiO_2 catalyst towards *n*-butanol oxidation was investigated. Time on-Line (TOL) data for this catalyst is shown below in Figure 4.8.

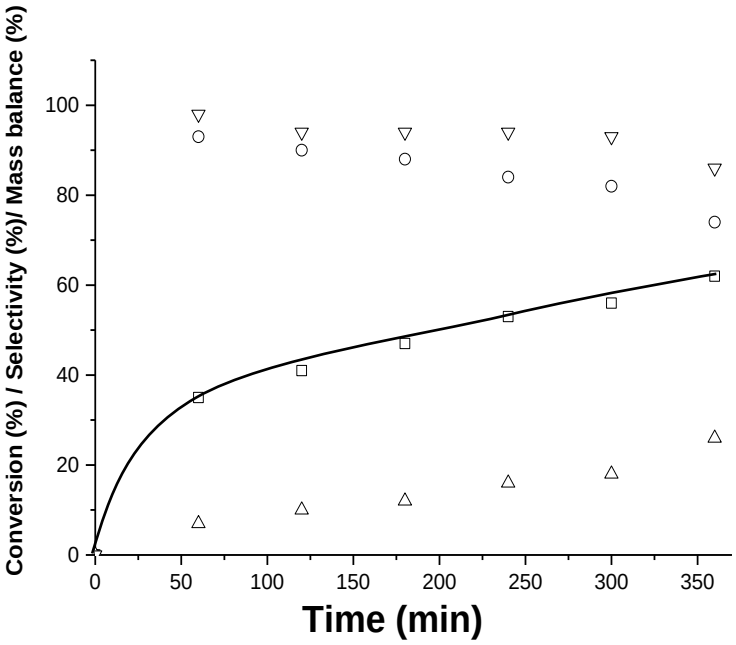

Figure 4.8. Time on-line data with 1 wt.%Pt-0.5 wt.%Pb/TiO_2 catalyst for selective oxidation of *n*-butanol. ***Reaction conditions*****:** 100 °C, 2 bar O_2, *n*-butanol (10 mL, 0.54 M), catalyst (15 mg), 750 rpm. □ Conversion of *n*-Butanol, ○ Butyraldehyde Selectivity, △ Butyric Acid Selectivity, ▽ Carbon Mass balance.

The graph shows that conversion of *n*-butanol starts to increase from 0 % to 62 %. There is significant increase of conversion after 4 h of reaction. The selectivity of butyraldehyde decreases from 93 % to 74 %, due to formation of butyric acid. The addition of lead as a promoter results in profound modification of the activity of the catalyst; the presence of the Pb promoter seems to suppress the poisoning observed with Pt alone, and improves the catalyst performance,[43] and high conversion was achieved with *n*-butanol, though the mass balance decreased from 92 % (1 wt.%Pt/TiO_2) to 86 % (1 wt.%Pt-0.5 wt.%Pb/TiO_2) at 6 h. Considering the time on-line results, it has been observed that the 1 wt.%Pt/TiO_2 (Figure 4.4) without promoter after 6 h the conversion of the *n*-butanol was 54 %. The addition of the Pb promoter to 1 wt.%Pt/TiO_2 enhances the activity of the catalyst to 62 % conversion after 6 h. At similar levels of conversion (41 and 54 %) the promoted catalyst demonstrates slightly higher butyraldehyde selectivity, 90 % and 84 % compared to 85 % and 75 %, respectively.

With the aim to demonstrate the stability of the 1 wt.%Pt 0.5 wt.% Pb/TiO_2 catalyst, the catalyst was tested, recovered and retested under the standard conditions (100 ^{0}C, 2 h and 2 bar O_2). The results are reported in Table 4.6.

Table 4.6. Reusability of 1 wt.% Pt-0.5 wt.%Pb/TiO_2 catalyst for 3 cycles.

Test cycle	Conv. *n*-BuOH (%)	Sel. (%)		Leaching (%)		Mass Balance (%)
		BuALD	BuAC	Pt	M	
1st	41	90	10	1.2	0.6	94
2nd	35	90	10	0.5	0.7	97
3rd	33	91	9	0.4	0.5	97

Conversion (Conv.), Selectivity (Sel.), *n*-Butanol (n-BuOH), Butyraldehyde (BuALD), Butyric Acid (BuAC). ***Reaction Conditions:*** 100 °C, 2 bar O_2, 2 h, *n*-butanol (10 mL, 0.54 M), 15 mg of catalyst**.**

The data shows that after 3 tests the conversion of *n*-butanol decreased. However, the selectivity toward butyraldehyde remains the same across the tests (~90 % to 91 %). In parallel, the selectivity to butyric acid remained the same across the tests; 9 % to 10 %. The first statement which can be made from these data is that the catalyst is losing activity with every test cycle. Given that the previously identified error in this reaction to be $\pm$ 4% these values are within experimental error.

The second statement which can be made is that the selectivity toward butyraldehyde and butyric acid remain the same. The leaching of platinum continues with each cycle, although it decreases. The ICP analysis has shown that 1.2 % of Pt from the catalyst is leached after 2 h reaction time. After the 2nd and 3rd use, the Pt leaching decreases to 0.5 and 0.4 %, respectively.

The effects of thermal pre-treatment conditions on the 1 wt.%Pt-0.5 wt.%Pb/TiO_2 catalyst was investigated, using calcination in air or reduction in hydrogen.

The time of pre-treatments under air or under hydrogen was maintained the same, *i.e.* 2 h at 200 °C, and a ramp rate from ambient of 5 °C/min. The results are reported in Table 4.7, Appendix E.

Table 4.7. Catalyst performance of 1 wt.%Pt-0.5 wt.%Pb/TiO_2 for *n*-butanol oxidation following different thermal pre-treatments.

Catalyst pre-treatment	Conv. (%)	Sel. (%)		Leaching (%)		Mass Balance (%)
		BuALD	BuAC	Pt	M	
1 wt. % Pt - 0.5 wt.%Pb/TiO_2 (Fresh)	41	90	10	1.2	0.6	94
1 wt. % Pt - 0.5 wt.%Pb/TiO_2 (Calcined)	16	95	5	0.1	0.5	96
1 wt. % Pt - 0.5 wt.%Pb/TiO_2 (5 vol.% H_2/Ar at 200 °C)	40	93	7	0.2	0.8	91

Conversion (Conv.), Selectivity (Sel.), Butyraldehyde (BuALD), Butyric Acid (BuAC)

Reaction Conditions: 100 °C, 2 h, 2 bar O_2, *n*-butanol (10 mL, 0.54 M), 15 mg of catalyst.

***Catalysts pre-treated*:** Calcined under air or A flow of 5 vol.%H_2/Ar for 2 h at 200 °C (5 °C/min).

Table 4.7 shows that when the catalysts are calcined under air for 2 h, the conversion of the *n*-butanol is decreased when compared to the catalysts that are freshly prepared. Furthermore, when the catalysts are treated under 5 vol.%H_2/Ar , the conversion of *n*-butanol is the same as when compared to the catalysts that are freshly prepared (as-obtained).

Again, it is important to notice here that the pretreatment plays an important role in the distribution of the products of the reaction and seems to confirm the hypothesis made previously for 1 wt.%Pt/TiO_2 reactions (Section 3.6.1).

From the observation it is possible to suggest that the particle size could influence the reaction rate, and therefore lower rates of activity with the time of use, suggesting a potential deactivation mechanism. This could imply that nanoparticle size is one of the reasons for the difference in catalyst activities on successive reuse. The XPS indicates the Pt to still be in a metallic form, exhibiting the previously noted low-binding energy (*ca.* 70.2 eV) after pre-treatment.

The ICP-MS results reported in Table 4.7 shows that the leaching of platinum from the 1 wt.%Pt-0.5 wt.% Pb/TiO_2 fresh catalyst is 1.2 %.

Selected SEM images of the 1 wt.%Pt - 0.5 wt.%Pb/TiO_2 fresh, calcined, 5 vol.%H_2/Ar treated, and used catalysts (after 2 h reaction) are presented in Figure 4.9.

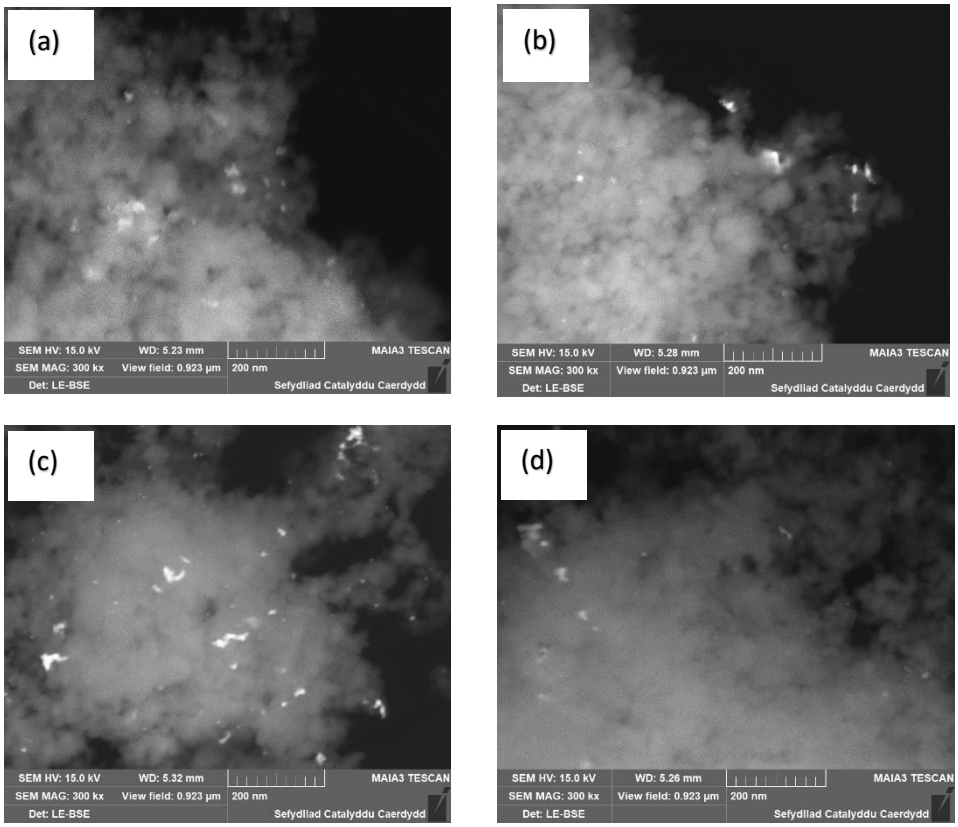

Figure 4.9. Representative SEM image of the 1 wt.%Pt - 0.5 wt.%Pb/TiO_2 (a) fresh (b) Used (after 2 h reaction) (c) Calcined (d) 5 vol.%H_2/Ar at 200 °C treatment. ***Reaction conditions :*** 100 °C, 2 h, 2 bar O_2, *n*-Butanol (0.54 M), 15 mg of catalyst, 750 rpm. ***Catalysts pre-treated:*** Calcined under air or A flow of 5 vol % H_2/Ar for 2 h at 200 °C (5 °C/min).

From the SEM (Figure 4.9) no difference can be detected between the 1 wt.%Pt - 0.5 wt.%Pb/TiO_2 catalysts before or after any treatment. SEM indicates that there are metals present, showing nanoparticles and that these nanoparticles are agglomerated. From the SEM images conclusions on particle size couldn't be made.

As mentioned in Chapter 3, Section 3.6.2 the SEM characterisation of the monometallic 1 wt.%Pt/TiO_2 catalyst shows that catalyst pretreatment affects the average particle size. The different activities observed could therefore likely be attributed to different pretreatment (Table 3.10) which cannot be observed by bimetallic 1 wt.%Pt- 0.5 wt.%Pb/TiO_2 catalysts.

4.6.3. 1 wt.%Pt – 1 wt.%M/TiO_2

The aim of this section is to show the effect of different promoter loadings with Pt on TiO_2 on the conversion of *n*-butanol and on the selectivity towards the different products. A series of 1 wt.%Pt/TiO_2 catalyst with M weight loadings of 1 wt. (M = Al, Sn, Bi, Zn and Pb) were prepared and tested for the oxidation of *n*-butanol at 100 °C, 2 bar O_2 for 2 h. Table 4.8 reports the conversion of *n*-butanol with bimetallic catalysts with a ratio 1 wt.% Pt-1 wt.%M/TiO_2, Appendix F.

Table 4.8. Conversion of 4 wt.%*n*-butanol and selectivity towards butyraldehyde and butyric acid over 1 wt.%Pt/TiO_2 and 1 wt.%Pt-1 wt.%M/TiO_2 (M= Bi, Pb, Al, Zn, Sn).

Catalysts Supported on TiO_2	Conv. (%)	Sel. (%)		Leaching (%)		Mass Balance (%)
		BuALD	BuAC	Pt	M	
1 wt.% Pt	38	84	16	3.10	-	96
1 wt.% Pt-1 wt.% Al	6	100	0	0.03	0.9	98
1 wt.% Pt-1 wt.% Sn	39	90	10	2.70	0.7	94
1 wt.% Pt-1 wt.% Bi	29	87	13	0.03	0.1	96
1 wt.% Pt-1 wt.% Zn	25	93	7	0.40	4.6	98
1 wt.% Pt-1 wt.% Pb	22	92	8	1.30	10.4	98

Conversion (Conv.), Selectivity (Sel.), Butyraldehyde (BuALD), Butyric Acid (BuAC)**.**
***Reaction Conditions*:** 100 °C, 2h, 2 bar O_2, *n*-butanol (10 mL, 0.54 M), 15 mg of catalyst.

The data show that all the bimetallics show an activity lower than the monometallic catalyst, except for 1 wt. %Pt-1 wt.%Sn/TiO_2 which shows comparable conversion (39 %) to the 1 wt.%Pt/TiO_2 (38 %). Another point is that the platinum leaching is reduced with the addition of the second metal. From Table 4.5 it is possible to see that the leaching of Pt can be increased (3.7 %, Table 4.5) when using a low metal loading of tin (0.5 wt.%Sn).

4.6.3.1. 1 wt.%Pt–1 wt.%Sn/TiO_2

Based on previous studies, promoter metals such as tin have generated significant interest. In the work reported here, the use of PtSn as a catalyst for the oxidation of *n*-butanol in water is presented. PtSn has been studied as a catalyst for alcohol (methanol[52-54] and ethanol[54-57]) oxidation over the last decade; it is currently the most active electrocatalyst used for ethanol oxidation[58, 59] in direct ethanol fuel cells,[60] even though the main products of this process are acetaldehyde and acetic acid.[61] The major difference between PtSn and Pt is the different shifts in lattice structure.[62] When Sn is incorporated into the fcc structure of Pt, the diffraction peaks of the resulting alloy are shifted slightly to lower 2θ values compared to corresponding peaks for a pure platinum catalyst.[62] This indicates that solid solutions of Pt and Sn have formed, which may lead to different energies for alcohol molecules to adsorb onto the catalyst, and for the formation of reaction intermediates, when compared to the energies on a pure Pt catalyst. Moreover, the introduction of Sn atoms alters the electron distribution in the orbitals of Pt. Colmati *et al*.[63, 64] found that a decrease in Pt 5*d*-band vacancies could be attributed to the donation of electrons from the Sn 5*p* and *s* bands to the Pt 5*d* band, which is a strong acceptor.

The study reported in this section focusses on oxidation of *n*-butanol on PtSn Figure 4.10. The following graph shows TOL with the bimetallic catalyst 1 wt.%Pt 1 wt.%Sn/TiO_2.

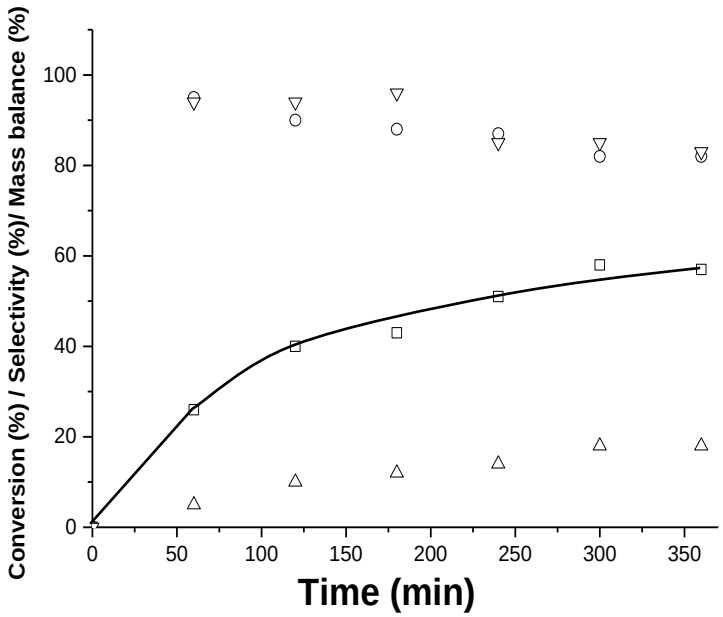

Figure 4.10. Time on-line data with 1 wt.%Pt - 1 wt.%Sn/TiO_2 catalyst for selective oxidation of *n*-butanol. ***Reaction conditions*****:** 100 °C, 2 bar O_2, *n*-butanol (10 mL, 0.54 M), catalyst (15 mg), 750 rpm. □ Conversion of *n*-butanol, ○ Butyraldehyde Selectivity, △ Butyric Acid Selectivity, ▽ Carbon Mass balance.

The data shows that after 6 h the conversion of *n*-butanol increases from 0 % to 56.6 %. There is significant increase of conversion after 4 h; this observation seems to indicate that the catalyst was still active after 4 h of reaction and was still active for the conversion of butyraldehyde into butyric acid. The selectivity of butyraldehyde decreased from 95 % to 82 %, due to formation of butyric acid (5 to 18 %). Another point is that the platinum leaching is increasing with the time (Table 4.9). Compare to Figure 4.4, it seems that the addition of tin enhance the conversion of *n*-butanol and selectivity towards butyraldehyde, although the mass balance is lower.

Table 4.9. Time on-line (TOL) data with 1 wt.%Pt-1 wt.%Sn/TiO_2 catalyst for Pt leaching (%).

TOL (h)	**1**	**2**	**3**	**4**	**5**	**6**
Pt leaching (%)	0.8	2.7	2.8	4.7	5.4	5.9
Sn leaching (%)	0.4	0.7	0.1	0.5	0.2	0.8

Reaction conditions**:** 100 °C, 2 bar O_2, *n*-butanol (10 mL, 0.54 M), catalyst (15 mg), 750 rpm.

In order to assess the stability of the 1 wt.%Pt 1 wt.% Sn/TiO_2 catalyst, the catalyst has been tested, recovered and retested under the standard conditions (100 °C, 2 h and 2 bar O_2). The results are reported in Table 4.10.

Table 4.10. Reusability of 1 wt.%Pt - 1 wt.%Sn/TiO_2 catalyst for 3 cycles

Test cycle	Conv. *n*-BuOH(%)	Sel. (%)		Leaching (%)		Mass Balance (%)
		BuALD	BuAC	Pt	M	
1st	39	90	10	2.7	0.7	94
2nd	35	92	8	1.4	1.4	94
3rd	31	92	8	1.1	1.1	95

Conversion (Conv.), Selectivity (Sel.), *n*-Butanol (n-BuOH), Butyraldehyde (BuALD), Butyric Acid (BuAC). ***Reaction Conditions:*** 100 °C, 2 bar O_2, 2 h, *n*-butanol (10 mL, 0.54 M), 15 mg of catalyst.

The data shows that after 3 cycles the conversion of *n*-butanol decreases. However, the selectivity toward butyraldehyde remains the same across the runs: ~ 90 % to 92 % from the first test to the third run. The selectivity toward butyric acid also remains the same throughout the test, increasing slightly from 8 to 10 % between the 1st and 3rd test, respectively. The first statement which can be made from this data is that after each test the catalyst still converts *n*-butanol, but still deactivated after 1st and 2nd use. It is also clear that the catalyst can convert *n*-butanol into butyraldehyde and butyric acid. The leaching of platinum decreases after the 1st cycle from 2.7 % to 1.4 % and 1.1 % for 2nd and 3rd cycles, respectively. This may suggest that these nanoparticles are agglomerated after each use.

The effect of catalyst thermal pre-treatments on *n*-butanol selective oxidation are reported in Table 4.11, Appendix G.

Table 4.11. Effect of thermal pre-treatment of 1 wt.%Pt - 1 wt.%Sn/TiO_2 catalyst for *n*- butanol selective oxidation..

Catalyst pre-treatment	Conv. (%)	Sel. (%)		Leaching (%)		Mass Balance (%)
		BuALD	BuAC	Pt	M	
1 wt.%Pt - 1 wt.%Sn/TiO_2 (Fresh)	39	90	10	2.7	0.7	94
1 wt.%Pt - 1 wt.%Sn/TiO_2 (Calcined)	40	91	9	2.0	0.2	94
1 wt.%Pt - 1 wt.%Sn/TiO_2 (5% H_2/Ar at 200 °C)	31	92	8	1.3	0.3	96

Conversion (Conv.), Selectivity (Sel.), Butyraldehyde (BuALD), Butyric Acid (BuAC)
Reaction Conditions: 100 °C, 2 h, 2 bar O_2, *n*-butanol (10 mL, 0.54 M), 15 mg of catalyst. ***Catalysts pre-treated*****:** Calcined under air or A flow of 5 vol.%H_2/Ar for 2 h at 200 °C (5 °C/min).

In the case of the 1 wt.%Pt - 1 wt.%Sn/TiO_2, when the catalyst is calcined, the conversion of *n*-butanol remains the same (Table 4.11). When the catalyst is pre-treated under 5 vol.%H_2/Ar the conversion of *n*-butanol reduces from 39 % to 31 % when compared to the fresh catalyst (as-obtained). It can be observed from data reported in Table 4.10 that the amount of leached platinum decreases from 2.7 % for fresh catalyst to 2.0 % and 1.3 % for calcined and pre-treated under 5 vol.% H_2/Ar, respectively.
Figure 4.11 shows the SEM images of 1 wt. % Pt - 1 wt.%Sn/TiO_2 catalysts when fresh, used (after 2 h reaction), calcined, and after 5 vol.% H_2/Ar treatment.

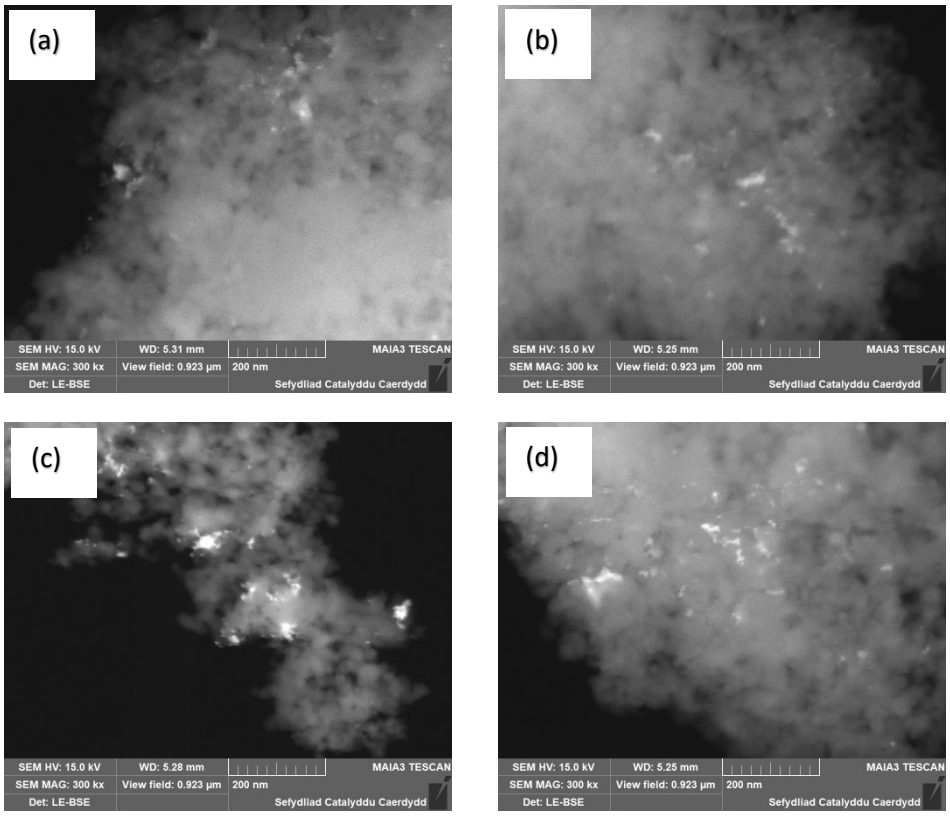

Figure 4.11. SEM image of the 1 wt.%Pt - 1 wt.%Sn/TiO_2 (a) Fresh (b) Used (after 2 h reaction) (c) Calcined (d) 5 vol.% H_2/Ar at 200 °C treatment. ***Reaction conditions:*** 100 °C, 2 h, 2 bar O_2, *n*-butanol (0.54 M), 15 mg of catalyst, 750 rpm. ***Catalysts pre-treated:*** Calcined under air or A flow of 5 vol.% H_2/Ar for 2 h at 200 °C (5 °C/min).

From the SEM images in Figure 4.11, it can be concluded that there are metal nanoparticles present on the surface, however, there are no clear differences between the fresh, used, calcined and 5 vol.% H_2/Ar treated catalysts. Its only shows that there are nanoparticles and that these nanoparticles are agglomerated.

4.7. XPS characterisation of 1 wt.%Pt–0.5 wt.%Pb/TiO_2 and 1 wt.%Pt-1 wt.%Sn/TiO_2 catalysts

Figure 4.12 reports XPS data for catalyst before and after pre-treatment.

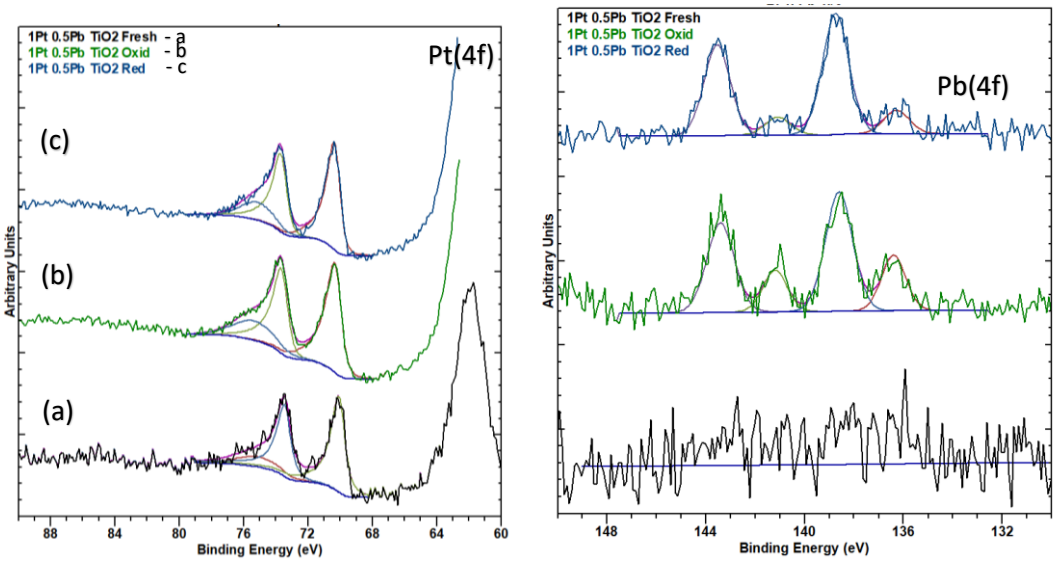

Figure 4.12. XPS analysis of 1 wt.%Pt–0.5 wt.%Pb/TiO_2 catalysts (a) Fresh, (b) Calcined, (c) Under 5% H_2/Ar. ***Catalysts pre-treated*:** Calcined under air or A flow of 5 vol.%H_2/Ar for 2 h at 200 °C (5 °C/min).

For the 1 wt.%Pt – 0.5 wt.%Pb/TiO_2 catalysts, 0.5 wt.%Pb sample, no Pb is readily evident in the freshly prepared sample, which may be attributed to Pt encapsulation or very large particles with poor dispersion. The samples calcined in air show a Pb (II) signal, again potentially a "skin" of oxide is formed on top of the elemental Pb. Despite the reductive treatment, we still observe a Pb oxide, which we attribute to re-oxidation of the Pb species during preparation and insertion into the XPS system.

For the equivalent Sn samples, we observe a similar case to that of the Pb data, where there is no significant shift in Pt(4f) binding energy, with all values within experimental error of metallic Pt (*ca.* 71 eV). The Sn(3d) region is less diagnostic to the formation of an oxide, since there is no significant shift between metallic Sn and Sn(I) or Sn(II) oxides.

The addition of lead and tin as promoters improves the catalyst performance. Previous studies by Colmati *et al*.[63, 64] show that the introduction of Sn atoms alters the electron distribution in the orbitals of Pt, stating that a decrease in the Pt 5*d*-band vacancies could be attributed to the donation of electrons from the Sn 5*p* and *s* bands to the Pt 5*d* band, which is a strong acceptor.

It seems that lead and tin suppress the poisoning observed with Pt alone, and improves the catalyst activity the platinum catalyst.

4.8. Conclusion

The oxidation of *n*-butanol was performed with a 1 wt.%Pt/TiO_2 catalyst under different conditions. Alternative cycles of oxygen/air and nitrogen were performed to better understand the activation of the catalyst. It was found that by alternating aerobic and anaerobic cycles that it was possible to limit the deactivation of the catalyst and to improve its performance. Characterization by XPS of the catalyst after the different cycles showed no significant change in Pt oxidation state or concentration, with the Pt remaining metallic and *ca.*0.3 at % concentration of the total elemental concentration. It was found that using air instead of oxygen increased the selectivity toward butyraldehyde. Based on this observation the effect of the concentration of oxygen was studied by varying the partial pressure. It was found that the best pressure, which gives the highest conversion, was 2 bar. The time on-line studies at this pressure were performed, and the catalysts show a higher life-time than when the pressure was 3 bar. Addition of promoters show an enhancement of catalytic activity for the Pt catalysts.

The *n*-Butanol oxidation has been performed with a 1 wt.%Pt-0.5 wt.%Pb/TiO_2 catalyst. The 1 wt.%Pt-0.5 wt.%Pb/TiO_2 presents the highest activity towards the conversion of *n*-butanol. The time online data has shown that different steps are occurring during the oxidation of *n*-butanol at different times of the reaction. The addition of lead as a promoter seems to suppress the poisoning observed with Pt alone, and improves the catalyst performance. The 1 wt.%Pt-0.5 wt.%Pb/TiO_2 showed sensitivity to such treatment and it has been concluded that there is a strong correlation between the pre-treated catalyst and the rate of *n*-butanol conversion. XPS analysis of 1 wt.%Pt-0.5 wt.%Pb/TiO_2 samples reveal that Pt exclusively is in the metallic state. The reusability of the catalyst has been tested over 3 cycles and the results have shown that the catalyst is still active towards the conversion of *n*-butanol, but the catalyst is losing activity with every test cycle.

The 1 wt.%Pt-1 wt.%Sn/TiO_2 catalyst also showed comparable conversion (39 %) to the 1 wt.%Pt/TiO_2 (38 %) for the *n*-butanol oxidation. The time on-line shows that after 6 h the conversion of *n*-butanol increases to 56.6 %. The 1 wt.%Pt-1 wt.%Sn/TiO_2 catalyst was still active after 4 h of reaction and was still active for the conversion of butyraldehyde into butyric acid. The reusability test shows that after each test the catalyst still converts *n*-butanol, but deactivates after 1st and 2nd use. It is also clear that the leaching of platinum decreases after the 1st cycle from 2.7 % to 1.4 % and 1.1 % for

2nd and 3rd cycles, respectively. When the 1 wt.%Pt-1 wt.%Sn/TiO_2 catalyst is calcined, the conversion of *n*-butanol remains the same. On the other hand when the catalyst is pre-treated under 5 vol.%H_2/Ar the conversion of *n*-butanol reduces from 39 % to 31 %, this may suggest that these nanoparticles are agglomerated after pre-treatment and this was confirmed by SEM characterisation.

4.9. References

1. A. P. Markusse, B. F. M. Kuster, D. C. Koningsberger and G. B. Marin, Catal. Lett., 1998, 55, 141-145.

2. J. W. Nicoletti and G. M. Whitesides, J. Phys. Chem., 1989, 93, 759-767.

3. M. Besson and P. Gallezot, Catal. Today, 2000, 57, 127-141.

4. P. J. M. Dijkgraaf, H. A. M. Duisters, B. F. M. Kuster and K. Van der Wiele, J. Catal., 1988, 112, 337-344.

5. Y. Ukisu, React. Kinet., Mech. Catal., 2015, 114, 385-394.

6. C. Shen, Y. J. Wang, J. H. Xu, K. Wang and G. S. Luo, Langmuir, 2012, 28, 7519-7527.

7. A. Barau, V. Budarin, A. Caragheorgheopol, R. Luque, D. J. Macquarrie, A. Prelle, V. S. Teodorescu and M. Zaharescu, Catal. Lett., 2008, 124, 204-214.

8. T. Kim, M. Takahashi, M. Nagai and K. Kobayashi, Electrochem. Acta., 2004, 50, 817-821.

9. J. S. Bradley, E. W. Hill, S. Behal, C. Klein, A. Duteil and B. Chaudret, Chem. Mater., 1992, 4, 1234-1239.

10. T. Teranishi and M. Miyake, Chem. Mater., 1998, 10, 594-600.

11. T. Teranishi, M. Hosoe, T. Tanaka and M. Miyake, J. Phys. Chem. B, 1999, 103, 3818-3827.

12. I. Gandarias, E. Nowicka, B. J. May, S. Alghareed, R. D. Armstrong, P. J. Miedziak and S. H. Taylor, Catal. Sci. Technol., 2016, 6, 4201-4209.

13. T. Lu, Z. Du, J. Liu, H. Ma and J. Xu, Green Chem., 2013, 15, 2215-2221.

14. T. Mallat and A. Baiker, Catal. Today, 1994, 19, 247-283.

15. T. Mallat, Z. Bodnar, A. Baiker, O. Greis, H. Strubig and A. Reller, J. Catal., 1993, 142, 237-253.

16. S. Szabó and I. Bakos, ACH - Models in Chemistry, 1996, 133, 83-92.

17. U. W. Hamm, D. Kramer, R. S. Zhai and D. M. Kolb, Electrochemica. Acta., 1998, 43, 2969-2978.

18. J. Clavilier, J. M. Feliu and A. Aldaz, J. Electroanal. Chem., 1988, 243, 419-433.

19. E. Herrero, L. J. Buller and H. D. Abruña, Chem. Rev., 2001, 101, 1897-1930.

20. S. Szabo, Int. Rev. Phys. Chem., 1991, 10, 207-248.

21. T. Mallat, Z. Bodnar and A. Baiker, in Studies in Surface Science and Catalysis, eds. M. Guisnet, J. Barbier, J. Barrault, C. Bouchoule, D. Duprez, G. Pérot and C. Montassier, Elsevier, 1993, vol. 78, pp. 377-384.

22. F. Alardin, B. Delmon, P. Ruiz and M. Devillers, Catal. Today, 2000, 61, 255-262.

23. H. H. C. M. Pinxt, B. F. M. Kuster and G. B. Marin, Appl. Catal. A Gen., 2000, 191, 45-54.

24. P. C. C. Smits, B. F. M. Kuster, K. van der Wiele and H. S. van der Baan, Carbohydrate Research, 1986, 153, 227-235.

25. M. Akada, S. Nakano, T. Sugiyama, K. Ichitoh, H. Nakao, M. Akita and Y. Morooka, Bull. Chem. Soc. Jpn., 1993, 66, 1511-1515.

26. R. M. Rioux, R. Komor, H. Song, J. D. Hoefelmeyer, M. Grass, K. Niesz, P. Yang and G. A. Somorjai, J. Catal., 2008, 254, 1-11.

27. J. I. Villegas, N. Kumar, T. Heikkilä, V. P. Lehto, T. Salmi and D. Y. Murzin, Chem. Eng. J., 2006, 120, 83-89.

28. H. Armendáriz, A. Guzmán, J. A. Toledo, M. E. Llanos, A. Vázquez and G. Aguilar-Ríos, Appl. Catal. A Gen., 2001, 211, 69-80.

29. S. A. Bocanegra, A. Guerrero-Ruiz, S. R. de Miguel and O. A. Scelza, Appl. Catal. A Gen., 2004, 277, 11-22.

30. G. J. Siri, J. M. Ramallo-López, M. L. Casella, J. L. G. Fierro, F. G. Requejo and O. A. Ferretti, Appl. Catal. A Gen., 2005, 278, 239-249.

31. J. Völter, G. Lietz, M. Uhlemann and M. Hermann, J. Catal., 1981, 68, 42-50.

32. A. Palazov, C. Bonev, G. Kadinov, D. Shopov, G. Lietz and J. Völter, J. Catal., 1981, 71, 1-8.

33. C. Roychowdhury, F. Matsumoto, P. F. Mutolo, H. D. Abruña and F. J. DiSalvo, Chem. Mater., 2005, 17, 5871-5876.

34. L. R. Alden, C. Roychowdhury, F. Matsumoto, D. K. Han, V. B. Zeldovich, H. D. Abruña and F. J. DiSalvo, Langmuir, 2006, 22, 10465-10471.

35. F. Matsumoto, C. Roychowdhury, F. J. DiSalvo and H. D. Abruna, J. Electrochem. Soc., 2008, 155, B148-B154.

36. J. Prabhuram, T. S. Zhao, Z. K. Tang, R. Chen and Z. X. Liang, J. Phys. Chem. B, 2006, 110, 5245-5252.

37. H. Abe, F. Matsumoto, L. R. Alden, S. C. Warren, H. D. Abruña and F. J. DiSalvo, J. Am. Chem. Soc., 2008, 130, 5452-5458.

38. G. Saravanan, T. Hara, H. Yoshikawa, Y. Yamashita, S. Ueda, K. Kobayashi and H. Abe, Chem. Commun., 2012, 48, 7441-7443.

39. B. Gurau, R. Viswanathan, R. Liu, T. J. Lafrenz, K. L. Ley, E. S. Smotkin, E. Reddington, A. Sapienza, B. C. Chan, T. E. Mallouk and S. Sarangapani, The J. Phys. Chem. B, 1998, 102, 9997-10003.

40. E. Antolini, J. R. C. Salgado and E. R. Gonzalez, J. Power Sources, 2006, 160, 957-968.

41. G. Saravanan, H. Abe, Y. Xu, N. Sekido, H. Hirata, S.-i. Matsumoto, H. Yoshikawa and Y. Yamabe-Mitarai, Langmuir, 2010, 26, 11446-11451.

42. S. Mukerjee and R. C. Urian, Electrochemica. Acta., 2002, 47, 3219-3231.

43. D.-J. Chen, Z.-Y. Zhou, Q. Wang, D.-M. Xiang, N. Tian and S.-G. Sun, Chem. Commun., 2010, 46, 4252-4254.

44. A. Capon and R. Parsons, J. Electroanal. Chem. Interfacia. Electrochem., 1973, 45, 205-231.

45. S. G. Sun, J. Clavilier and A. Bewick, J. Electroanal. Chem. Interfacia. Electrochem., 1988, 240, 147-159.

46. W. P. Zhou, A. Lewera, R. Larsen, R. I. Masel, P. S. Bagus and A. Wieckowski, J. Phys. Chem. B, 2006, 110, 13393-13398.

47. J. Ge, Y. Zhang, C. Liu, T. Lu, J. Liao and W. Xing, J. Phys. Chem. C, 2008, 112, 17214-17218.

48. J.-Y. Wang, Y.-Y. Kang, H. Yang and W.-B. Cai, J. Phys. Chem. C, 2009, 113, 8366-8372.

49. L. V. Minevski and R. R. Adžić, J. Appl. Electrochem., 1988, 18, 240-244.

50. M. D. Macia, E. Herrero and J. M. Feliu, J. Electroanal. Chem., 2003, 554-555, 25-34.

51. S. Uhm, S. T. Chung and J. Lee, Electrochem. Commun., 2007, 9, 2027-2031.

52. F. Colmati, E. Antolini and E. R. Gonzalez, Electrochemica. Acta., 2005, 50, 5496-5503.

53. Z. Liu, B. Guo, L. Hong and T. H. Lim, Electrochem. Commun., 2006, 8, 83-90.

54. A. S. Arico, P. Creti, P. L. Antonucci and V. Antonucci, Electrochem. Solid-State Lett., 1998, 1, 66-68.

55. C. Lamy, E. M. Belgsir and J.-M. Léger, J. Appl. Electrochem., 2001, 31, 799-809.

56. W. J. Zhou, S. Q. Song, W. Z. Li, Z. H. Zhou, G. Q. Sun, Q. Xin, S. Douvartzides and P. Tsiakaras, J. Power Sources, 2005, 140, 50-58.

57. A. Kowal, S. L. Gojković, K. S. Lee, P. Olszewski and Y. E. Sung, Electrochem. Commun., 2009, 11, 724-727.

58. S. Meenakshi, P. Sridhar and S. Pitchumani, RSC Adv., 2014, 4, 44386-44393.

59. A. C. Queiroz, W. O. Silva, I. A. Rodrigues and F. H. B. Lima, Appl. Catal. B Environ., 2014, 160-161, 423-435.

60. L. An, T. S. Zhao and Y. S. Li, Renewable and Sustainable Energy Reviews, 2015, 50, 1462-1468.

61. S. Beyhan, C. Coutanceau, J.-M. Léger, T. W. Napporn and F. Kadırgan, Int. J. Hydrogen Energy, 2013, 38, 6830-6841.

62. R. G. C. S. dos Reis and F. Colmati, J. Solid State Electrochem., 2016, 20, 2559-2567.

63. F. Colmati, E. Antolini and E. R. Gonalez, J. Electrochem. Soc., 2007, 154, B39-B47.

64. M. C. Roman-Martinez, D. Cazorla-Amoros, S. De Miguel and O. Scelza, J. Jpn. Pet. Inst., 2004, 47, 164-178.

Chapter 5: The behavior of Vulcan XC-72R Carbon as a support for Pt

5.1. Introduction

Many researches are interested in finding the most appropriate catalyst support, since it will influence the metal particle size, structure, charge, and the form of the specific active sites at the metal–support boundary.[1] This Chapter is concerned with the use of Vulcan XC-72R carbon as a support material for Pt nanoparticles. The interaction between the carbon and Pt plays an important role in the properties of the Pt/C catalyst. It has been demonstrated that this interaction is attributed to the electron transfer from the Pt nanoparticles to the carbon support. Furthermore, the electronic structure change of platinum catalyst particles by this interaction leads to the change of the catalyst properties.[2] Generally, this electronic interaction has a positive effect towards the enhancement of catalytic properties and stability.[2] In fuel cell catalyst studies, it has been shown that metal-carbon support interactions influences the oxidation of both CO and methanol.[3, 4] For *n*-butanol oxidation, previous work has shown that when carbon was used as a support the selectivity toward butyric acid was 78.9 %, whilst for TiO_2 the selectivity was 21.2 %.[5] More effort is needed to further understand the mechanism of the interaction between Pt and carbon support.

In order to determine how the catalytic performance was affected by the support, Pt was prepared by sol-immobilisation using a carbon support, as it was previously reported.[5] The catalyst testing protocol are described in detail in Chapter Two (section 2.2.3).

5.2. Time on-line with Pt/C at 3 bar O_2

Initial studies of the XC72R carbon support alone exhibited negligible activity towards the oxidation of *n*-butanol when run under standard reaction conditions, and no conversion to oxidised C_4 products was found.

Addition of 1 wt.%Pt to the carbon support induced activity, and hence selectivity and conversion of n-butanol to butyraldehyde and butyric acid as shown in Figure 5.1. The carbon mass balance is also shown.

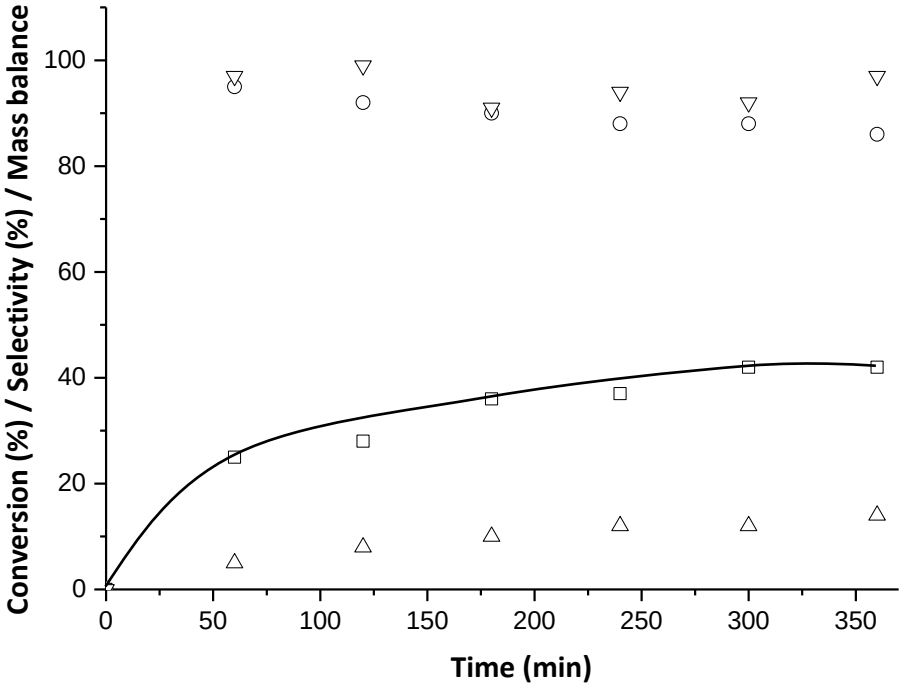

Figure 5.1. Time on-line data with 1 wt.%Pt/C catalyst for selective oxidation of *n*- butanol. ***Reaction conditions*****:** 100 °C, 3 bar O_2, *n*-butanol (10 mL, 0.54 M), catalyst (15 mg), 750 rpm. □ Conversion of *n*-butanol, ○ Butyraldehyde Selectivity, △ Butyric Acid Selectivity, ▽ Carbon Mass balance.

Time on-line studies were carried out by following the normal oxidation method, but with the time being changed accordingly, the 1 wt.%Pt/C catalysts were used and tested at 100 °C, 3 bar O_2 for 6 h Figure 5.1.

Figure 5.1 shows that as the alcohol is consumed in the reaction over time, the selectivity towards butyraldehyde is decreased and it is converted into butyric acid. The conversion of *n*-butanol starts to increase from 25 % to ~ 40 %. The conversion of *n*- butanol increased up to ~ 40 %, after 3 h the conversion remains the same until the end of the 6 h reaction. There was no significant increase after 3 h. This implies that the catalyst had deactivated after 3 h (also observed previously Chapter 3, section 3.4). The selectivity of butyraldehyde decreases from 95 % to *ca.* 86 % and the selectivity toward butyric acid increases from 5 % to 14 %.

Using carbon as the support reduced Pt leaching by a large amount compared to TiO_2 (Chapter 3, section 3.6). Under standard conditions, 2.8 % of the Pt loading was leached from Pt/C, this is a significant improvement when compared to the TiO_2

catalyst, which leached 5.2 % Pt. For the 1 wt.%Pt/TiO_2 catalyst the conversion of *n*- butanol was 30 % (Figure 3.7) and in the case of 1 wt.%Pt/C catalyst the conversion was 28 %, this decrease in leaching has not significantly influenced the catalyst activity in the oxidation of *n*-butanol.

5.2.1. Effect of catalyst pre-treatment

5.2.1.1. Reaction under 3 bar O_2

Additional experiments were conducted over 1 wt.%Pt/C fresh (as-obtained), calcined and 5 vol.%H_2/Ar pretreated for 2 h at 200 °C (5 °C/min) to study the effect of pre-treatment on the catalyst activity. Table 5.1 shows the affect of pre-treatment of 1 wt.%Pt/C on catalyst performance.

Table 5.1. Conversion of *n*-butanol and product selectivity over 1 wt.%Pt/C under different catalyst pre-treatments.

Catalyst pre-treatment	Conv. *n*-BuOH (%)	Sel. (%)		Mass balance (%)	Leaching (%)
		BuALD	BuAC		
1 wt.%Pt/C Fresh (as-obtained)	28	95	5	97	2.8
1 wt.%Pt/C (Calcined)	23	98	2	97	2.2
1 wt.% Pt /C (5 vol.%H_2/Ar at 200 °C)	19	100	0	97	2.4

Conversion (Conv.), Selectivity (Sel.), *n*-Butanol (*n*-BuOH), Butyraldehyde (BuALD), Butyric Acid (BuAC)

***Reaction Conditions*:** 100 °C, 2 h, 3 bar O_2, *n*-butanol (10 mL, 0.54 M), 15 mg of catalyst, 750 rpm.

Catalysts pre-treated: Calcined under air and pre-treated under 5 vol.%H_2/Ar for 2 h at 200 °C (5 °C/min).

Table 5.1 shows that when the catalysts were pre-treated, the conversion of the *n*- butanol was decreased compared to when the catalysts are fresh (as-obtained). All the pre-treatments were performed at 200 °C and for 2 h.

Table 5.1 shows that when the catalysts were calcined under air for 2 h, the conversion of the *n*-butanol was decreased slightly (23 %) compared to the fresh catalyst (28 %).

Furthermore, the selectivity towards butyraldehyde increases slightly from 95 % to 98 % compared to the fresh catalyst.

However, when the catalysts were pre-treated under 5 vol.%H_2/Ar at 200 °C, the *n*- butanol conversion decreases. It can be seen that the conversion of *n*-butanol for pre-treated catalyst under 5 vol.%H_2/Ar reaches 19 % after 2 h and butyraldehyde is the only primary product (100 %), Table 5.1. The ICP-MS analysis for the fresh catalyst has showed that 2.8 % of Pt from the catalyst was leached after 2 h reaction. On the other hand, the amount of Pt leached for the calcined and under 5 vol.%H_2/Ar were 2.2 % and 2.4 %, respectively. This observation using carbon support show a lower Pt leaching compared to that observed for the TiO_2-supported catalyst (Section 3.6.1).

5.3. Time on-line with Pt/C at 2 bar O_2

To compare how the conversion and selectivity is influenced by pressure, and based on the findings in Chapter 4, the catalysts were tested under 2 bar O_2, and a time on-line study is shown in Figure 5.2. The time on-line studies were carried out under 2 bar O_2, 15 mg of catalyst at 100 °C (750 rpm).

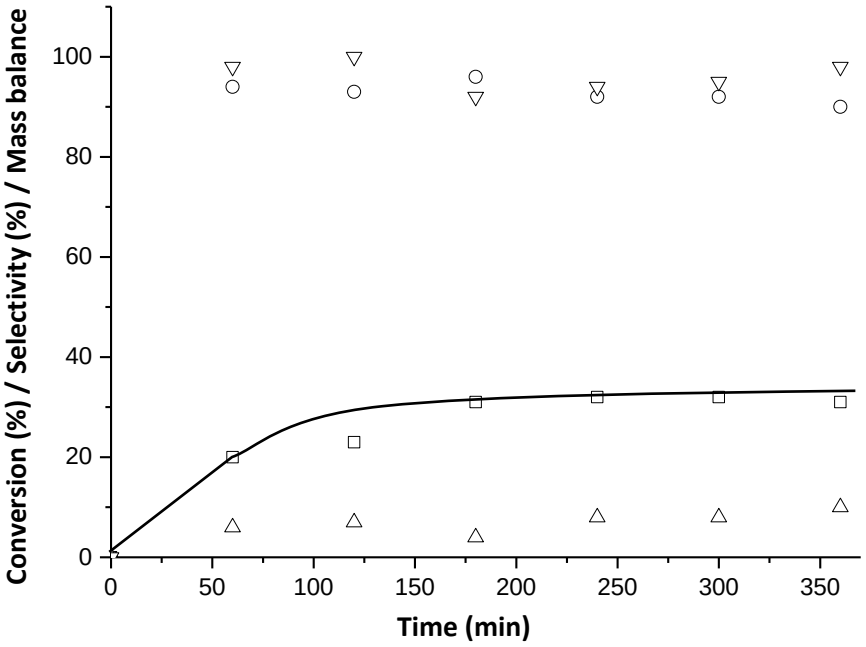

Figure 5.2. Time on-line data with 1 wt.%Pt/C catalyst for selective oxidation of *n*- butanol. ***Reaction conditions*****:** 100 °C, 2 bar O_2, *n*-butanol (10 mL, 0.54 M), catalyst (15 mg), 750 rpm. □ Conversion of *n*-Butanol, ○ Butyraldehyde Selectivity, △ Butyric Acid Selectivity ▽ Carbon Mass balance.

For 1 wt.%Pt/C the conversion reached 20 % after 1 h and the selectivity towards butyraldehyde and butyric acid was 94 % and 6 %, respectively, Figure 5.2. After 3 h, the conversion of *n*-butanol over 1 wt.%Pt/C under 2 bar O_2 increased up to 31 % and remained the same until 6 h of reaction. The selectivity toward butyraldehyde went through different steps during this time. Butyric acid is the secondary product, the selectivity increased up to 10 %, which appears when the selectivity of butyraldehyde starts to decrease.

From this result, it can be observed that 1 wt.%Pt/C tested for 6 h reaction showed that the conversion of *n*-butanol remained almost the same after 3 h, and the selectivity toward butyraldehyde remains the same after 6 h. This observation seems to indicate that the catalyst is partially deactivated after 3 h reaction. The conversion of *n*-butanol stops after 3 h and the catalyst is still active for the conversion of butyraldehyde into butyric acid.

Based on the observations made from the reactions at 2 and 3 bar O_2, it can be seen that the rate of reaction after 1 h is higher at 3 bar than 2 bar, with 25 % and 20 % conversion respectively. There is a clear deactivation in the catalyst during the reaction at 2 bar O_2 after 3 h. A complete deactivation of the catalyst does not appear to occur at 3 bar O_2, although the rate of reaction does slow down. This is in contrast to what was observed over Pt/TiO_2 (Chapter 3, Section 3.4 and Chapter 4, Section 4.5), with Pt/C the higher oxygen pressure may assist with the removal or oxidation of inhibiting species.

5.3.1. Effect of catalyst pre-treatment

5.3.1.1. Reaction under 2 bar O_2

Catalyst pretreatment has an important effect on the Pt metal and support interaction. The catalyst was calcined and pre-treated under 5 vol.%H_2/Ar, which may affect the conversion rate of *n*-butanol. Table 5.2 reports the effect of pre-treatment of 1 wt.%Pt/C on catalyst behaviour, Appendix H.

Table 5.2 Conversion of *n*-butanol over 1 wt.%Pt/C under different pre-catalyst treatments.

Catalyst and pre-treatment	Conv. *n*-BuOH (%)	Sel. (%)		Mass balance (%)	Leaching (%)
		BuALD	BuAC		
1 wt.%Pt/C	23	93	7	100	1.5
1 wt.% Pt /C (Calcined)	24	95	5	94	2.2
1 wt.% Pt /C (5% H_2/Ar at 200 °C)	17	93	7	94	0.6

Conversion (Conv.), *n*-Butanol (*n*-BuOH), Butyraldehyde (BuALD), Butyric Acid (BuAC), Selectivity (Sel.).

***Reaction Conditions*:** 100 °C, 2 h, 2 bar O_2, *n*-butanol (10 mL, 0.54 M), 15 mg of catalyst, 750 rpm.

Catalysts pre-treated: Calcined under air or A flow of 5 vol.%H_2/Ar for 2 h at 200 °C (5 °C/min).

Table 5.2 shows that when the catalysts were calcined under air for 2 h, the conversion of the *n*-butanol was increased slightly (24 %), compared to when the catalysts were freshly prepared (23 %). Furthermore, when the catalysts were heat treated in 5 vol.%H_2/Ar at 200 °C and tested, the conversion of *n*-butanol decreases to 17 %. All the pre-treatments were performed at 200 °C and for 2 h (5 °C/min). In the case of the heat-treated of 1 wt.%Pt/C under 5 vol.%H_2/Ar the % of leached Pt decreased to 0.6 % compared to the calcined catalyst and fresh (as-obtained) catalyst, 2.2 % and 1.5 %, respectively.

With the aim to demonstrate the stability of the 1 wt.%Pt/C catalyst, the catalyst has been tested, recovered and retested under the standard conditions (100 °C, 2 h and 2 bar O_2). The results are reported in Table 5.3.

Based on studies in Sections 5.2 and 5.3, comparing 2 and 3 bar oxygen, when 3 bar of oxygen is used, the conversion of *n*-butanol is slightly increased to 28 % compared to 2 bar O_2, 23 %, after 2 h reaction. Furthermore, it is important to notice here that the selectivity towards butyraldehyde is slightly higher than for 2 bar O_2. The amount of leached Pt, which decreased from 2.8 % (3 bar O_2) to 1.5 % (2 bar O_2), after 2 h reaction.

Based on these observations it was decided that the best pressure to work with is 2 bar O_2.

5.3.2. Reusability tests

Reusability studies, shown in Table 5.3, show the conversion of *n*-butanol and the selectivity toward butyraldehyde and butyric acid.

Table 5.3. Reusability of 1 wt.%Pt/C for 3 cycles.

Test cycle	Conv. *n*-BuOH (%)	Sel. (%)		Leaching (%)	Mass Balance (%)
		BuALD	BuAC		
1st	23	93	7	1.5	100
2nd	20	100	0	1.4	100
3rd	24	100	0	2	97

Conversion (Conv.), Selectivity (Sel.), *n*-Butanol (*n*-BuOH), Butyraldehyde (BuALD), Butyric Acid (BuAC).

Reaction conditions: 100 °C, 2 h, 2 bar O_2, *n*-butanol (10 mL, 0.54 M), 15 mg of catalyst.

The data shows that after 3 repeated experiments the conversion of *n*-butanol remained unchanged. However, the selectivity toward butyraldehyde increased with subsequent repeat experiments from 93 % from the first test to 100 % to the third reusability experiment. In parallel the selectivity to butyric acid decreases with the reusability test, from 7 % from the first test to 0 % for the third test.

It was found that after each test the catalyst was still converting *n*-butanol and the conversion reached the same level after 2 h reaction. It is clear that the catalyst can convert *n*-butanol into butyraldehyde.

During the tests the selectivity toward butyraldehyde and butyric acid changes. The catalyst presented here is still active toward the conversion of *n*-butanol at the same level after repeated cycles. The reusability test shows that the selectivity towards the products is affected after every reuse.

5.3.3. Characterisation of Pt/C

The catalysts were characterised by X-ray Photoelectron Spectroscopy (XPS) and Transmission Electron Microscopy (TEM) in order to study the metal chemical state and particle size and dispersion.

5.3.3.1. Transmission Electron Microscopy (TEM)

In order to determine the platinum particle size and dispersion on the carbon support, detailed Transmission Electron Microscopy (TEM) studies were performed.

Figure 5.3 shows representative micrographs obtained from TEM.

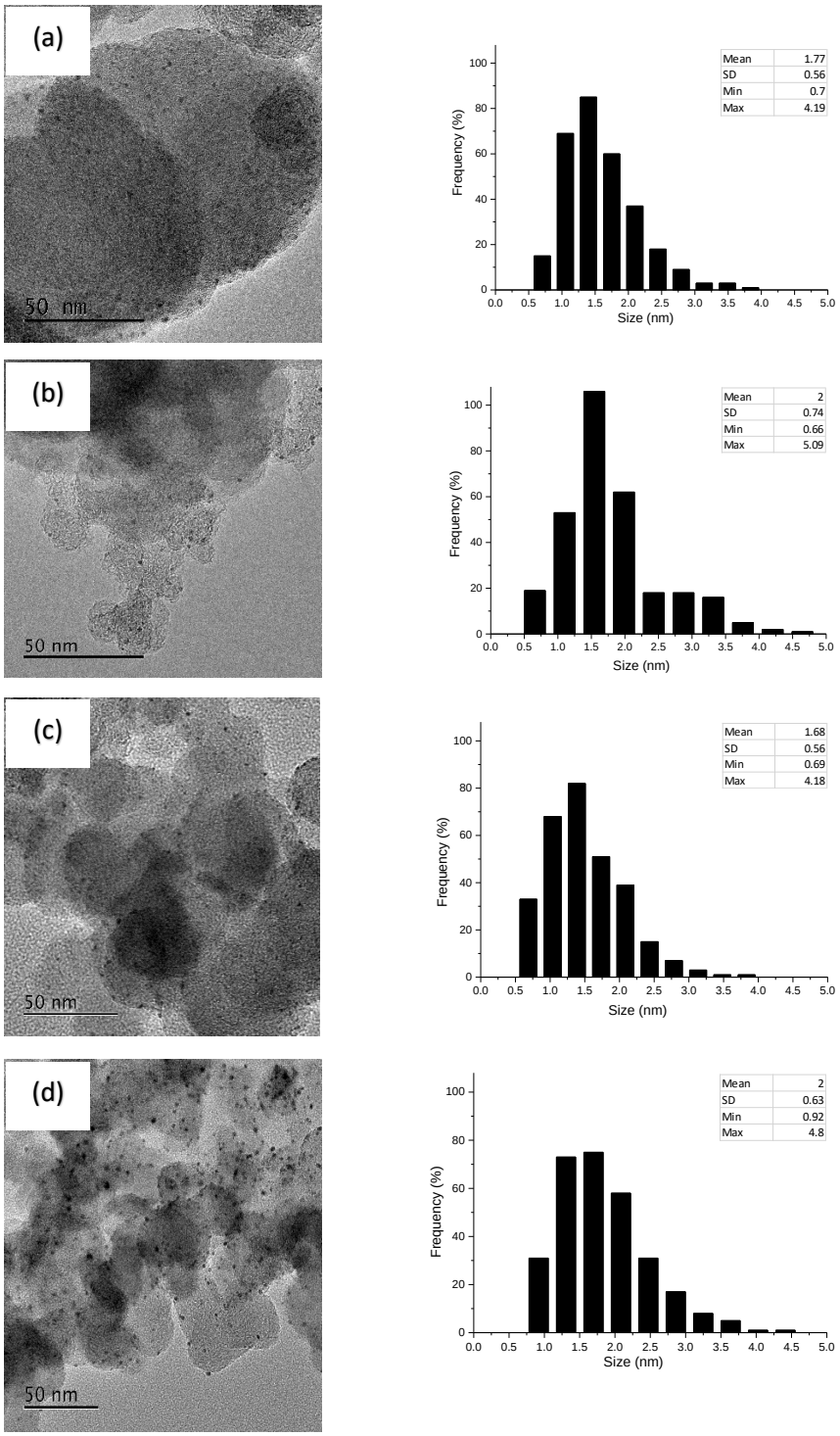

Figure 5.3. Transmission Electron Microscopy (TEM) image and Particle size distribution of (a) Fresh (as-obtained), (b) calcined, (c) 5 vol.%H_2/Ar for 2 h at 200 °C (5 °C/min) treatment and (d) Used catalyst (after 2 h reaction) of 1 wt.%Pt/C. ***Reaction conditions:*** 100 °C, 2 h, 2 bar O_2, *n*-butanol (0.54 M), 15 mg of catalyst, 750 rpm. ***Catalysts pre-treated:*** Calcined under air or A flow of 5 vol.%H_2/Ar for 2 h at 200 °C (5 °C/min).

TEM analysis was carried out on fresh (as-obtained), calcined, 5 vol.%H_2/Ar at 200 °C treatment and used (after 2 h reaction) catalysts. The 5 vol.%H_2/Ar at 200 °C treatment, calcined and fresh (as-obtained) catalysts have comparable mean particle sizes, as shown in Table 5.4.

Table 5.4. Mean NP diameter of 1 wt.%Pt/TiO_2 under different pre-treatments catalysts.

Catalyst and pre-treatment	Mean NP diameter	SD
1 wt.%Pt/C (Fresh)	1.77	0.56
1 wt.%Pt/C (Used)	2.00	0.63
1 wt.%Pt/C (Calcined)	2.00	0.74
1 wt.%Pt/C (5 vol.%H_2/Ar at 200 °C)	1.68	0.56

Nanoparticles (NP), Standard Deviation (SD). ***Reaction conditions:*** 100 °C, 2 h, 2 bar O_2, *n*-butanol (0.54 M), 15 mg of catalyst, 750 rpm. ***Catalysts pre-treated*****:** Calcined under air or A flow of 5 vol.%H_2/Ar for 2 h at 200 °C (5 °C/min).

From results described in Table 5.2 and 5.4 the catalyst activity is slightly affected by the mean nanoparticle size, which are 1.77 nm, 2 nm and 1.68 nm for fresh, calcined, 5 vol.%H_2/Ar at 200 °C treatment, respectively. The different activities observed could therefore likely be attributed to either the physicochemical properties of the different catalysts after different pre-treatment under air or 5 vol.%H_2/Ar for 2h at 200 °C (5 °C/min). The mean nanoparticle size of the fresh catalyst increased to 2 nm after 2 h of reaction.

For the 5 vol.%H_2/Ar at 200 °C treatment catalyst the mean nanoparticles size was 1.68 nm and in the case of calcined catalyst the mean diameter size 2 nm, Table 5.2. For the calcined catalyst conversion is 24 %, on the other hand under 5 vol.%H_2/Ar at 200 °C treatment the catalyst conversion is 17 %. The different activities observed could therefore likely be attributed to different factors beyond particle size effects.

5.3.3.2. X-ray Photoelectron Spectroscopy (XPS) analysis

XPS was performed on 1 wt.%Pt/C Fresh (as-obtained), calcined and pre-treated under 5 vol.%H_2/Ar catalysts (Figure 5.4).

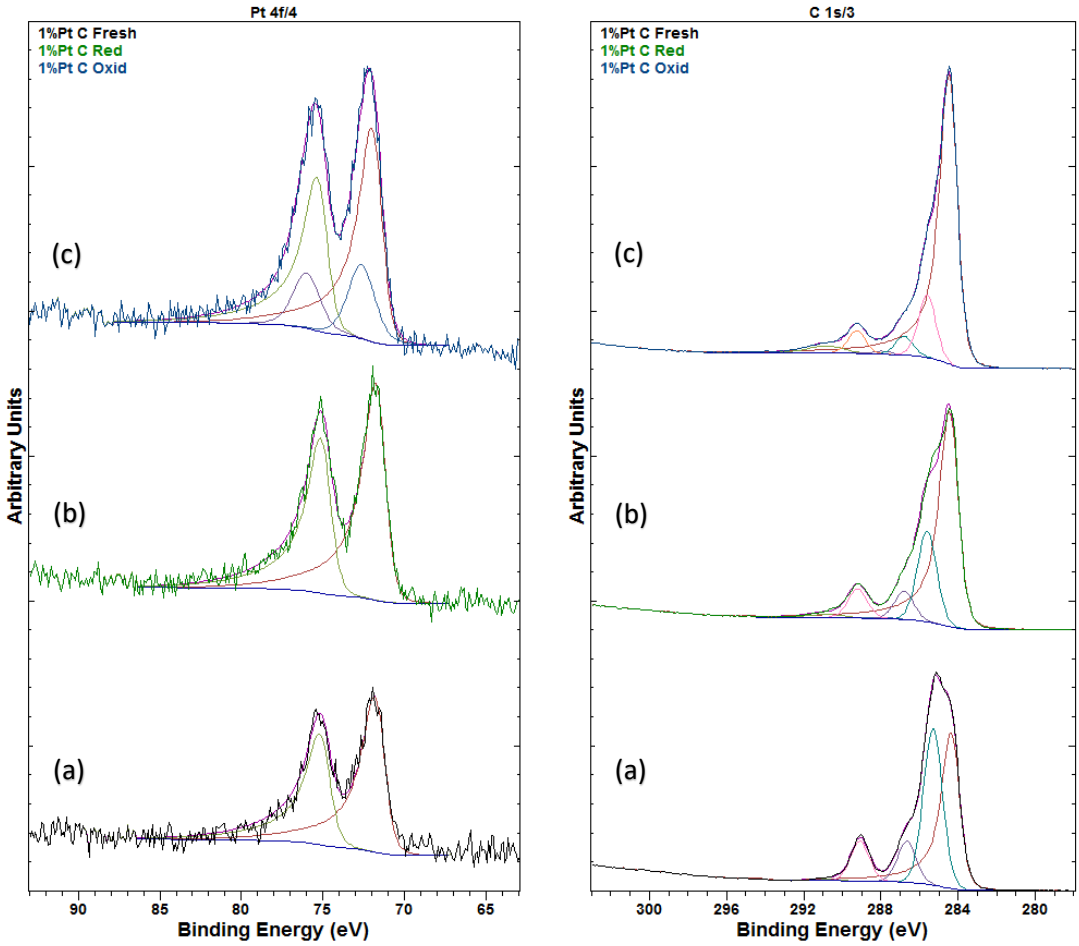

Figure 5.4. Pt(4f) and C(1s) core-level spectra for (a) Fresh (as-obtained), (b) 5 vol.% H_2/Ar treatment and (c) Calcined for 2 h at 200 °C (5 °C/min) 1 wt.%Pt/C catalysts. ***Catalysts pre-treated*****:** Calcined under air or A flow of 5 vol.%H_2/Ar for 2 h at 200 °C (5 °C/min).

Table 5.5. XPS derived concentrations (at%) and binding energies

Sample	Concentration (at%)			Pt4f binding energy (eV)
	O 1s	C 1s	Pt 4f	
1 wt.%Pt/C (Fresh)	14.06	85.90	0.04	71.60
1 wt.%Pt/C (5 vol.%H_2/Ar at 200 °C)	11.96	87.98	0.05	71.60
1 wt.%Pt/C (Calcined)	7.26	92.67	0.07	71.8 (0.05 at%) & 72.6 (0.02 at%)

Catalysts pre-treated: Calcined under air or A flow of 5 vol.%H_2/Ar for 2 h at 200 °C (5 °C/min).

As seen in Figure 5.4, all catalysts have Pt present predominantly as Pt^0, with a binding energy of 71.8 eV (+/-0.2 eV), this binding energy is greater than that of bulk Pt (*ca.* 71 eV),[6] and the increased binding energy is attributed to the small particle size. The sol used in the preparation of the fresh catalysts is clearly evident in the corresponding C(1s) spectra, and reduction and oxidation treatments serve to remove some of this organic coating, with the oxidative treatment decreasing the intensity of the C(1s) peak around 285-285.5 eV, coincident with this is the loss of intensity of the peaks above 287 eV. The presence of the pi-pi* structure appearing after oxidative treatment (Figure 5.5(c)) suggests that the conductive carbon support is not being attenuated by species on top of it, and we attribute this to the loss of organic species (i.e. the sol stabilizing ligands) from the surface. This oxidative treatment also reveals a broadening of the Pt(4f) peaks, revealing potentially a second Pt species characterised by a binding energy of 72.6 eV, typical of Pt^{2+} species in PtO or $Pt(OH)_2$,[7-13] and consistent with the oxidising atmosphere.

5.3.4. Addition of Pb as promoter

The enhancement of catalytic properties of Pt by adding a second metal may occur through the change of the local bonding geometry (structure effects), the distribution of active sites (ensemble effects) or directly by modifying the reactivity of platinum surface atoms (electronic effects). A number of studies have shown that lead has a promoting effect on the electrooxidation of alcohols and other organic molecules.[14-19] Recent studies showed that lead has been found as a good catalyst for the oxidation of ethanol in alkaline solutions.[20] A previous study of Liu et al. showed that a PtPb/C catalyst

displayed enhanced electrocatalytic activity towards both formic acid and methanol oxidation compared with Pt/C.[17] In this study the focus will be on two types of metallic surfaces: monometallic platinum (as shown above) and bimetallic surfaces based on platinum with lead added, previously both were prepared on a titania support, Chapter 4, with the PtPb showing the best activity towards *n*-butanol oxidation. Because of the higher activity exhibited from using the lead-platinum bimetallic supported titania (Chapter 4, Section 4.6.2.1), it was decided to also prepare this catalyst on a carbon support. 1 wt.%Pd - 0.5 wt.%Pb/C catalyst have been prepared using the preparation method presented in Chapter 2 (Section 2.2.1), and the activity towards the oxidation of *n*- butanol have been evaluated.

5.3.5. Time on-line studies with 1 wt.%Pt-0.5 wt.%Pb/C

Many researches show that the addition of metals such as lead to platinum catalysts can significantly enhance their activity.[21-24] A previous study showed that the Pb has a good promoting effect on the electrooxidation of alcohols and other organics.[14, 15, 17, 25, 26] A study by Li and Pickup,[14] reported that Pb addition led to improvements in the catalytic activity of carbon-supported Pt catalysts in the oxidation of ethanol in acidic conditions. Liu et *al.,*[17] revealed that a PtPb/C bimetallic catalyst enhanced the electrocatalytic activity in the oxidation of both formic acid and methanol compared to Pt/C.[27-29] Based on a previous study by Wang et *al.,*[19] the addition of lead facilitates the oxidative removal of adsorbed CO from the surface of the Pt, which is considered to be a common poison in Pt catalysts.

A time on-line study on 1 wt.%Pt-0.5 wt.%Pb/C catalyst was performed. The data for 1 wt.%Pt-0.5 wt.%Pb/C are shown in Figure 5.5.

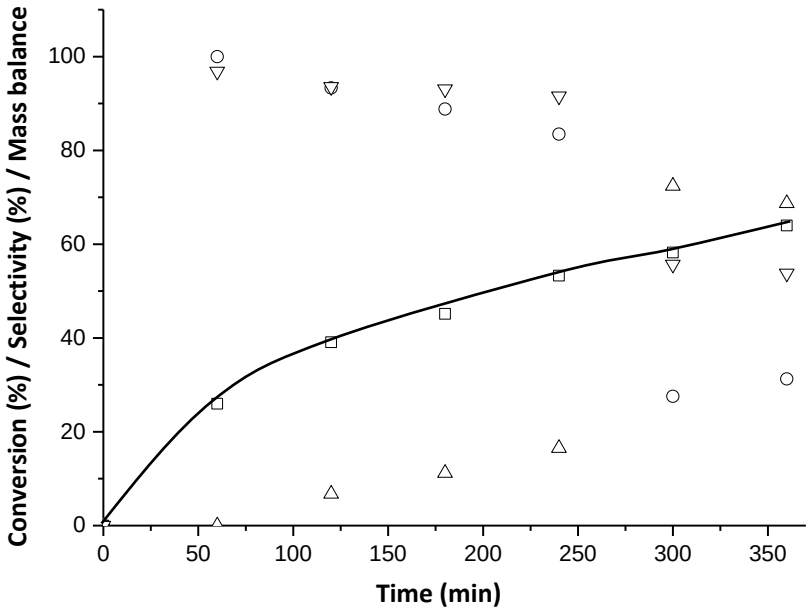

Figure 5.5. Time on-line data with 1 wt.%Pt 0.5 wt.%Pb/C catalyst for selective oxidation of *n*-butanol. ***Reaction conditions*****:** 100 °C, 2 bar O_2, *n*-butanol (10 mL, 0.54 M), catalyst (15 mg), 750 rpm. □ Conversion of *n*-Butanol, ○ Butyraldehyde selectivity △ Butyric Acid selectivity, ▽ Carbon mass balance.

For 1 wt.%Pt 0.5 wt.%Pb/C the conversion reached 26 % after 1 h and butyraldehyde was the primary product (100 %), Figure 5.5. After 2 h the conversion of *n*-butanol increased and the selectivity toward butyraldehyde decreased to the end of the 6 h reaction period. Furthermore, butyric acid selectivity increased to ~ 70 %, it is a secondary product, as it is formed when the selectivity of butyraldehyde starts to decrease, until it reaches ~ 31 %. This indicates that the catalyst is still active and it seems to promote the conversion of butyraldehyde into butyric acid. After 5 h there are increases of conversion (remaining ~ 60 %), there is a relatively large decrease in the selectivity towards the butyraldehyde, with a significant increase in selectivity towards butyric acid. This indicates that the catalyst is still active after 5 h.

5.3.6. Effect of 1 wt.%Pt 0.5 wt.%Pb/C catalyst pre-treatment

The effect of thermal treatments on activity towards *n*-butanol oxidation has been studied for 1 wt. %Pt 0.5 wt.%Pb/C. The results of experiments are reported in Table 5.6.

Table 5.6 The influence of thermal pre-treatment of 1 wt.%Pt 0.5 wt.%Pb/C catalyst for the selective oxidation of *n*-Butanol.

Catalyst and pre-treatment	Conv. *n*-BuOH (%)	Sel. (%)		Mass balance (%)	Leaching (%)	
		BuALD	BuAC		Pt	Pb
1 wt.%Pt 0.5 wt.%Pb/C (Fresh)	39	93	7	94	0.1	3.1
1 wt.%Pt 0.5 wt.%Pb/C (Calcined)	46	87	13	92	0.1	5.7
1 wt.%Pt 0.5 wt.%Pb /C (5 vol.%H_2/Ar at 200 °C)	31	92	8	96.4	0.1	5.3

Conversion (Conv.), Selectivity (Sel.), *n*-Butanol (*n*-BuOH), Butyraldehyde (BuALD), Butyric Acid (BuAC). ***Reaction Conditions*****:** 100 °C, 2 h, 2 bar O_2, *n*-butanol (10 mL, 0.54 M), 15 mg of catalyst, 750 rpm. ***Catalysts pre-treated:*** Calcined under air or A flow of 5 vol.%H_2/Ar for 2 h at 200 °C (5 °C/min).

Table 5.6 shows that when the catalysts are calcined under air for 2 h, the conversion of the *n*-butanol is increased compared to when the catalysts are freshly prepared. Table 5.6 shows the conversion of the *n*-butanol is decreased slightly to 31 % compared to when the catalysts are freshly prepared (39 %). Furthermore, when the catalysts are calcined at 200 °C and tested, the conversion of *n*-butanol increases to 46 %. It can be seen that there is an increase of conversion of *n*-butanol for the calcined catalyst compared with the heat treated one under 5 vol.%H_2/Ar.

With the aim to demonstrate the stability of the 1 wt.%Pt 0.5 wt.%Pb/C catalyst, the catalyst has been tested, recovered and retested under the standard conditions (100 °C, 2 h and 2 bar O_2).

5.3.7. Reusability test of the 1 wt.%Pt 0.5 wt.%Pb/C catalyst

Reusability studies, shown in Table 5.7, show that the conversion of *n*-butanol and the selectivity toward butyraldehyde and butyric acid after consecutive catalyst use.

Table 5.7 Reusability of 1 wt.% Pt 0.5 wt.% Pb/C for 3 cycles.

Test cycle	Conv. *n*-BuOH(%)	Sel. (%)		Leaching (%)		Mass Balance (%)
		BuALD	BuAC	Pt	Pb	
1st	39	93	7	0.1	3.1	94
2nd	32	94	6	0.1	0.5	97
3rd	31	92	8	0.1	0.9	96

Conversion (Conv.), Selectivity (Sel.), *n*-Butanol (*n*-BuOH), Butyraldehyde (BuALD), Butyric Acid (BuAC). ***Reaction Conditions*****:** 100 °C, 2 h, 2 bar O_2, *n*-butanol (10 mL, 0.54 M), 15 mg of catalyst, 750 rpm.

The data in Table 5.7 shows the conversion of *n*-butanol after 3 repeated experiments over 1 wt.% Pt 0.5 wt.% Pb/C. It was found that after each test the catalyst was still converting *n*-butanol and the conversion was different after every test after 2 h reaction. The conversion of *n*-butanol after the second and third tests decreased to ~ 30 %.

During the tests the selectivity toward butyraldehyde and butyric acid changed slightly. Although the catalyst activity toward the conversion of *n*-butanol decreased after the 2nd test. The reusability test shows that the selectivity towards the products was not affected after every reuse. The addition of Pb to Pt suppressed the quantity of Pt leached after 2 h of reaction; the monometallic Pt catalyst exhibited 1.5 % Pt leaching after 2 h of reaction, whereas this was significantly reduced to 0.1 % after the incorporation of Pb. It was also observed however, that Pb leaching occurred during these reactions, but did appear to decrease upon subsequent used; from 3.1 % after 1st use to 0.5 and 0.9 % for the 2nd and 3rd use, respectively.

5.3.8. Characterisation of 1 wt.%Pt 0.5 wt.%Pb/C catalyst

5.3.8.1. Scanning Electron Microscopy (SEM)

Figure 5.6 shows representative Scanning Electron Microscopy images of a 1 wt.%Pt - 0.5 wt.%Pb/C fresh (as-obtained), calcined and 5 vol.%H_2/Ar at 200 °C treatment for the used catalysts (after 2 h reaction).

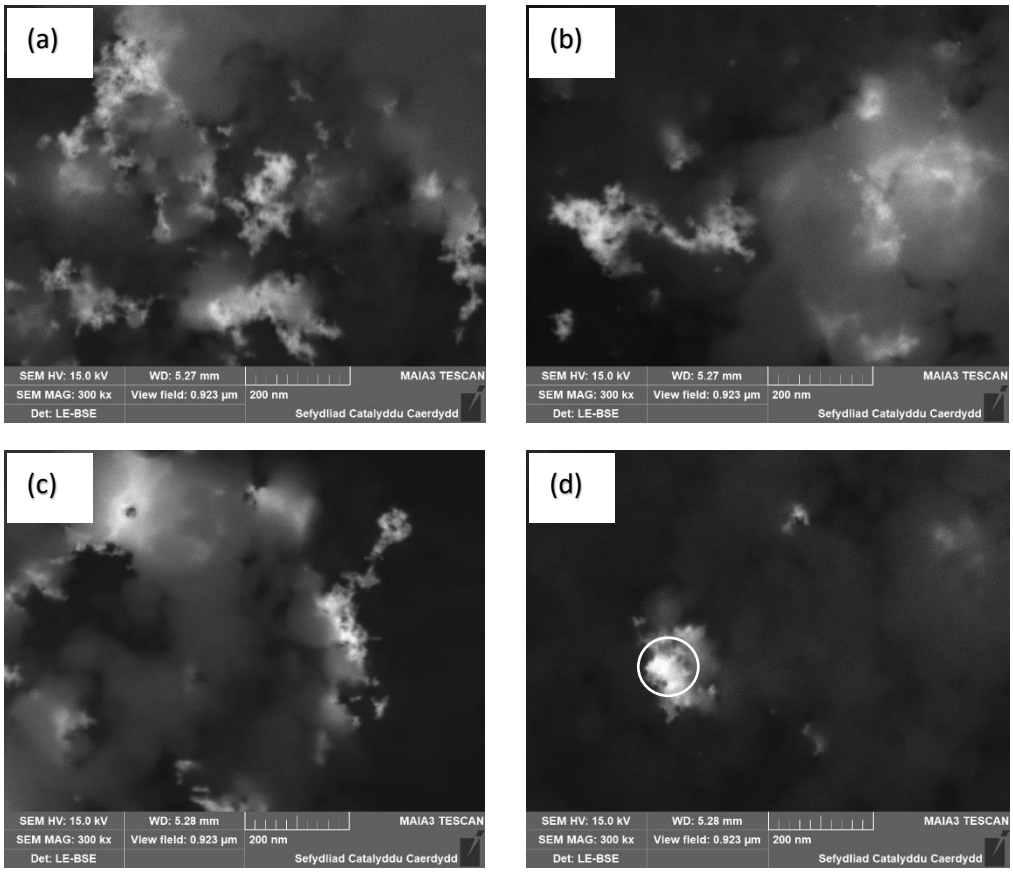

Figure 5.6. Scanning electron microscopy (SEM) images of (a) Fresh (as-obtained) (b) used (after 2 h reaction) (c) Calcined and (d) 5 vol.%H_2/Ar at 200 °C treatment of 1 wt.%Pt 0.5 wt.%Pb/C. ***Reaction Conditions*****:** 100 °C, 2 h, 2 bar O_2, *n*-butanol (10 mL, 0.54 M), 15 mg of catalyst, 750 rpm. ***Catalysts pre-treated:*** Calcined under air or A flow of 5 vol.%H_2/Ar for 2 h at 200 °C (5 °C/min).

From the Scanning Electron Microscopy (Figure 5.6) no difference can be detected between fresh (as-obtained) and different pre-treatment. SEM indicates that there are metal species present on the surface, however, there are no observable differences between the fresh, used, calcined and treated under 5 vol.%H_2/Ar catalysts. Its only shows that there are nanoparticles and these nanoparticles are large and non-uniform agglomerates. From the SEM images, conclusions on particle size couldn't be made.

A study by Chen *et al.*[30] showed that when PtPb/C catalyst were synthesised through two step method without using any surfactant and organometallic precursor, the average particle size of a PtPb nanoparticle is about 8.7 nm.

5.3.8.2. X-ray Photoelectron Spectroscopy (XPS) Analysis

XPS analysis of the 1 wt.%Pt 0.5 wt.%Pb/C catalyst revealed significant changes in the concentration of Pb and the binding energy of Pt, depending on the catalyst treatment or reaction time. Figure 5.7 shows both Pt(4f) and Pb(4f) regions for fresh (as- obtained), calcined, and reduced under 5 vol.%H_2/Ar and used (after 2 h reaction) catalysts respectively. Table 5.8 shows the XPS derived atomic concentrations.

Table 5.8. XPS derived at % for 1 wt.%Pt-0.5 wt.%Pb/C Catalysts.

Sample	Concentration (at%)				
	O 1s	**C 1s**	**S 2p**	**Pt 4f**	**Pb 4f**
1 wt.%Pt-0.5 wt.%Pb/C (Fresh)	2.44	97.32	0.18	0.04	0.01
1 wt.%Pt-0.5 wt.%Pb/C (Calcined)	8.93	90.84	0.18	0.05	0.01
1 wt.%Pt-0.5 wt.%Pb/C (Under 5 vol.%H_2/Ar)	2.70	97.06	0.19	0.04	0.01
1 wt.%Pt-0.5 wt.%Pb/C (Used)	9.28	90.48	0.16	0.07	0.00

Reaction Conditions*:** 100 °C, 2 h, 2 bar O_2, *n*-butanol (10 mL, 0.54 M), 15 mg of catalyst, 750 rpm. ***Catalysts pre-treated: Calcined under air or A flow of 5 vol.%H_2/Ar for 2 h at 200 °C (5 °C/min).

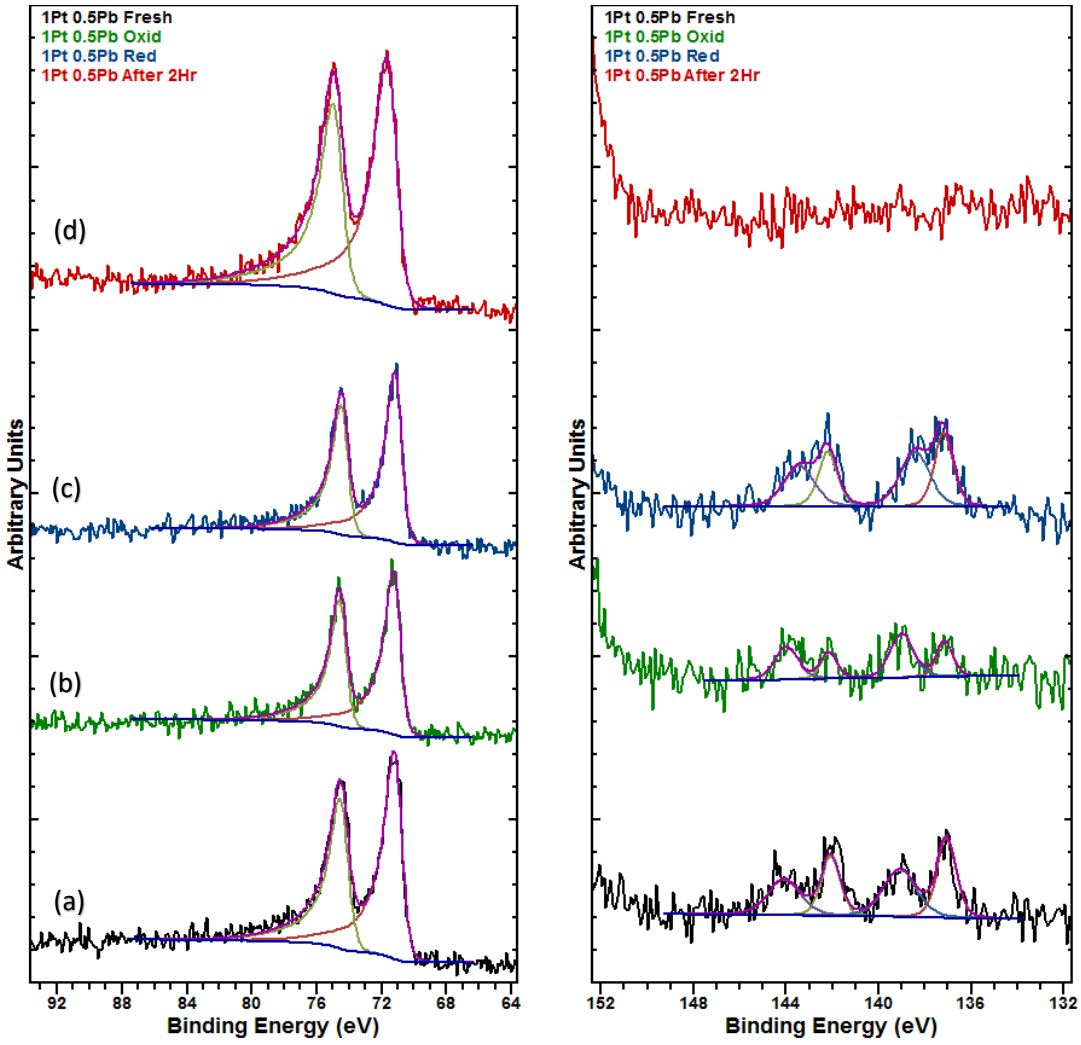

Figure 5.7. XPS analysis of 1 wt.%Pt-0.5 wt.%Pb/C (a) Fresh (as-obtained), (b) Calcined, (c) Under 5 vol.%H_2/Ar and (d) Used catalysts. ***Reaction Conditions*****:** 100 °C, 2 h, 2 bar O_2, *n*-butanol (10 mL, 0.54 M), 15 mg of catalyst, 750 rpm. ***Catalysts pre-treated:*** Calcined under air or A flow of 5 vol.%H_2/Ar for 2 h at 200 °C (5 °C/min).

All treatments show the presence of both metallic and oxide Pb states, although we believe the distribution of the Pb changes with heat treatment, as suggested by the variation in signal intensity. The Pt was observed at a binding energy of 71.3 eV for all catalysts containing Pd and was assigned to metallic Pt. After reaction however, there was clear loss of Pb from the surface and this is coincident with a shift upwards in binding energy of the Pt(4f) peak to 71.5 eV, and a broadening of the peak width. The shift upwards in energy is above that of bulk Pt, so this shift is indicative of a decrease in particle size, and potentially a greater interaction of the smaller particles with defects within the carbon surface.[31]

5.4. Conclusions

Pt and PtPb nanoparticles supported on Vulcan XC-72R carbon have been prepared by sol-immobilisation. Based on Chapter four observation, the effect of the concentration of oxygen have been studied at 2 and 3 bar O_2. The time on-line studies at these pressures were performed and the catalysts show a catalyst deactivation after 3 h, when the pressure is 2 and 3 bar. It was found in Chapter 4 (Section 4.5) that the best pressure used with Pt/TiO_2 was 2 bar of oxygen, which gave the highest conversion. This is different to what is observed with Pt/C, where the oxygen may assist with the removal or oxidation of surface inhibiting species. Changing the support is likely have an effect, the leaching tests have shown that the amount of Pt leached decreased from 3.1 % for theTiO_2-support, to 1.5 % (C-support) after 2 h reaction under 2 bar O_2, with high selectivity towards butyraldehyde (95 %). The reusability of the catalyst has been tested over 3 cycles and the results have shown that the catalyst is still active toward the conversion of *n*-butanol at the same level after all cycles. Transmission electron microscopy (TEM) analysis results show that the mean nanoparticles size for fresh 1 wt.%Pt/C catalyst was 1.77 nm, on the other hand the calcined and heat treated under 5 vol.%H_2/Ar showed particle sizes of 2.00 nm and 1.68 nm, respectively. The addition of Pb to Pt catalyst enhanced the activity towards *n*-butanol oxidation compared with Pt, from 23 % (1 wt.%Pt/C) to 39 % (1 wt.%Pt- 0.5 wt.%Pb/C) at 2 bar O_2 after 2 h. The reusability test of 1 wt.%Pt- 0.5 wt.%Pb/C shows *n*-butanol conversion decreased after the 1st cycles and the selectivity towards the products was not affected after each reuse. The SEM images of 1 wt.%Pt-0.5 wt.%Pb/C for fresh (as-obtained), used, calcined and treated under 5 vol.%H_2/Ar catalyst show that there are nanoparticles and these nanoparticles are agglomerated. XPS analysis of 1 wt.%Pt- 0.5 wt.%Pb/C samples show that the Pt is found at a binding energy of 71.3 eV for all catalysts containing Pd and is assigned to metallic Pt.

5.5. References

1. Z. Qu, W. Huang, S. Zhou, H. Zheng, X. Liu, M. Cheng and X. Bao, J. Catal., 2005, 234, 33-36.

2. X. Yu and S. Ye, J. Power Sources, 2007, 172, 133-144.

3. M. Kim, J.-N. Park, H. Kim, S. Song and W.-H. Lee, J. Power Sources, 2006, 163, 93-97.

4. A. L. Dicks, J. Power Sources, 2006, 156, 128-141.

5. I. Gandarias, E. Nowicka, B. J. May, S. Alghareed, R. D. Armstrong, P. J. Miedziak and S. H. Taylor, Catal. Sci. Technol., 2016, 6, 4201-4209.

6. https://srdata.nist.gov/xps/.

7. J. S. Hammond and N. Winograd, J. Electroanal. Chem. Interfacia. Electrochem., 1977, 78, 55-69.

8. K. S. Kim, N. Winograd and R. E. Davis, J. Am. Chem. Soc., 1971, 93, 6296-6297.

9. G. Wang, Y. Lin, X. Xiao, X. Li and W. Wang, Surf. Interface Anal., 2004, 36, 1437-1440.

10. G. N. Derry and P. N. Ross, Surf. Sci., 1984, 140, 165-180.

11. C. Puglia, A. Nilsson, B. Hernnäs, O. Karis, P. Bennich and N. Mårtensson, Surf. Sci., 1995, 342, 119-133.

12. D. Y. Petrovykh, H. Kimura-Suda, A. Opdahl, L. J. Richter, M. J. Tarlov and L. J. Whitman, Langmuir, 2006, 22, 2578-2587.

13. P. Gambardella, Z. Sljivancanin, B. Hammer, M. Blanc, K. Kuhnke and K. Kern, Phys. Rev. Lett., 2001, 87, 056103/056101-056103/056104.

14. G. Li and P. G. Pickup, Electrochimica. Acta., 2006, 52, 1033-1037.

15. A. Kelaidopoulou, E. Abelidou and G. Kokkinidis, Journal of Appl. Electrochem., 1999, 29, 1255-1261.

16. L. Zhang, X. Yan, G. Zhu, Z. Zeng, M. Shen and A. Pohlers, Zhenkong Kexue yu Jishu Xuebao/J. Vac. Sci. Technol., 2006, 26, 268-271.

17. Z. Liu, B. Guo, S. W. Tay, L. Hong and X. Zhang, J. Power Sources, 2008, 184, 16-22.

18. X. Yu and L. Hu, 2009.

19. Y. Wang, T. S. Nguyen, X. Liu and X. Wang, J. Power Sources, 2010, 195, 2619-2622.

20. J. Ye, J. Liu, C. Xu, S. P. Jiang and Y. Tong, Electrochem. Commun., 2007, 9, 2760-2763.

21. J.-L. Sculfort, A. Etcheberry and J. Gautron, J. Electroanal. Chem. Interfacia. Electrochem., 1985, 189, 143-154.

22. L. V. Minevski and R. R. Adžić, J. Appl. Electrochem., 1988, 18, 240-244.

23. M. D. Macia, E. Herrero and J. M. Feliu, J. Electroanal. Chem., 2003, 554-555, 25-34.

24. S. Uhm, S. T. Chung and J. Lee, Electrochem. Commun., 2007, 9, 2027-2031.

25. L. J. Zhang, Z. Y. Wang and D. G. Xia, J. Alloys and Compd., 2006, 426, 268-271.

26. X. Yu and P. G. Pickup, J. Power Sources, 2009, 192, 279-284.

27. C. Roychowdhury, F. Matsumoto, V. B. Zeldovich, S. C. Warren, P. F. Mutolo, M. Ballesteros, U. Wiesner, H. D. Abruña and F. J. DiSalvo, Chem. Mater., 2006, 18, 3365-3372.

28. L. R. Alden, C. Roychowdhury, F. Matsumoto, D. K. Han, V. B. Zeldovich, H. D. Abruña and F. J. DiSalvo, Langmuir, 2006, 22, 10465-10471.

29. S. Maksimuk, S. Yang, Z. Peng and H. Yang, J. Am. Chem. Soc., 2007, 129, 8684-8685.

30. D.-J. Chen, Z.-Y. Zhou, Q. Wang, D.-M. Xiang, N. Tian and S.-G. Sun, Chem.l Commun., 2010, 46, 4252-4254.

31. G. Zhang, D. Yang and E. Sacher, J. Phys. Chem. C, 2007, 111, 565-570.

Chapter 6: Conclusions and Future Work

6.1. Conclusions

This thesis has attempted to investigate and develop a catalyst which will be active, selective and stable for the oxidation of *n*-butanol to butyraldehyde, and to identify the features of the catalyst that make them active, thereby informing the design of future catalysts. Many approaches have been examined, based on the literature that was presented in Chapter 1. This work aimed to understand the physico-chemical parameters affecting the activity of 1 wt.%Pt/TiO_2 for the oxidation of *n*-butanol. The progress of the work is summarised in the following Table (Table 6.1).

Table 6.1. Conversion of solution containing 4 %*n*-butanol and selectivity toward butyraldehyde and butyric acid.

Catalyst Studied	Conv. *n*-BuOH (%)	Sel. (%)		Mass balance (%)	Leaching (%)	
		BuALD	BuAC		Pt	M
3 bar O_2, 2 h, 100 °C						
1 wt.%Pt/TiO_2 (Fresh)	30	91	9	96	5.2	-
1 wt.%Pt/TiO_2 (5 vol.%H_2/Ar at 200 °C)	43	93	7	89	3.1	-
1 wt.%Pt/TiO_2 (Fresh)						
N_2 cycles	63	77	11	67	-	-
Air	51	79	16	87	-	-
2 bar O_2, 2 h, 100 °C						
1 wt.%Pt/TiO_2 (Fresh)	38	84	16	96	3.1	-
Addition of promoters						
0.5 wt.%Pb	41	90	10	94	1.2	0.6
1 wt.%Sn	39	90	10	94	2.7	0.7
C-support (2 bar O_2, 2 h, 100 °C)						
1 wt.%Pt/C (Fresh)	23	93	7	100	1.5	-
Addition of promoters						
0.5 wt.%Pb (Fresh)	39	93	7	94	0.1	3.1
0.5 wt.%Pb (Calcined)	46	87	13	92	0.1	5.7

Conversion (Conv.), Selectivity (Sel.), *n*-Butanol (n-BuOH), Butyraldehyde (BuALD), Butyric Acid (BuAC). ***Catalysts pre-treated*****:** Calcined under air or A flow of 5 vol.%H_2/Ar for 2 h at 200 °C (5 °C/min).

The starting point of the thesis was to study of Pt/TiO_2 catalysts. The catalysts were prepared by sol immobilisation. To investigate the effect of different loadings of platinum on TiO_2 on the conversion of *n*-butanol and on the selectivity toward the different products, a series of wt.%Pt/TiO_2 catalysts with various Pt weight loadings were prepared. 1 wt.%Pt/TiO_2 showed the highest activity towards the conversion of *n*-butanol.

To determine if the oxidation of *n*-butanol was diffusion limited, differing masses of the 1 wt%Pt/TiO_2 were tested. The study showed that below 50 mg catalyst used the reaction is under a kinetic regime, and above it was under a diffusion limited regime. Base on this observation 15 mg catalysts have been used for all further catalytic tests.

In order to determine how the catalytic performance proceeded over time, time on-line studies were conducted. The conversion of *n*-butanol stops after 2 h, and the selectivity of butyraldehyde decreases as butyric acid is formed. This data suggested that the inhibition of the reaction by the presence of butyraldehyde affects the conversion of *n*-butanol and the selectivity toward the different products of the reaction.

The influence of varying reaction temperatures showed that measurable activity is obtained above 40 °C.

The potential role of leached Pt on the reaction was investigated. The tests showed that the catalyst is leaching, and that sintering can affect the conversion of the reaction. Catalyst characterisation by XPS and SEM suggests that the observed Pt leaching is related to both the metal–support interaction and the size of the metal nanoparticles.

The effect of surface treatments on activity towards *n*-butanol oxidation was studied on Pt/TiO_2. It can be seen that Pt/TiO_2 showed significant sensitivity to such treatment, and it has been concluded that there is a strong correlation between the pre-treated catalyst and the rate of *n*-butanol conversion.

To demonstrate the stability of the 1 wt.%Pt/TiO_2 catalyst, the catalyst has been tested over 3 cycles and the results showed that the catalyst was consistently active toward the conversion of *n*-butanolacross all cycles. Additionally, the selectivity toward butyraldehyde increased with the 3rd experiments to 100% and butyraldehyde was the main product.

Studies in the thesis then investigated the causes for catalyst deactivation. Two approaches concentration of oxygen on the performance, and addition of promoters were examined. The aim of the study in Chapter 4 was to investigate the effect of these changes on the stability of the 1 wt.%Pt/TiO_2 catalysts towards leaching, and also towards the conversion of *n*-butanol.

Alternating steps of oxygen/air followed by a purge with an inert gas (nitrogen) were performed to better understand the deactivation of the catalyst. These purges helped

to avoid/slow down the deactivation of the catalyst. XPS showed no significant change in Pt oxidation state or concentration. It was found that using air instead of oxygen increased the selectivity toward butyraldehyde.
Based on this observation the effect of the concentration of oxygen was studied. It was observed that a low concentration of oxygen didn't allow for sufficient oxidation of *n*-butanol, whilst a higher concentration of oxygen contributes to the catalyst deactivation. It has been found that the best oxygen pressure, which gives the highest conversion, is 2 bar. The time on-line studies at this pressure were performed and the catalysts show a higher life-time than when the pressure is 3 bar.

To improve the performance of platinum catalysts, the preparation of Pt-based bimetallic catalysts were investigated. The performance of the Pt metallic phase could be enhanced by addition of inactive metals of Group 14, such as Sn and Pb.
The *n*-Butanol oxidation was performed with a 1 wt.%Pt-0.5 wt.%Pb/TiO_2 catalyst. With the aim to demonstrate the stability of 1 wt.%Pt-0.5 wt.%Pb/TiO_2, time on-line studies were performed. The addition of lead as a promoter results in profound modification of the activity of the catalyst; the presence of the Pb promoter seems to suppress the poisoning observed with Pt alone, and improved the catalyst performance. With the PtPb catalyst for example, the activity was comparable to the monometallic Pt catalyst, the mass balance is 7 % lower, but the quantity of Pt leached is decreased (from 3.1 % to 1.2 %). The effects of thermal pre-treatment conditions on the 1 wt.%Pt-0.5 wt.%Pb/TiO_2 catalyst were investigated, using calcination in air or under 5 vol.%H_2/Ar.

When the 1 wt.%Pt-1 wt.%Sn/TiO_2 catalyst was calcined, the conversion of *n*-butanol remained the same. On the other hand when the catalyst was pre-treated under 5 vol.%H_2/Ar the conversion of *n*-butanol reduced from 39 % to 31 %, this may suggest that these nanoparticles are agglomerated after pre-treatment and this was confirmed by SEM analysis. XPS analysis revealed that Pt was exclusively in the metallic state. The catalyst was tested over 3 cycles and the results showed that the catalyst was still active towards the conversion of *n*- butanol, but the catalyst lost activity with every test cycle.
The addition of tin to the platinum catalyst also showed comparable conversion (39 %) to platinum alone (38 %) for the *n*-butanol oxidation. The time on-line study of 1 wt.%Pt-1 wt.%Sn/TiO_2 showed that after 6 h the conversion of *n*-butanol increases from 0 % to 56.6 %. The reusability test shows that after each test the catalyst still converts *n*-butanol, but deactivates after each cycle. The leaching of platinum decreases from 2.7 % in the 1st cycle to 1.1 % after the 3rd cycle.

In order to determine how the catalytic performance was affected by the support, which is disclosed in Chapter 5, a carbon support was investigated (Cabot Vulcan XC-72R), with sol-immobilisation as the preparation used as the synthesis method.

The catalyst formed by Pt nanoparticles supported on Vulcan XC72R was shown to be very stable and reactive for the selective oxidation of *n*-butanol by O_2 in an aqueous phase, under standard conditions (100 °C, 2 bar O_2).

The effect of the concentration of oxygen was studied at 2 and 3 bar O_2, based on results obtained in Chapter 4. According to the previous Chapter's time on-line studies at 2 and 3 bar pressures, reactions were performed to compare how the conversion and selectivity was influenced by pressure. The catalysts show deactivation after 3 h, when the pressure is 2 and 3 bar. Comparing 2 bar with 3 bar, it is important to notice here that the selectivity towards butyraldehyde is slightly higher than at 3 bar O_2. The amount of leached Pt, which decreased from 2.8 % (3 bar O_2) to 1.5 % (2 bar O_2), despite the fact that the conversion at 3 bar (28 %) is higher than at 2 bar (23 %) after 2 h. Based on these observations it was decided that the best pressure to work with is 2 bar O_2.

The best pressure for Pt/TiO_2 was 2 bar of oxygen, which gave the highest conversion. This is different to what was observed with Pt/C, where the oxygen may assist with the removal or oxidation of inhibiting species. By changing the catalyst support Pt leaching was reduced from 3.1 % (TiO_2-support) to 1.5 % (C-support) after 2 h reaction under 2 bar O_2.

After 3 repeated experiments on Pt/C the conversion of *n*-butanol changed, at 2 bar O_2. The results have shown that the catalyst was still active toward the conversion of *n*-butanol at the same level along 3 cycles. TEM characterisation of the Pt/C catalyst shows that catalyst pretreatment affects slightly the average particle size. From TEM analysis it was seen that the mean nanoparticles size for fresh 1 wt.%Pt/C catalyst was 1.77 nm on the other hand the TEM of calcined and under 5 vol.%H_2/Ar are it was 2.00 nm and 1.68 nm, respectively.

Based on Chapter 4, the PtPb showed the best activity towards *n*-butanol oxidation. Because of the higher activity exhibited from using the lead-platinum bimetallic (41 %conversion of 1 wt.%Pt- 0.5 wt.%Pb/ TiO), it was decided to prepare this catalyst on a carbon support. The addition of Pb to the Pt catalyst enhanced the activity towards *n*-butanol oxidation compared with Pt, from 23 % (1 wt.%Pt/C) to 39.10 % (1 wt.%Pt- 0.5 wt.%Pb/C) at 2 bar O_2 after 2 h. The reusability test of PtPb/C showed decreased *n*-butanol conversion after the 1st cycle, whilst the selectivity towards the products was not affected after every reuse. The SEM images of PtPb/C for fresh (as-obtained), used, calcined and treated under 5 vol.%H_2/Ar catalyst showed that there

were nanoparticles and these nanoparticles are agglomerated. XPS analysis of lead-platinum bimetallic samples show that the Pt is assigned to metallic Pt^0.

In summary, studies carried out during the course of this thesis have led to a significant enhancement in the performance of supported platinum catalysts, for the catalytic oxidation of *n*-butanol. Whilst future work is required to fully understand these catalytic systems, the detailed investigations presented here provide key information. Indeed *n*- butanol can be made from biomass and propylene a petroleum derivative so, biobutanol could become a key building block in future biorefineries.

6.2. Recommended Future Work

There are a number of further studies that could be pursued. Some further characterisation of the catalysts could be undertaken to gain a full understanding why certain methods are causing an improvement to stability and selective oxidation. Despite the progress in improving catalyst stability for this reaction in this thesis, further improvements may be achievable. Further work in this area is therefore aimed at developing a more stable catalyst, which could investigate the use of other catalyst supports such as metal oxides, such as SnO_2 and CeO_2, and other carbon supports, such as acetylene black and Ketjen Black. Establishing how supports with different acidic/basic properties, reducibility and electronic conductivity could provide insight on the desirable properties required to improve the catalyst performance. Other non-precious metals (Cu, Co, Ni) could also be studied instead of Pt. Replacing Pt with other more abundant elements could reduce the cost associated with the catalyst, and thus make it more viable.

As discussed, previous work has suggested that the presence of an alcohol can reduce the over oxidation of butyraldehyde to butyric acid.[1] This would ultimately lead to a higher reaction selectivity to the desired butyraldehyde product. This was also evidenced in this work, see Chapter 3. For this reason, it would be of interest to assess how different alcohols, used as additives, could affect and perhaps, enhance this inhibition. For this a series of different alcohols could be used, to establish whether the size of the alcohol chain, or functionality of the alcohol (primary, secondary, tertiary) influences the inhibition. Furthermore, the involvement of radical inhibitors may also be assessed as an additive, as they may inhibit the auto oxidation of the desired aldehyde product. Preliminary studies have been conducted to investigate this; in the absence of any catalyst, butyraldehyde oxidation was determined to be 83 % after 2 h under standard reaction conditions. In the presence of hydroquinone (2 mg) the conversion was reduced to 76 %. These studies were only preliminary, but provide a good foundation to study moving forward. If auto-oxidation of the butyraldehyde is indeed problematic, it would be beneficial to conduct a more in-depth temperature study, to try and enhance reaction selectivity to butyraldehyde.

The use of different catalyst preparation methods would also be of use, to establish how changes in the Pt dispersion effects the activity, selectivity and stability. For instance particle size is crucial the use of reducible support to enhance strong metal support interaction (SMSI), and consequently control activity and stability. Completion of this work will require further characterisation studies to fully understand the catalytic systems studied.

In order to investigate the surface species formed the mechanism, DRIFT spectroscopic studies would be a useful technique to be performed on the monometallic and bimetallic Pt supported catalysts dosed with small quantities of the substrate and reaction intermediates.

6.3. Reference

1. I. Gandarias, E. Nowicka, B. J. May, S. Alghareed, R. D. Armstrong, P. J. Miedziak and S. H. Taylor, Catal. Sci. Technol., 2016, 6, 4201- 4209.

Appendix A

Time online study with different metal loaded Pt on TiO_2 support of catalyst for selective oxidation of *n*-butanol.

Catalyst wt.%Pt/TiO_2	Time (min)	Conv. *n*-BuOH (%)	Sel. (%)		Mass balance (%)
			BuALD	BuAC	
0.25 wt.%	0	0	0	0	100
	10	0	0	0	100
	20	0	0	0	100
	30	0	0	0	100
	60	0	0	0	100
	120	0	0	0	100
	180	0	0	0	100
	240	0	0	0	100
	300	0	0	0	100
	360	0	0	0	100
0.1 wt.%	0	0	0	0	100
	10	0	0	0	100
	20	0	0	0	100
	30	0	0	0	100
	60	0	0	0	100
	120	0	0	0	100
	180	0	0	0	100
	240	0	0	0	100
	300	0	0	0	100
	360	0	0	0	100

Conversion (Conv.), Selectivity (Sel.), *n*-Butanol (*n*-BuOH), Butyraldehyde (BuALD), Butyric Acid (BuAC). ***Reaction Conditions:*** 100 °C, 3 bar O_2, *n*-Butanol (0.54 M), 15 mg of catalyst.

Appendix B

Conversion of *n*-Butanol over 1 wt.%Pt/TiO_2 catalysts following different pre-treatments.

Catalyst	Conv. *n*-BuOH (%)	Sel. (%)		Mass balance (%)
		BuALD	BuAC	
1 wt.%Pt /TiO_2 (Calcined)	23	93	7	100
	23	94	6	100
1 wt.%Pt /TiO_2 (5 vol.% H_2/Ar)	43	93	7	89
	36	95	5	94

Conversion (Conv.), Selectivity (Sel.), *n*-Butanol (*n*-BuOH), Butyraldehyde (BuALD), Butyric Acid (BuAC). ***Reaction Conditions:*** 100 °C, 2 h, 3 bar O_2, *n*-Butanol (0.54 M), 15 mg of catalyst. ***Catalysts pre-treated:*** Calcined under air or A flow of 5 vol.%H_2/Ar for 2 h at 200 °C (5 °C/min).

Appendix C

Time on-line data (TOL) for 1 wt.%Pt/TiO_2 catalyst for selective oxidation of *n*-Butanol.

TOL (h)	Conv. *n*-BuOH (%)	Sel. (%)		Mass balance (%)
		BuALD	BuAC	
	25	91	9	100
1	29	91	9	95
	29	89	11	96
	39	85	15	100
2	35	84	16	97
	41	83	17	91
	36	86	14	100
3	45	83	17	90
	43	85	15	90
	42	82	18	100
4	46	82	18	91.9
	50	78	22	96
5	50	80	20	88
	54	74	25	90
6	50	76	24	94

Conversion (Conv.), Selectivity (Sel.), *n*-Butanol (*n*-BuOH), Butyraldehyde (BuALD), Butyric Acid (BuAC). ***Reaction Conditions:*** 100 °C, 2 bar O_2, *n*-Butanol (0.54 M), 15 mg of catalyst.

Appendix D

Conversion of 4 wt.%*n*-butanol and selectivity towards butyraldehyde and butyric acid over 1 wt.%Pt- 0.5 wt.%M/TiO_2 (M= Bi, Pb, Al, Zn, Sn).

Catalysts Supported on TiO_2	**Conv. *n*-BuOH (%)**	**Sel. (%)**		**Mass balance (%)**
		BuALD	**BuAC**	
1 wt.% Pt - 0.5 wt.% Al	12 13	98 100	2 0	96 97
1 wt.% Pt - 0.5 wt.% Sn	39 41	90 87	10 13	97 100
1 wt.% Pt - 0.5 wt.% Bi	29 24	86 84	14 15	97 100
1 wt.% Pt - 0.5 wt.% Zn	22 24	93 94	7 6	99 96
1 wt.% Pt - 0.5 wt.% Pb	43 39	86 85	14 15	90 89

Conversion (Conv.), Selectivity (Sel.), *n*-Butanol (*n*-BuOH), Butyraldehyde (BuALD), Butyric Acid (BuAC). ***Reaction Conditions:*** 100 °C, 2 h, 2 bar O_2, *n*-Butanol (0.54 M), 15 mg of catalyst.

Appendix E

Conversion of *n*-Butanol over 1 wt.%Pt-0.5 wt.%Pb/TiO_2 catalyst following different pre-treatments.

Catalyst	Conv. *n*-BuOH (%)	Sel. (%)		Mass balance (%)
		BuALD	BuAC	
1 wt.%Pt-0.5 wt.%Pb/TiO_2 Fresh (as-obtained)	43 39 42	91 91 90	9 9 10	95 94 94
1 wt.%Pt-0.5 wt.%Pb/TiO_2 (Calcined)	16 15	96 95	5 5	95 97

Conversion (Conv.), Selectivity (Sel.), *n*-Butanol (*n*-BuOH), Butyraldehyde (BuALD), Butyric Acid (BuAC). ***Reaction Conditions:*** 100 °C, 2 h, 2 bar O_2, *n*-Butanol (0.54 M), 15 mg of catalyst.

Catalysts pre-treated: Calcined under air or A flow of 5 vol.%H_2/Ar for 2 h at 200 °C (5 °C/min).

Appendix F

Conversion of 4 wt.%*n*-butanol and selectivity towards butyraldehyde and butyric acid over 1 wt.%Pt- 1 wt.%M/TiO_2 (M= Bi, Pb, Al, Zn, Sn).

Catalysts Supported on TiO_2	**Conv. (%)**	**Sel. (%)**		**Mass Balance**
		BuALD	**BuAC**	
1 wt.% Pt - 1 wt.% Al	8 5	100 100	0 0	98 97
1 wt.% Pt - 1 wt.% Sn	36 36	89 88	11 12	96 100
1 wt.% Pt - 1 wt.% Bi	32 26	87 88	4 12	95 97
1 wt.% Pt - 1 wt.% Zn	25 24	94 92	6 8	97 98
1 wt.% Pt - 1 wt.% Pb	21 23	93 91	7 9	95 100

Conversion (Conv.), Selectivity (Sel.), Butyraldehyde (BuALD), Butyric Acid (BuAC). ***Reaction Conditions:*** 100 °C, 2 h, 2 bar O_2, *n*-Butanol (0.54 M), 15 mg of catalyst.

Appendix G

Conversion of *n*-Butanol over 1 wt.%Pt -1 wt.%Sn/TiO_2 catalyst following different pre-treatments.

Catalyst	Conv. *n*-BuOH (%)	Sel. (%)		Mass balance (%)
		BuALD	BuAC	
1 wt.%Pt-1 wt.%Sn/TiO_2 Fresh (as-obtained)	36 41 40	88 91 91	12 9 9	98 91 93
1 wt.%Pt-1 wt.%Sn/TiO_2 (Calcined)	31 31	92 92	8 8	97 95
1 wt.%Pt-1 wt.%Sn/TiO_2 (5 vol.% H_2/Ar)	42 39	91 91	9 9	91 96

Conversion (Conv.), Selectivity (Sel.), *n*-Butanol (*n*-BuOH), Butyraldehyde (BuALD), Butyric Acid (BuAC). ***Reaction Conditions:*** 100 °C, 2 h, 2 bar O_2, *n*-Butanol (0.54 M), 15 mg of catalyst. ***Catalysts pre-treated:*** Calcined under air or A flow of 5 vol.%H_2/Ar for 2 h at 200 °C (5 °C/min).

Appendix H

Conversion of *n*-Butanol over 1 wt.%Pt/C catalyst following different pre-treatments.

Catalyst	Conv. *n*-BuOH (%)	Sel. (%)		Mass balance (%)
		BuALD	BuAC	
1 wt.%Pt/C	20	94	6	98
Fresh (as-obtained)	23	93	7	100
1 wt.%Pt/C	24	95	5	95
(Calcined)	25	95	6	94
1 wt.%Pt/C	18	94	7	93
(5 vol.% H_2/Ar)	16	93	7	95

Conversion (Conv.), *n*-Butanol (*n*-BuOH), Butyraldehyde (BuALD), Butyric Acid (BuAC), Selectivity (Sel.).

Reaction Conditions**:** 100 °C, 2 h, 2 bar O_2, *n*-butanol (10 mL, 0.54 M), 15 mg of catalyst, 750 rpm.

Catalysts pre-treated: Calcined under air or under 5 vol.%H_2/Ar for 2 h at 200 °C (5 °C/mi